

DEVELOPMENT OF SPUTTERED TECHNIQUES FOR THRUST CHAMBERS

FINAL REPORT

(NASA-CR-135153)	DEVELOPMENT OF SPUTTERED	N77-17146
TECHNIQUES FOR THRUST CHAMBERS	Final Report	
(Pratt and Whitney Aircraft Group)	71 p HC	
A04/MF A01	CSCI 21H	Unclas
		G3/20 16492

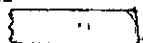
November 1976

by: J. R. Mullaly, R. J. Hecht, J. W. Broch,
and
P. A. Allard

Pratt & Whitney Aircraft Group
Division of United Technologies Corporation
Contract NAS 3-17792-Mod 4
National Aeronautics and Space Administration
NASA - Lewis Research Center

J. M. Kazaroff, Program Manager

65

1. Report No. NASA CR-135153	2. Government Accession No	3. Recipient's Catalog No.	
4. Title and Subtitle DEVELOPMENT OF SPUTTERED TECHNIQUES FOR THRUST CHAMBERS FINAL REPORT		5. Report Date November 1976	6. Performing Organization Code
		8. Performing Organization Report No FR-8027	
7. Author(s) J. R. Mullaly, R. J. Hecht, J. W. Broch, P. A. Allard		10. Work Unit No	
9. Performing Organization Name and Address Pratt & Whitney Aircraft Group Division of United Technologies Corporation Government Products Division P. O. Box 2691 West Palm Beach, Florida 33402		11. Contract or Grant No NAS3-17792 MOD 4	
		13. Type of Report and Period Covered Contractor Report	
12. Sponsoring Agency Name and Address National Aeronautics and Space Administration Washington, D. C. 20546		14. Sponsoring Agency Code	
		15. Supplementary Notes John Kazaroff, Project Manager NASA Lewis Research Center Cleveland, Ohio 44135	
16. Abstract Procedures for closing out coolant passages in regeneratively cooled thrust chambers by triode sputtering, using post and hollow Cu-0.15% Zr cathodes, were developed. The effects of aluminum-CERROTRU® filler materials, substrate preparation, sputter cleaning, substrate bias current density and system geometry on closeout layer bond strength and structure were evaluated. High strength closeout layers were sputtered over aluminum fillers. The tensile strength and microstructure of continuously sputtered Cu-0.15% Zr deposits were determined. These continuous sputtered deposits were as thick as 0.75 cm. Tensile strengths were consistently twice as great as the strength of the material in wrought form. <p style="text-align: center;">ORIGINAL PAGE IS OF POOR QUALITY</p>			
17. Key Words (Suggested by Author(s)) Sputtering Thrust Chambers CERROTRU® AMZIRC® Aluminum		18. Distribution Statement Unclassified-Unlimited	
19. Security Classif. (of this report) Unclassified	20. Security Classif. (of this page) Unclassified	21. No. of Pages 74	22. Price* 

* For sale by the National Technical Information Service, Springfield Virginia 22161

CONTENTS

<i>Section</i>		<i>Page</i>
	ILLUSTRATIONS.....	iv
	TABLES.....	vi
I	SUMMARY.....	1
II	INTRODUCTION.....	2
III	TASK I - CLOSEOUT LAYER APPLICATION TECHNIQUES.....	3
	A. Equipment and Procedures.....	3
	B. Filler Material Selection and Filling Techniques.....	8
	C. Final Substrate Preparation and Closeout Layer Deposition Parameters	26
	D. Results.....	32
	E. Conclusions.....	51
IV	TASK II - PROPERTIES OF TRIODE SPUTTERED COPPER - 0.15 WT% ZIRCONIUM (AMZIRC®) MATERIAL.....	54
	A. Equipment and Procedures.....	54
	B. Hollow Cathode Results and Discussion.....	56
	C. Post Cathode Results and Discussions.....	58
	D. Conclusions.....	62
V	PROGRAM SUMMARY.....	64
VI	REFERENCES.....	65
	DISTRIBUTION LIST.....	66

ILLUSTRATIONS

<i>Figure</i>		<i>Page</i>
1	Schematic of System No. 1 Shown for Post Cathode.....	4
2	Flat Cathode Coater (Some Ground Potential Shields Not Shown for Clarity)..	5
3	Task I Substrates.....	6
4	Burst Test Rig - Shown for Closeout Layer Deposited in a Hollow Cathode.....	7
5	Flat Tensile Specimen (Shown for Hollow Cathode Deposit).....	7
6	Schematic of Filler Systems.....	9
7	Details of Grooves on Flat Substrate, Sputtered Aluminum Filler Work.....	12
8	Details of Grooves on Cylindrical Substrates - Sputtered Aluminium Filler Work - Post Cathode Substrate Shown. Hollow Cathode Substrates Had Identically Sized Grooves on the OD.....	13
9	Microstructure of Closeout Layer Over Filled 0.152 cm Wide by 0.120 cm Deep Grooves.....	16
10	Microstructure of Closeout Layer Over Partially Filled (Porous) Grooves.....	17
11	Example of Groove on Flat Substrate 1-2A Not Completely Filled with Sputtered Aluminum - Illustration of Filler Growth.....	18
12	Filling Grooves by Sputtering from a Hollow Cathode - Effect of Bias.....	20
13	Typical Detail of Sputtered Aluminum Filling on 0.152 cm Wide by 0.102 cm Deep Grooves as a Function of Substrate Bias - Void Formation - Hollow Cathode	21
14	Typical Filling of 0.127 cm Wide by 0.127 cm Deep Grooves With Sputtered Aluminum as a Function of Substrate Bias - Hollow Cathode.....	22
15	Typical Filling of 0.127 cm Wide by 0.127 cm Deep Grooves With Sputtered Aluminum as a Function of Substrate Bias - Post Cathode.....	24
16	Aluminum Wire Before Machining.....	25
17	Closeout Layer Over Correctly and Incorrectly Indexed Cast CERROTRU® - Substrate 1-4.....	36
18	Typical Closeout Layer Microstructure Over Capped Cast CERROTRU® Filler - Substrate 1-5.....	37
19	Closeout Layer Over Correctly and Incorrectly Indexed Encased CERROTRU® - Substrate 1-7.....	38

20	Typical Closeout Layer Microstructure Over Encased CERROTRU® - Substrate I-7.....	39
21	Growth of Closeout Layer Over Large Defect in Surface of Filler - Void Formation Substrate I-7.....	39
22	Typical Microstructure of Closeout Layer Over Aluminum Wire Filler - Substrate I-6.....	40
23	Typical Closeout Layer Microstructure Over Capped Aluminum Wire - Substrate I-8.....	41
24	Typical Microstructure Over Aluminum Wire Filler - Origin Of Leaders - Substrate I-9.....	42
25	Microstructure Over Surface Sanded With 1000 Grit SiC Paper - No Leaders - Substrate I-11.....	43
26	Typical Microstructure of Closeout Layer on Substrate I-12.....	44
27	Microstructure Near Burst Specimen Failure Showing Crack Propagation - Substrate I-13.....	46
28	Microstructure of Closeout Layer Deposited at Two Different Rates Showing Effect of Bias Current Density, Substrate I-14.....	47
29	Coarse and Fine Microstructure for Two Closeout Layer Growth Rates; Substrate I-4P, 50V Bias.....	48
30	Coarse and Fine Microstructure for Two Closeout Layer Rates; Substrate I-5P, -25V Bias.....	49
31	Microstructure Showing Coarse and Fine Regions for Substrate I-6P.....	50
32	Microstructure of Sputtered AMZIRC® at Higher Voltage and Higher Rate, Substrate II-1.....	57
33	Typical Microstructure for Substrate II-2; Cathode Voltage -1000V.....	58
34	Typical Longitudinal and Traverse Microstructure for Substrate II-3.....	59
35	Microstructure of Deposit Formed at Two Rates Showing Effect of Bias Current Density - Substrate II-4.....	60
36	Microstructure of Deposit From Post Cathode Showing Onset of Fine Structure at Two Deposit Rates; -50 Volt Bias, Substrate II-10.....	61
37	Microstructure of Deposit II-28 at Low Rate -25V Bias.....	62

TABLES

<i>Table</i>		<i>Page</i>
1	Sputter Cleaning and Deposition Parameters for CERROTRU® Capped With Aluminum.....	10
2	Sputter Cleaning and Deposition Parameters for CERROTRU® Encased in Aluminum.....	11
3	Sputter Deposition Parameters for Sputtered Aluminum and Copper on Flat Grooved Substrates (System No. 4).....	15
4	Volume Percent of Groove Filled in Flat Substrates.....	15
5	Sputter Deposition Parameters and Filling Data for OD Grooved Cylindrical Substrates (1100 Series Aluminum Hollow Cathode, System No. 1..	18
6	Sputter Deposition Parameters for ID Grooved Cylindrical Substrates (1100 Series Aluminum Post Cathode, System No. 2).....	23
7	Summary of Task I Closeout Substrate Preparation and Sputter Cleaning Parameters.....	27
8	Summary of Task I Closeout Deposition Parameters.....	28
9	Burst Test Results for Task I Hollow Cathode Sputtered Specimens.....	33
10	Tensile Properties of AMZIRC® Closeout Layers (Room Temperature).....	34
11	Vickers Hardness for As-Deposited AMZIRC® Closeout Layers for Task I.....	34
12	Summary of Task II Substrate Preparation.....	54
13	Summary of Task II Deposition Parameters.....	55
14	Tensile Properties of Deposited and Wrought AMZIRC® (Room Temperature)	55
15	Vickers Hardness for As-Deposited AMZIRC® for Task II.....	56
16	Gas Content of Task II Deposits.....	56

SECTION I SUMMARY

The purpose of this program was to develop procedures for closing out the cooling passages in regeneratively cooled thrust chambers and to determine the effect of sputtering parameters on the mechanical properties of the closeout layer. The program was divided into two work tasks.

In Task I, aluminum wire, sputtered aluminum and CERROTRU® were used in several combinations for filling grooves machined in copper cylinders. The filler materials were machined flush with the substrate surface and AMZIRC® (Cu-0.15%Zr) was sputtered over the filled substrate. The best filler system, judging by the quality of the sputtered AMZIRC closeout layer and ease of removal was aluminum wire covered by a thin layer of sputtered aluminum. By use of careful surface preparation techniques, nearly equal results were obtained using aluminum wire alone. The bulk of Task I experiments were performed with wire filled substrates.

Experiments were performed to show the effect of substrate surface roughness, sputter cleaning, substrate bias current density, system geometry and other parameters on the closeout layer structure and burst strength. It was shown that substrate bias current density could effectively modify columnar growth habit and "cure" defect structures originating at the comparatively rough substrate surfaces.

AMZIRC closeout layers triode sputtered both from post and hollow cathodes exhibited tensile strengths far superior to conventionally wrought processed AMZIRC. For example, 0.2% offset yield strengths (room temperature) of 640 MN/m^2 (93 ksi) at 15% elongation were achieved in a hollow cathode deposit. AMZIRC closeout layers 0.076 cm (0.030 in.) thick (filler leached out) withstood hydrostatic burst test pressures of 68.8 MN/m^2 (10,000 psi) without failure.

The objective of Task II was to determine the effect of sputtering parameters on the properties of AMZIRC deposits sputtered continuously from hollow and post cathodes in the triode discharge. A hollow cathode deposit 0.76 cm (0.303 in.) thick was made at a deposition rate of 6.7 mm/s (0.95 mils/hr) and -50 volts bias. Offset yield strength was 861 MN/m^2 (125 ksi) with 6% elongation. Substrate bias was shown to effectively reduce oxygen levels in these thick deposits.

SECTION II INTRODUCTION

In the development of advanced chambers for programs such as the Space Tug Experimental Engine Program, new fabrication techniques and/or materials will be needed to meet the projected chamber requirements. Of the techniques currently available for fabrication, deposition by sputtering offers the most potential for meeting the demands of the advanced designs. The application of sputtering techniques to the fabrication of thrust chambers permits relative freedom in materials selection for the chamber designer. Not being limited by the inability to electrodeposit a material and not having to sacrifice the material properties by elevated temperature joining operations, the chambers can be fabricated from practically any alloy or combination of alloys desired. Furthermore, the improved bonding obtainable with sputtering provides increased low-cycle fatigue life through improved materials and an elimination of joining materials at the bond interface.

Previous work by Mullaly, Hecht, Schmid, and Torrey (Reference 1) and McCalanahan, Busch and Moss (Reference 2) has shown that precipitation-hardened copper alloys synthesized by sputtering offer potential as materials for fabricating regeneratively cooled thrust chambers. Furthermore, it was shown that a sputtered copper-0.15 zirconium alloy can be stronger than the same alloy produced by conventional primary forming techniques.

The proposed method for chamber fabrication involves the sputtering of an inner or outer chamber wall, with subsequent machining to a ribbed wall configuration. The chamber channels are then filled with a suitable material and the final closeout layer applied. Fabrication by this approach requires that the filler material be compatible with the vacuum sputtering environment. The filler must be capable of being applied to the channeled configuration and completely removed without degrading the chamber material properties. The objectives of this program were (1) to develop procedures for closing out the chamber channels by triode sputtering AMZIRC from both a post and hollow cathode, and (2) to evaluate the effect of triode sputtering parameter variations on the tensile properties of AMZIRC.

The investigation performed in this program was divided into two work tasks. Task I involved the application of an AMZIRC closeout layer to a cylinder containing channels to yield a cylindrical structure representative of regeneratively cooled thrust chambers. Within this task an evaluation of four filler material systems to fill the grooved cylinder passages and selection of triode sputtering deposition parameters compatible with the filler materials were performed. Procedures for filling the channels with the selected materials were also developed. In Task II, the material properties of continuously sputtered thick deposits were determined. The effect of substrate bias voltage on the tensile properties of deposits sputtered from a post cathode and the effect of substrate and cathode power settings on the tensile properties of deposits sputtered from a hollow cathode were determined.

This report covers all the work performed in Tasks I and II of Contract NAS3-17792 MOD4. Previous work on NAS3-17792 was separately reported in the Interim Report NASA CR-134824 (Reference 1).

SECTION III
TASK I
CLOSEOUT LAYER APPLICATION TECHNIQUES

The objective of this task is the development of procedures for closing out coolant passages of regeneratively cooled thrust chambers by triode sputtering using both post and hollow cathode methods. This procedure development includes selection, placement, and removal of the filler materials as well as evaluating the effects of various sputtering parameters on the closeout layer material bond quality.

A. EQUIPMENT AND PROCEDURES

The three vacuum chambers used for sputter deposition from post and hollow cathodes are shown schematically in figure 1. The chambers were of welded stainless steel construction. The essential difference between chambers lies in the different anode and ground-shield geometry. The significance of the different geometries will be discussed later in this report. All systems were rough pumped with liquid nitrogen sorption pumps. System 1 was pumped to ultra-high vacuum with an ion pump. Systems 2 and 3 were each pumped with a liquid nitrogen trapped 6-inch diffusion pump.

Sputter deposition onto flat substrates was done in a chamber shown schematically in figure 2. This chamber was rough pumped with a copper wool trapped 17.7 cfm mechanical pump and pumped to ultra-high vacuum with a 4-inch liquid nitrogen trapped diffusion pump. This flat cathode system is designated system No. 4.

The hollow cathodes were the same size for each system; 10.2 cm ID, 12.7 cm OD by 22.8 cm long. All closeout layer work was done with a 0.15%Zr-Cu (AMZIRC®) alloy. Aluminum hollow cathodes were either type 1100 or 6061 aluminum. Post cathodes were 3.8 cm-diameter by 22.2 cm long. AMZIRC was used on all closeout layers and 1100 aluminum was used for all groove filling experiments from post cathodes. Flat cathodes were 7.3 cm wide by 10.2 cm high and 0.64 cm thick. In the flat cathode work, AMZIRC was used for closeout layers and both 1100 and 6061 aluminum were used for groove filling.

Hollow cathodes were held in water cooled stainless steel holders in systems 1 and 2 and were directly water cooled in system 3. Post cathodes were directly cooled by a coaxial tube arrangement. Flat plate cathodes were clamped to water cooled stainless steel holders.

Substrates used in conjunction with hollow and post cathode closeout layer depositions are shown schematically in figure 3. Both AMZIRC and OFHC copper were used. Grooves were cut in substrate OD by sawing. Grooves on substrate ID were machined by multiple passes with a shaper. The number of grooves in hollow cathode substrates varied from 10 to 72 (fully grooved) and will be noted in the appropriate text or tables. All post cathode substrates had 10 grooves on the ID. The final machining of all hollow and post cathode substrates was done on a lathe. Further surface preparation details are given in the report. Details on substrates used for sputtered aluminum groove filling experiments will be given in section B.3.

The cathode and anode power supplies for all systems were three-phase, full wave rectified, unfiltered DC. Substrate bias for system 2 was either single- or three-phase full wave rectified unfiltered DC. Bias for systems 1, 3 and 4 was provided by single-phase, full wave rectified, unfiltered DC power supplies. The filaments for all systems were AC powered.

ORIGINAL PAGE IS
OF POOR QUALITY

FIGURE 1a SCHEMATIC OF SYSTEM NO. 1 SHOWN FOR POST CATHODE

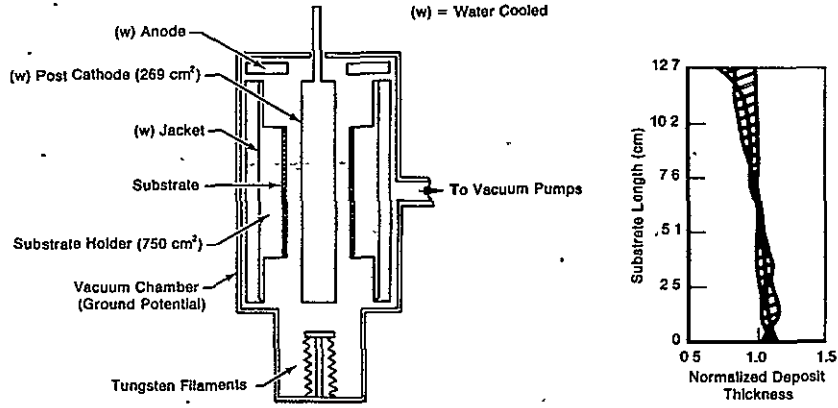


FIGURE 1b SCHEMATIC OF SYSTEM NO. 2 SHOWN FOR HOLLOW CATHODE

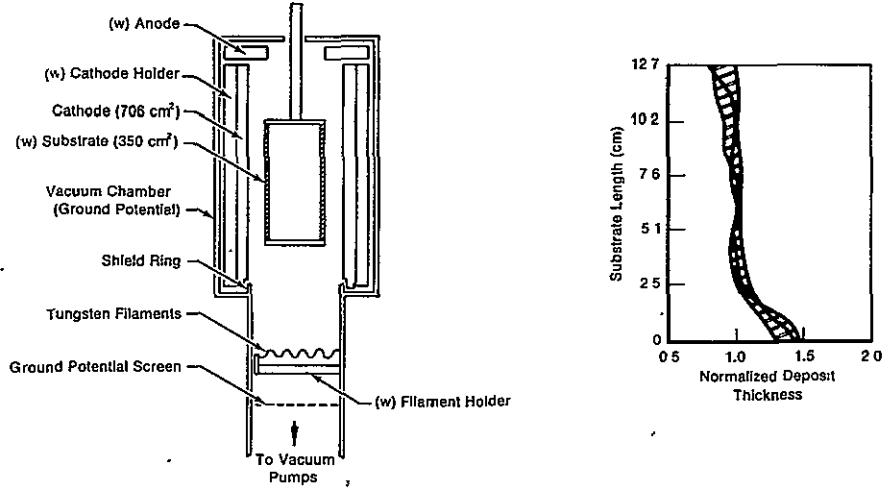
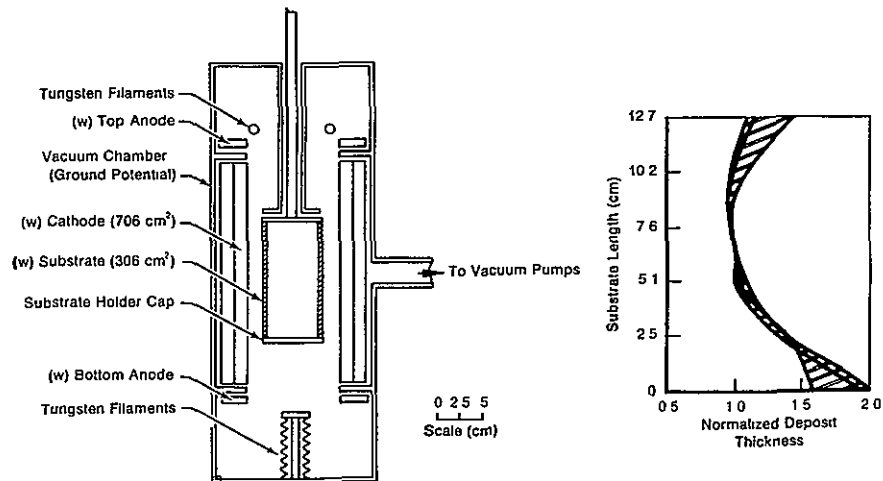


FIGURE 1c SCHEMATIC OF SYSTEM NO. 3 SHOWN FOR HOLLOW CATHODE



FD 104549

Figure 1. Schematic of System No. 1 Shown for Post Cathode

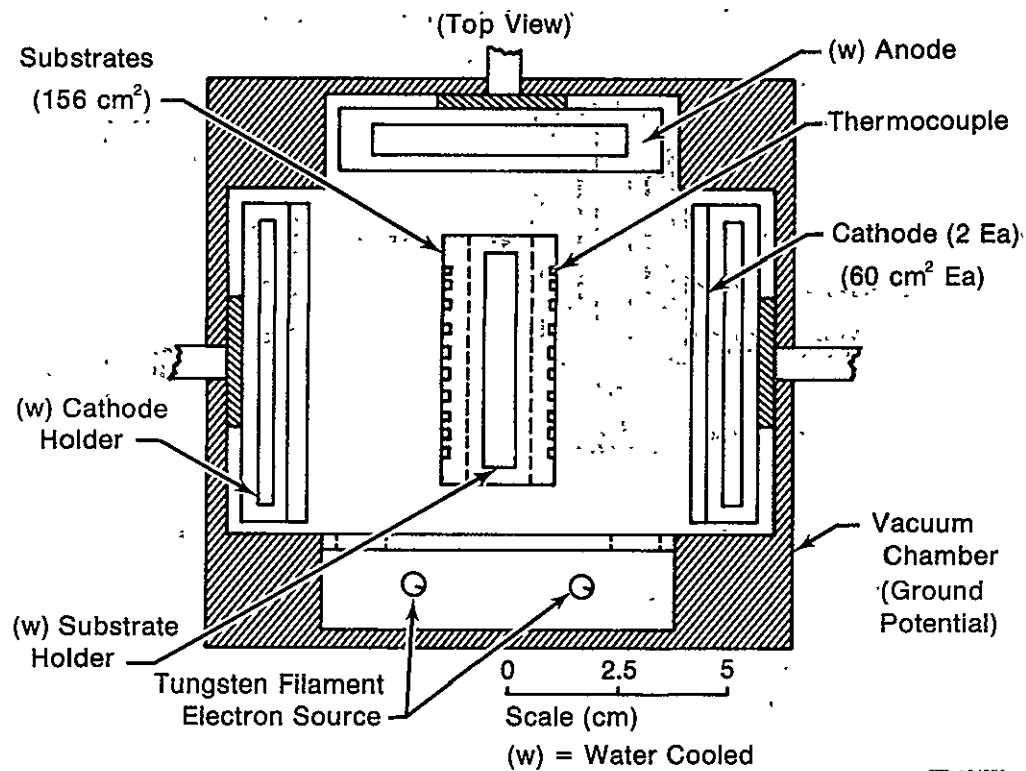


Figure 2. Flat Cathode Coater (Some Ground Potential Shields Not Shown for Clarity)

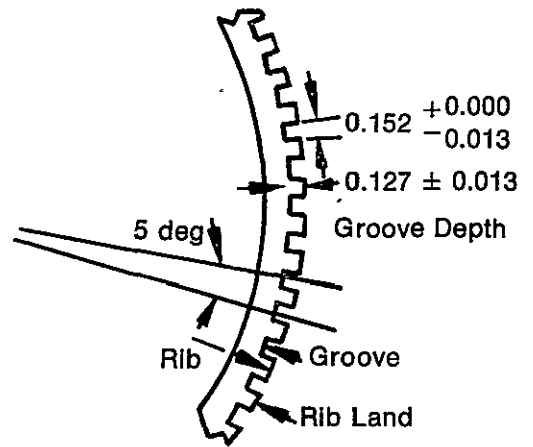
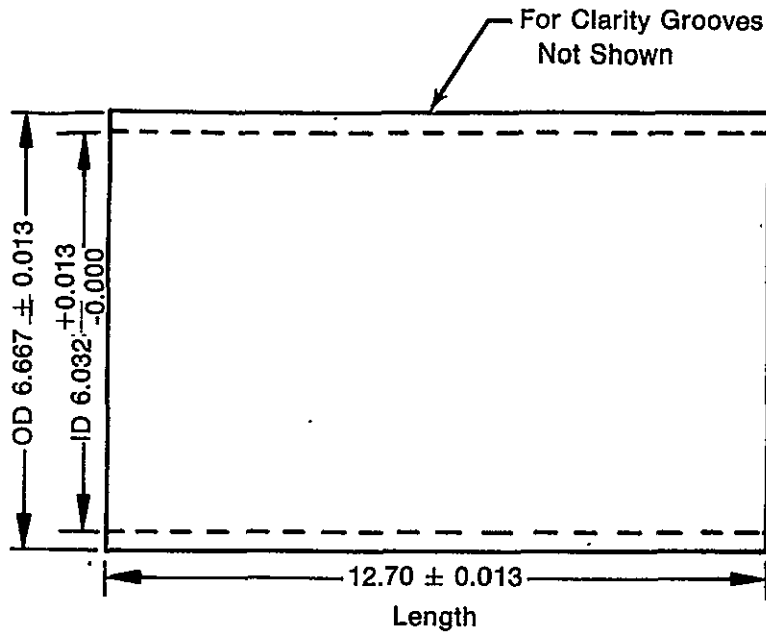
Pressure during sputtering was measured by a Pirani gage. Pressures given in data tables are gage readings corrected for krypton. Pump down to ultra-high vacuum is monitored by ion pump current in system 1 and by ion gages in systems 2, 3 and 4. Pressure was maintained by a bypass (from chamber to diffusion pump) throttle valve in systems 2, 3 and 4 and by a throttled liquid nitrogen trapped 2-inch diffusion pump on system 1:

A general procedure was used for all depositions performed in this evaluation. Substrates were cleaned and installed on their holders. Systems were pumped to the 10^{-8} torr range with filaments. Research grade (99.995%) krypton gas was bled into the system to a few millitorr and sputter cleaning of the substrate started. Usually several cycles of sputter cleaning, each followed by pump down to ultra-high vacuum, were necessary to reduce substrate and system outgassing to an acceptable level. Sputter cleaning of the cathode was done simultaneously with substrate cleaning and at the same voltage. Whenever the deposition cycle was stopped for more than about a minute a sputter cleaning cycle was performed before continuing the deposition.

Burst tests were done in the rig shown schematically in figure 4. The rig was design limited to 68.8 MN/m^2 (10,000 psi). Test sections were 1 inch long cylindrical sections cut from the overcoated substrates. The closeout layer was machined to 0.076 cm (0.030 inch) thickness for each specimen.

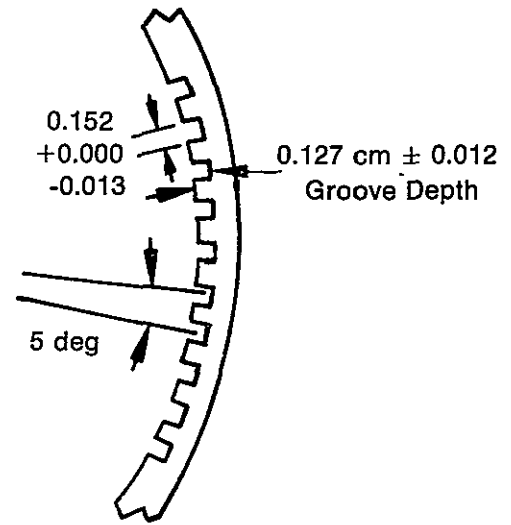
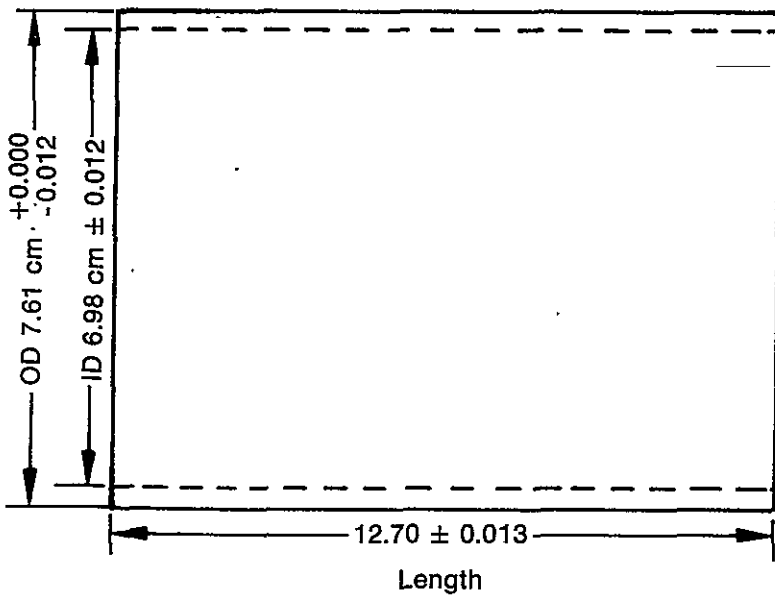
Where deposit tensile properties were to be determined flat tensile samples, figure 5, were machined and tested.

FIGURE 3a
 HOLLOW CATHODE GROOVED SUBSTRATE FOR TASK I CLOSEOUT LAYER WORK



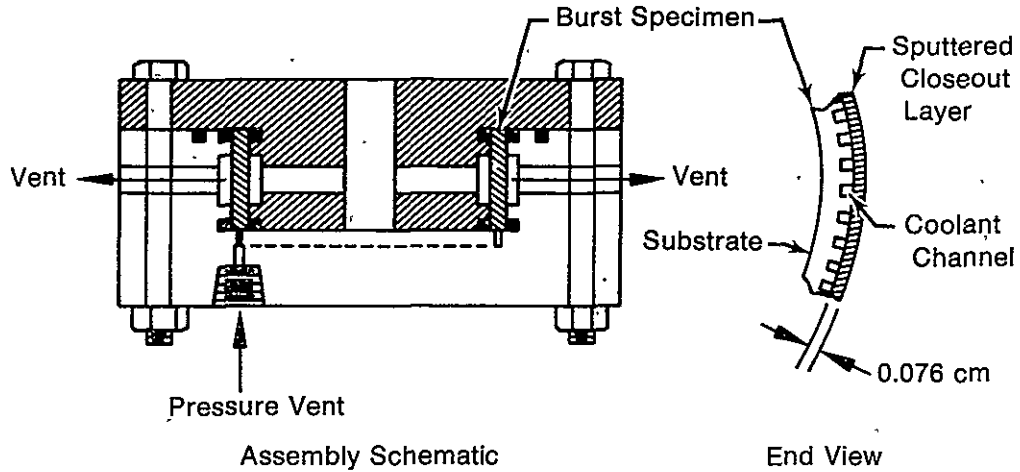
Note: Dimensions in cm

FIGURE 3b
 POST CATHODE GROOVED SUBSTRATE FOR TASK I CLOSEOUT LAYER WORK



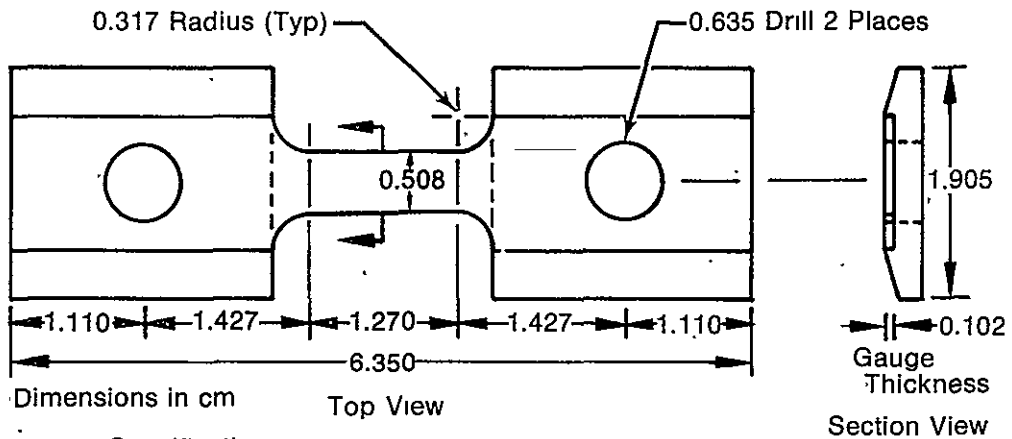
FD 104551

Figure 3. Task I Substrates



FD 104552

Figure 4. Burst Test Rig - Shown for Closeout Layer Deposited in a Hollow Cathode



Specifications

1. Gauge Section To Be Symmetric and Parallel Within 0.013 cm
2. Holes To Be Within 0.013 cm of Centerline
3. Dimensions \pm 0.013 cm Unless Noted
4. Finish 1.7 μ m RMS or Better

FD 104553

Figure 5. Flat Tensile Specimen (Shown for Hollow Cathode Deposit)

B. FILLER MATERIAL SELECTION AND FILLING TECHNIQUES

Previous work (reference 1) showed that CERROTRU® and flame sprayed aluminum had potential as filler materials. CERROTRU is a binary eutectic (Bi-42 wt% Sn) with a 411°K (281°F) melting point and a Brinell hardness of 22. This material is relatively easy to cast into channeled structures. A problem arises when backsputtering CERROTRU filled substrates prior to depositing the closeout layer. Overheating leads to rapid migration of Bi over the substrate surface which contaminates the rib lands and subsequently reduces the closeout layer-to-rib bond strength. Aluminum is compatible with vacuum and with the AMZIRC closeout layer material. In addition, aluminum with its higher melting point is not sensitive to heat generated in the back sputtering operation, does not back sputter (under voltages used) rapidly, and can be completely removed with NaOH without affecting the base copper alloy. Flame sprayed aluminum, however, was unacceptable due to excessive porosity in the filler as well as to poor bonding to the rib wall. The excessive porosity lead to excessive outgassing while the lack of rib bonding was often the source of defects in the closeout layer.

Based on the above preliminary work, several CERROTRU and aluminum filler schemes were evaluated in this program. The approaches are pictured in figure 6. A description of each approach and techniques for implementing are given in the following discussion.

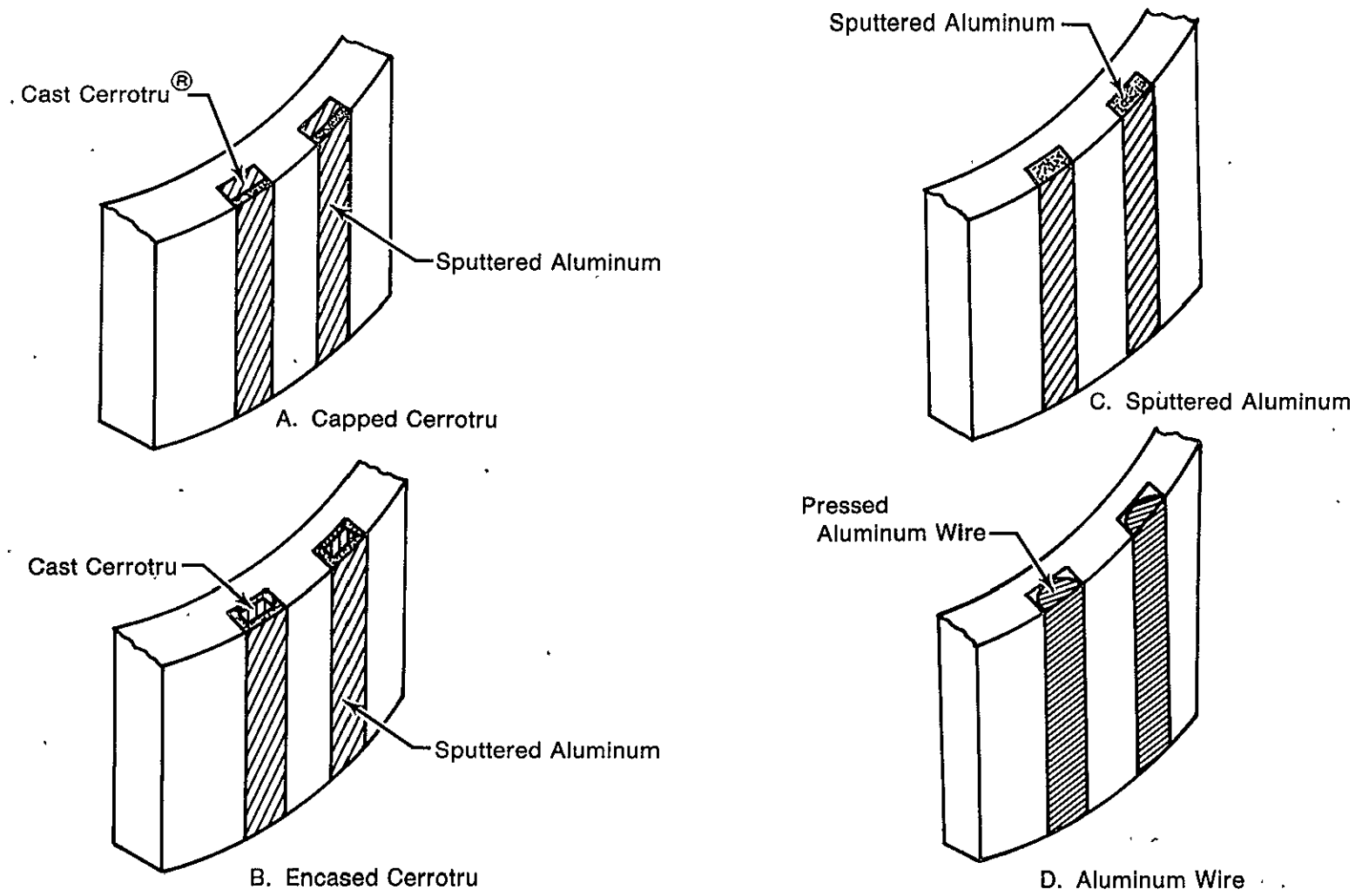
1. Cast CERROTRU Capped With Sputtered Aluminum

CERROTRU was cast into the substrate grooves. The alloy was then machined back 0.025 cm in each groove leaving a groove 0.025 cm deep by 0.152 cm wide which was filled with sputtered aluminum. This technique should provide a dense layer which can be sputter cleaned with a minimum of problems. Three substrates, I-3, I-4 and I-5 were filled by this method. They were OFHC copper with 10 grooves each on the OD.

Typically, the cylinder was prepared by vapor blasting the grooves to remove burrs and contaminants and washed with methanol. The ends of the cylinder were tightly plugged. The cylinder was then tightly wrapped with 0.0127 cm Ti-6Al-4V sheet so that it extended slightly beyond the copper cylinder ends. The titanium alloy sheet was secured with 0.025 cm diameter wire at two positions along the cylinder length. This assembly was then preheated for 120 to 180 sec in an air furnace at $477 \pm 10^\circ\text{K}$ ($399.2 \pm 20^\circ\text{F}$).

Approximately 3.9 kg of CERROTRU was melted in a PYREX container and the molten alloy skimmed to remove floating contaminants. The preheated cylinder was pushed vertically into the molten CERROTRU so that the top edge of the copper cylinder was below the surface of the molten CERROTRU. Since a difference in pressure exists, the molten CERROTRU is forced up the passages formed by the titanium alloy sheet and the grooved copper cylinder. Vibrating the assembly assisted the movement of entrapped bubbles up the grooves and assured complete filling of the passages. The whole assembly was then allowed to cool to room temperature. After removing the outer glass container, the excess CERROTRU was broken away, and the titanium alloy sheet and the end plugs removed to complete the process. The filled grooves were visually examined for porosity. The CERROTRU in the grooves was then machined to a level 0.025 cm below the rib land surface.

Due to misindexing during back machining, a thin layer of CERROTRU was visible on one rib wall in each groove of substrate I-3. This was not observed on substrates I-4 and I-5. The substrates were sanded lengthwise with 600 grit SiC paper, scrubbed with cleanser and rinsed in ethyl alcohol.



FD 104554

Figure 6. Schematic of Filler Systems

Substrate sputter cleaning and deposition parameters are given in table 1. Sputtering was done in system No. 1 from a type 1100 series hollow aluminum cathode. As noted on the table, the sputter cleaning, no matter how low a voltage and how short the cleaning cycle, was enough to melt the CERROTRU. Any lower voltage and shorter times would be completely ineffective. Sputter cleaning was done to ensure a reasonable bond between the aluminum cap and the rib wall. A poor bond could be the source of defects as discussed before and could lead to complete loss of the cap during the lathe machining of the substrate back to the original OD.

TABLE 1. SPUTTER CLEANING AND DEPOSITION PARAMETERS FOR CERROTRU® CAPPED WITH ALUMINUM

Sputter Cleaning						
Substrate Number	Cleaning Cycle No. ¹	Substrate		Time (ks)	Pressure	
		Current (ma/cm ²)	Voltage (volt)		(N)	(n/m ²)
I-3	1	4.0	-25	0.3	4.9	0.64
	2	3.9	-25	0.3	4.1	0.53
I-4	1	4.2	-15	0.3	4.6	0.60
I-5	1	3.8	-15	0.12	5.1	0.66
	2	3.8	-15	0.12	5.1	0.66
	3	4.3	-15	0.3	6.1	0.79

Deposition									
Substrate Number	Deposition Run No. ²	Substrate		Target		Time		Pressure	
		Current (ma/cm ²)	Voltage (volt)	Current (ma/cm ²)	Voltage (volt)	(ks)	(hr)	(N)	(n/m ²)
I-3	1	3.9	-25	4.0	-500	44.1	12.25	3.6	0.47
	2	4.0	-25	4.1	-500	48.6	13.5	4.1	0.53
I-4	1	3.7	-15	4.5	-500	136.8	38.0	2.7	0.34
I-5	1	4.3	-15	4.7	-500	52.2	14.5	5.3	0.69
	2	3.5	-15	4.5	-500	45.0	12.5	2.4	0.31
	3	4.1	-15	4.5	-500	57.6	16.0	3.7	0.48

¹ System typically pumped to low 10⁻⁴ micron range between cycles.

² System vented between cycles 2 and 3. CERROTRU in one complete groove had melted (pocked) surface.

³ System pumped to low 10⁻⁵ micron range between runs (run equals continuous sputtering time) and substrate sputter cleaned at -50v for 0.9 kiloseconds.

⁴ Pocked appearance of aluminum over grooves indicated melting of CERROTRU during cleaning cycle.

2. CERROTRU Encased In Sputtered Aluminum

This scheme is similar to the preceding one except that the substrate grooves were first coated with aluminum sputtered from the 1100 series hollow aluminum cathode. The substrate was machined back to its original OD before casting CERROTRU into the lined grooves. The aluminum liner was approximately 0.025 cm thick on the bottom of each groove and 0.013 cm thick on the walls. CERROTRU was cast into the lined grooves by the procedure outlined above. The aluminum liner along with the CERROTRU in each groove was cut back 0.025 cm in preparation for depositing the aluminum cap.

In addition to the advantages of the aluminum cap already discussed, this technique should minimize CERROTRU problems at the rib wall. One substrate, I-7, was filled by this method. The substrate was OFHC copper with 10 grooves on the OD. The substrate was scrubbed with cleaning powder and rinsed in ethyl alcohol before sputter deposition work.

Sputter cleaning and deposition parameters for both the liner and cap deposition are summarized in table 2. Sputtering was done in system No. 1.

TABLE 2. SPUTTER CLEANING AND DEPOSITION PARAMETERS FOR CERROTRU® ENCASED IN ALUMINUM

Sputter Cleaning									
Substrate									
Substrate Number	Cleaning Cycle No. ¹	Current (ma/cm ²)	Voltage (volt)	Time (ks)	Pressure (N)	Pressure (n/m ²)			
Before Aluminum Liner Deposition.									
I-7	1	4.0	-25	0.3	3.2	0.42			
	2	4.3	-50	1.8	4.9	0.64			
Before Aluminum Cap Deposition									
I-7	1	3.3	-25	0.3	2.4	0.31			
	2	3.7	-25	0.3	6.0	0.78			
	3	3.8	-50	1.5	2.5	0.33			

Deposition									
Substrate									
Substrate Number	Deposition Run No. ¹	Substrate		Target		Time		Pressure	
		Current (ma/cm ²)	Voltage (volt)	Current (ma/cm ²)	Voltage (volt)	(ks)	(hr)	(N)	(n/m ²)
Liner Deposition									
I-7	1	5.0	-50	5.5	-500	54	15	2.6	0.34
	2	5.1	-50	5.9	-500	57.6	16	4.9	0.64
Cap Deposition									
I-7	1	3.9	-50	4.8	-500	32.4	9	1.4	0.18
	2	4.1	-50	5.0	-500	144	40	1.2	0.16

¹System pumped to low 10⁻⁴ micron range between cleaning cycles and deposition runs. Substrate sputter cleaned at -50v for 0.9 kiloseconds between deposition runs.

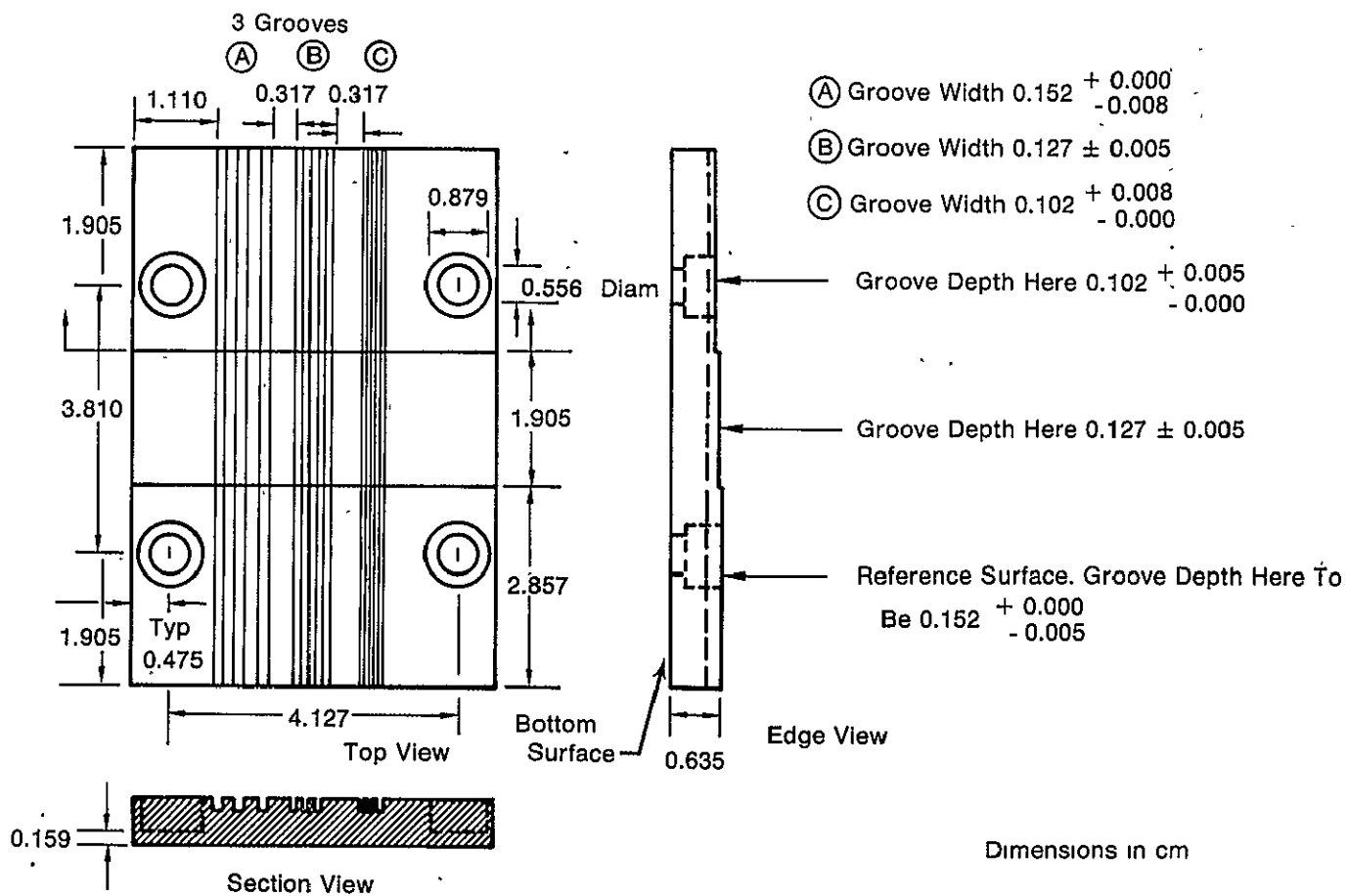
²Pocked appearance of aluminum over grooves indicated melting of approximately 60% of CERROTRU.

3. Sputtered Aluminum

Filling grooves with sputtered aluminum would completely eliminate the problems connected with CERROTRU. Irregularly shaped grooves could be filled and a good filler to rib wall bond could be obtained. Previous work in this laboratory showed that grooves 0.140 cm wide by 0.127 cm deep in a flat plate could be filled from a planar cathode. The filler was well bonded to the groove walls, but a void defect originated from the inside corners of each groove. The void was propagated upward as the filler closed up the groove leaving a defect at the surface of the filler.

Experiments were undertaken to determine what size grooves could be filled from flat, hollow and post cathodes. Substrates were grooved with combinations of groove widths and depths as shown in figures 7 and 8. The cylindrical substrates were cut from OFHC copper. The flat substrates were AMZIRC.

Due to the time required, no cylindrical substrates were completely filled for closeout layer application. The discussion of this filling technique will be completed in this section and will not be discussed further in the Results Section of this report.

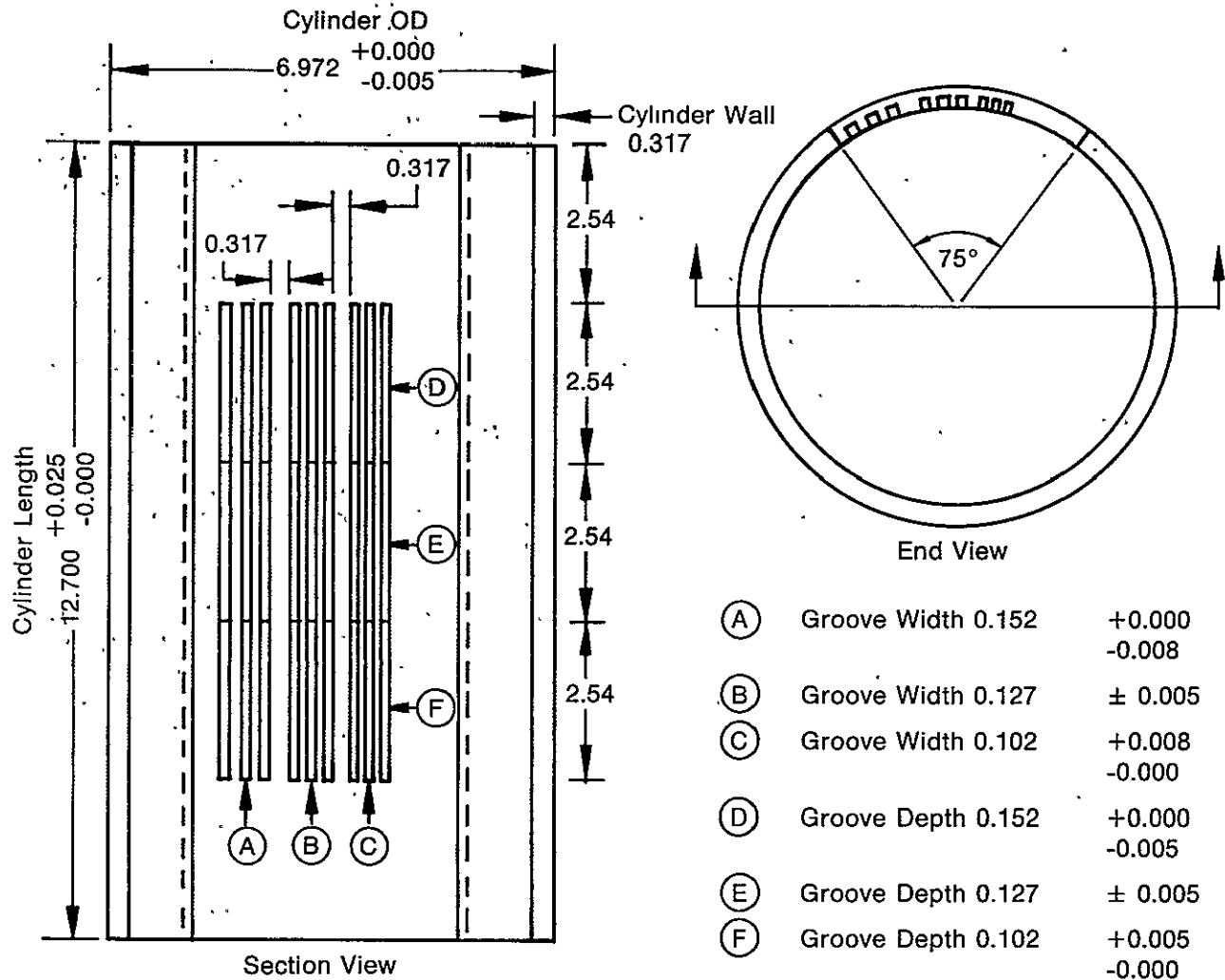


Note:

1. Tolerance Fractional Dim ± 0.025
2. Bottom Surface Flat To ± 0.013 and $1.7 \mu\text{m}$ RMS or Better Finish
3. Groove Tolerance Only Over 0.635 Length In Center of Each Indicated Groove Depth Region
4. Alternate Fabrication of Groove Widths and Depths Use, e.g. Grooves May be Sawed To Different Depth in A Smooth Face, or Grooves May Be Sawed For Short Length (0.635 minimum).
5. Land Width Between Grooves To Be Same Width As Groove

FD 104555

Figure 7. Details of Grooves on Flat Substrate, Sputtered Aluminum Filler Work



Dimensions in cm

Notes:

1. Tolerance Fractional Dim ± 0.025 . Other Dim As Noted
2. Cylinder OD and ID Surface Finish $0.81 \mu\text{m}$ RMS or Better
3. Groove Reference Surface is Cylinder ID
4. Groove Tolerance Only Over 0.635 Length in Center of Each Indicated Groove Depth Region
5. Grooves Should Be Machined By Most Economical Method
6. Land Width Between Grooves To Be Same As Groove Width
7. One Cylinder Should Be Sectioned Into 4 Parts and Groove Machined in Each Part. Then Cut Section From 4 Cylinders Such That a Complete Cylinder is Fabricated

FD 104556

Figure 8. Details of Grooves on Cylindrical Substrates - Sputtered Aluminium Filler Work - Post Cathode Substrate Shown. Hollow Cathode Substrates Had Identically Sized Grooves on the OD

The first filling was done on the flat substrates to test the viability of this technique before proceeding to cylindrical substrates. Type 1100 and 6061 series aluminum were used to test the effect of aluminum alloy on closeout layer microstructure. Preliminary substrate cleaning consisted of a cleaning powder scrub followed by an ethyl alcohol rinse. Ion bombardment cleaning typically was done for 300 seconds with $-25v$ on the substrate followed by pump down to the low 10^{-7} torr range then additional sputtering for 1800 seconds at $-50v$ before the initial deposition. If the discharge was interrupted for any length of time during a deposition cycle, the substrate was sputter cleaned for 900 seconds at $-50v$.

Deposition parameters are listed on table 3. The larger grooves were essentially filled at the end of several runs constituting deposition cycle Number 1. At the end of this first cycle, the substrates were ground back to the original surface. Then a thin layer of aluminum was deposited to cover the defects exposed by the first grinding. The substrates were again ground back prior to depositing the AMZIRC closeout layer. Substrates I-1A and I-2A were coated individually during cycle 1 and simultaneously for cycles 2 and 3. The substrates were sectioned after cycle 3.

The groove filling achieved for each groove is given in table 4. A typical microstructure for the closeout layers over 100% filled grooves is shown in figure 9. The closeout layer was dense and contained no defects. The microstructures over the type 1100 and 6061 aluminum are similar.

Filled grooves marked "*porous*" in table 4 were for the most part successfully overcoated. Figure 10 illustrates a typical microstructure over the porous aluminum, i.e., no defects emanating from the filler-rib wall interface; growth over gross defects defective for short distances and then "cured"; and a different structure over the filler material than over the AMZIRC substrate material. The different growth habit may be due to porosity and a reduced thermal conductivity through the porous aluminum. Hardness, however, does not decrease in the AMZIRC adjacent to the porous aluminum indicating that no gross overtemperature occurred. The thermocouple in the substrate registered a maximum of $433^{\circ}K$ ($310^{\circ}F$) during the closeout layer deposition.

Figure 11 shows a typical unfilled groove. The AMZIRC deposit illustrates how the sputtered filler grows rapidly into the groove from the rib walls and prevents any significant amount of material from reaching the bottom of the groove. A program of thin deposits alternating with machining back to the substrate surface would be needed to fill the deeper and narrower grooves.

The first work on filling cylindrical substrates was done in a hollow cathode. Substrates were grooved on the OD with the same combination of groove widths and depths as the flat substrates. (See figure 8.) The substrates were vapor blasted, scrubbed with a cleanser and rinsed in ethyl alcohol and sputter cleaned as described for the flat substrates.

Deposition parameters and filling data are given on table 5. Substrate I-10 was not filled as extensively as I-1 and I-2. A vacuum leak during deposition cycle No. 2 caused a poorly structured layer that could not be sputter cleaned for further filling.

The object of the experiments was to determine the effect of substrate bias on filling. The flat plate work showed that at the top of the groove the deposit grew rapidly into the groove effectively shielding the bottom of the groove from the sputtered aluminum. In the hollow cathode geometry, this growth from the walls was expected to be more severe due to the greater range of the angle of incidence (with the substrate) of the sputtered material. A bias of $-25v$ or higher should cause aluminum to be resputtered from the mouth of the groove and thereby keep the groove opened so groove filling could continue.

TABLE 3. SPUTTER DEPOSITION PARAMETERS FOR SPUTTERED ALUMINUM AND COPPER ON FLAT GROOVED SUBSTRATES (System No. 4)

Substrate Number	Deposition Cycle No.	Substrate		Cathode		Time		Pressure		Coating Thickness	
		Current (ma/cm ²)	Voltage (volts)	Current (ma/cm ²)	Voltage (volts)	(hr)	(ks)	(N)	(N/m ²)	(mils)	(mm)
Substrate filled from 6061 series flat aluminum cathode											
I-1A	1	5.3	-25	3.4	-1500	44	158.4	3.0	0.39		
	1	3.0	0	3.9	-1500	38	136.8	2.7	0.35		
	1	4.7	0	4.6	-1000	179	644.4	3.2	0.42	84	2.13
	2	4.3	0	4.6	-1000	32	115.2	2.6	0.34	10	0.25
Substrate filled from 1100 series flat aluminum cathode											
I-2A	1	4.3	0	4.6	-1000	183	658.8	2.9	0.38	73	1.85
	2	4.3	0	4.6	-1000	32	115.2	2.6	0.34	10	0.25
Substrate overcoated with AMZIRC from flat cathodes											
I-1A and I-2A	3	3.5	0	4.2	-1000	22	79.2	2.5	0.33	17	0.43

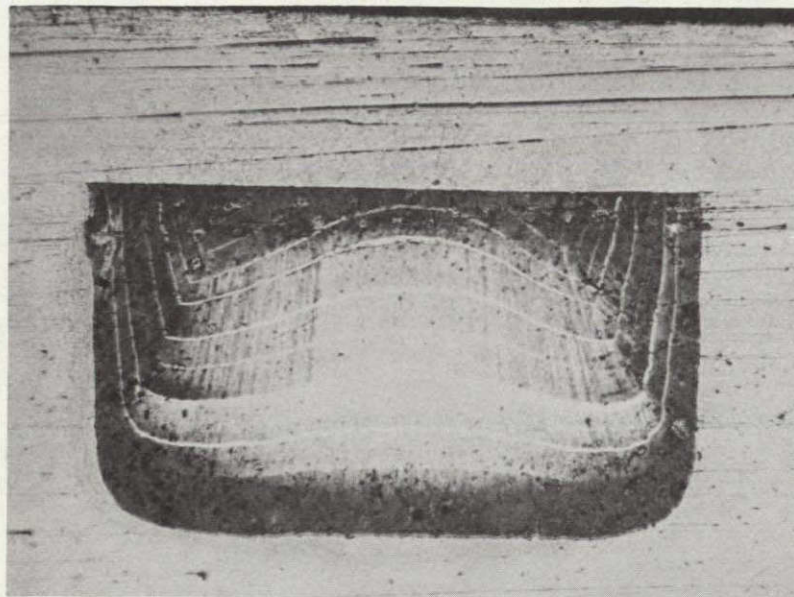
TABLE 4. VOLUME PERCENT OF GROOVE FILLED IN FLAT SUBSTRATES

Groove Width Depth	Substrate I-1A		
	0.102 cm	0.1278 cm	0.154 cm
0.102 cm	100 (porous ¹)	100 (porous)	100
0.127 cm	90	100 (porous)	100
0.154 cm	75	80	100
Substrate I-2A			
0.102 cm	100 (porous)	100	100
0.127 cm	90	100 (porous)	100
0.154 cm	75	75	90

¹ Estimated from photomicrograph of groove cross-section.

² Porous at top of filling due to propagation of corner originating defect.

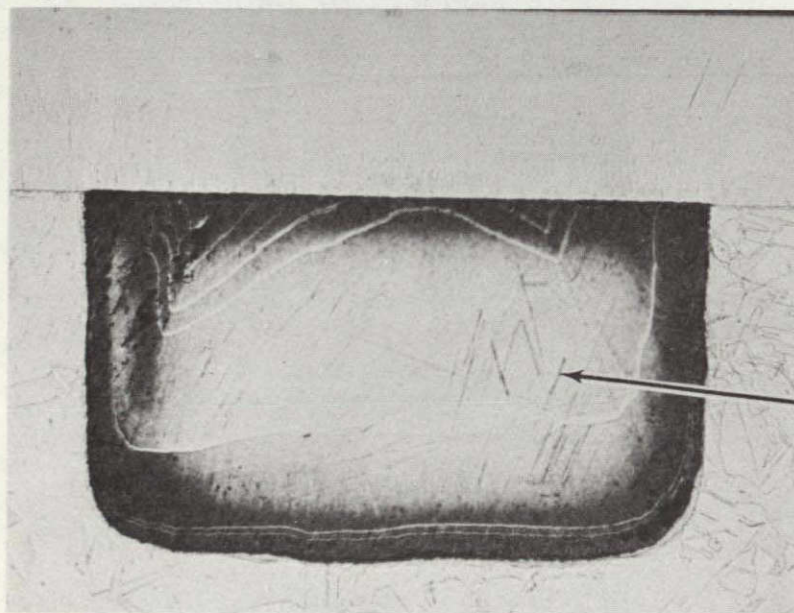
ORIGINAL PAGE IS
OF POOR QUALITY



Polishing
Scratch
(Typical)

Mag: 50X

Etched Filler In I-1A



Closeout
Layer

Interface

Rib

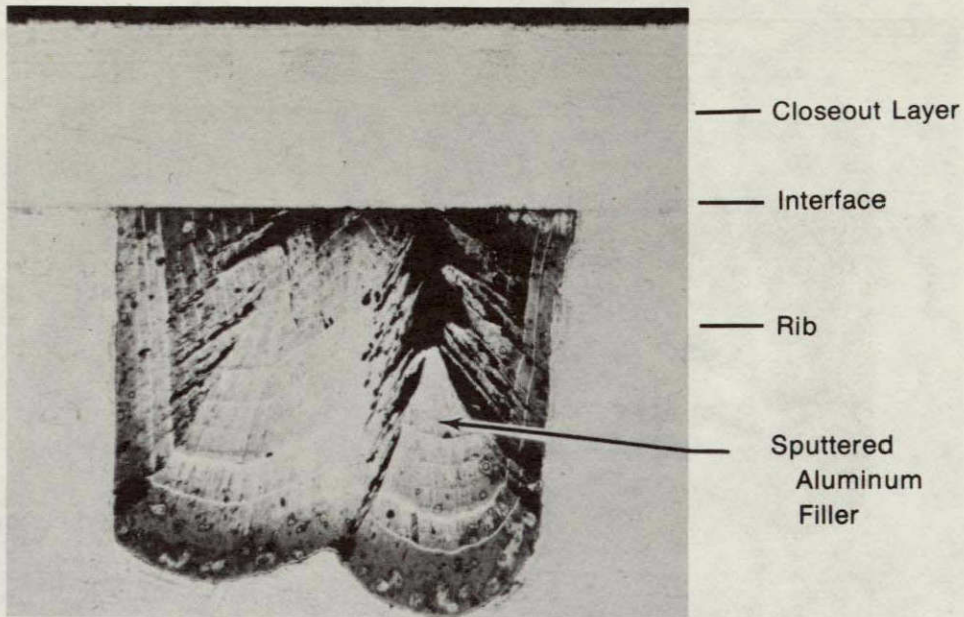
Sputtered
Aluminum
Filler

Mag: 50X

Etched Filler In I-2A

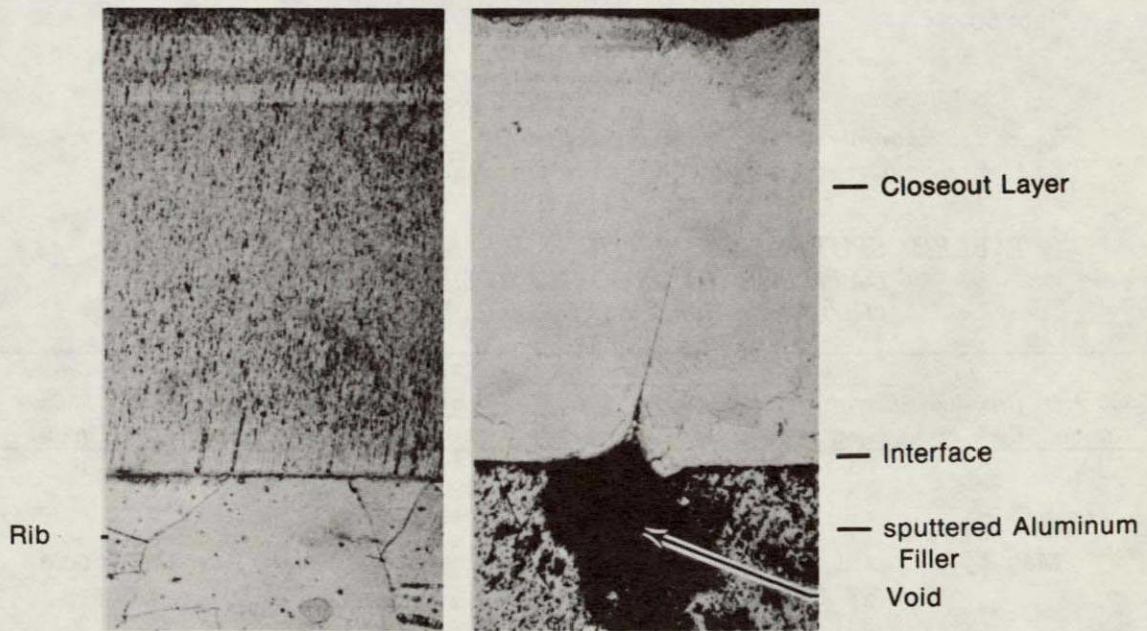
FD 104557

Figure 9. Microstructure of Closeout Layer Over Filled 0.152 cm Wide by 0.120 cm Deep Grooves



Mag: 50X

Etched Filler In I-1A

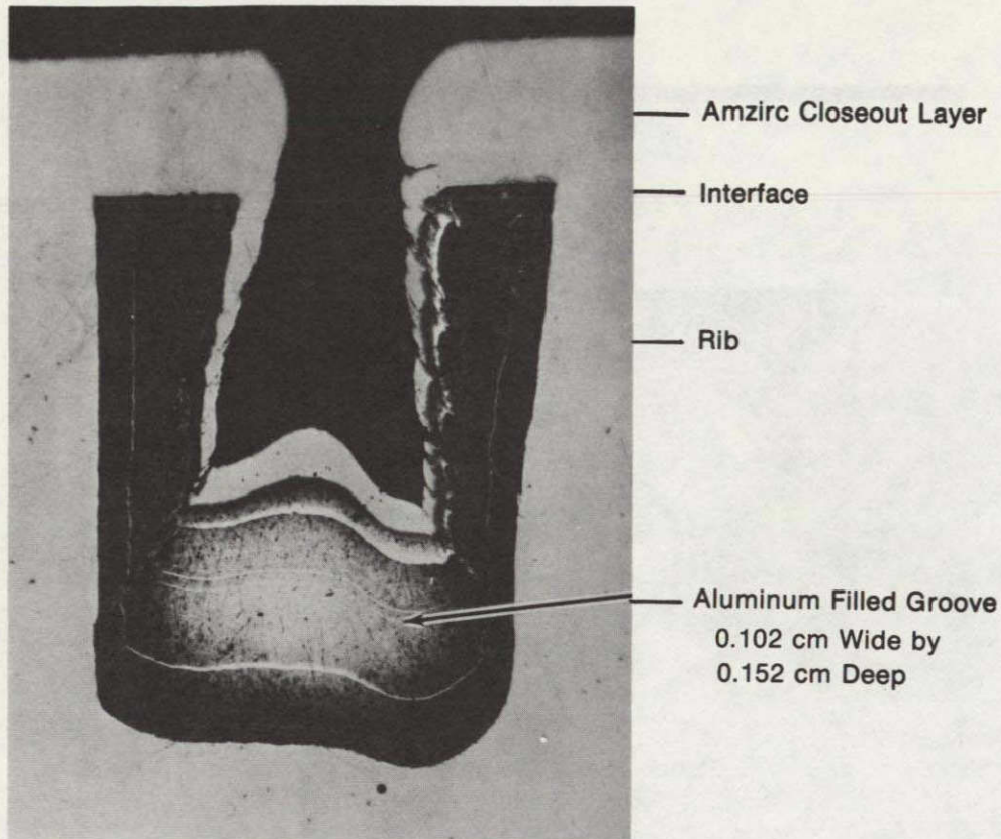


Mag: 250X

Etched Filler In I-2A

FD 104558

Figure 10. Microstructure of Closeout Layer Over Partially Filled (Porous) Grooves



Mag: 50X

Unetched

FD 104559

Figure 11. Example of Groove on Flat Substrate 1-2A Not Completely Filled with Sputtered Aluminum - Illustration of Filler Growth

TABLE 5. SPUTTER DEPOSITION PARAMETERS AND FILLING DATA FOR OD GROOVED CYLINDRICAL SUBSTRATES (1100 Series Aluminum Hollow Cathode, System No. 1)

Substrate Number	Deposition Cycle No. ¹	Substrate		Target		Time		Pressure		Coating Thickness ²		Groove Filling ³ (mils)
		Current (ma/cm ²)	Voltage (volts)	Current (ma/cm ²)	Voltage (volts)	(hr)	(ks)	(N)	(N/m ²)	(mils)	(mm)	
I-1	1	5.1	-25	4.8	-500	88	316.8	3.7	0.48	46	1.17	16
	2	4.3	-25	4.2	-500	111	399.6	3.7	0.48	52	1.32	32
	3	4.6	-25	4.4	-500	50	180	3.7	0.48	22	0.56	39 (filled)
	4	4.6	-25	5.0	-500	42	151.2	3.7	0.48	20	0.51	filled
	5	4.3	-25	4.5	-500	37	133.2	3.7	0.48	13	0.33	filled
I-2	1	3.3	0	4.5	-500	68	244.8	3.7	0.48	43	1.09	17
	2	3.1	0	4.4	-500	113	406.8	3.7	0.48	50	1.27	26
	3	3.6	0	5.1	-500	35	125	3.7	0.48	18	0.46	35
	4	3.6	0	5.0	-500	39	140.4	3.7	0.48	19	0.48	42 (filled)
I-10	1	4.1	-50	5.1	-500	169	608.4	3.7	0.48	75	1.90	20

¹ Aluminum machined back to substrate OD at end of each cycle. Cylinder orientation changed end for end on each reinstallation.

² Coating thickness calculated from increase in diameter at center of cylinder.

³ Height of aluminum deposit (bottom of groove to peak of deposit) in nominal 0.152 cm wide by 0.102 cm deep groove at the end of each deposition cycle (measured from 47 magnification photomicrograph of groove cross section for substrates I-1, I-2 and with depth probe for I-10).

As can be seen in figure 12 only substrate I-1 showed any practical filling. Grooves 0.127 cm and 0.152 cm wide by 0.102 cm deep and 0.152 cm wide by 0.127 cm deep were filled. However, the flat substrates showed that the narrower and deeper the groove the less the volume filled. Figure 13 shows each 0.152 cm wide by 0.102 cm deep groove at higher magnification. The groove filled at zero bias has a much greater corner defect problem and is not acceptably filled. The groove filled at -25v bias was filled during the third deposition cycle. The apparent bridging of the defect for the biased groove may be due in part to smearing of the aluminum during back machining. (Each back machining removed approximately 0.002 cm from the original substrate diameter.)

The expected reduction of wall growth in the -25v biased part was not observed. On the contrary, wall growth was greater for all groove sizes on the biased part. This is illustrated by the two 0.127 cm wide by 0.127 cm deep grooves shown on figure 14. Filling has effectively stopped in the unbiased groove during the second deposition cycle while the biased groove has continued filling through three deposition cycles despite the greater wall growth. As shown in table 5, nearly equal amounts of aluminum were deposited on each substrate per deposition cycle. The main effect of bias, then, is not back sputtering but most likely an ion plating type of mechanism where some fraction of the aluminum is ionized during transit from the cathode. The ionized material then follows the electric field lines into the substrate groove. All biased grooves were filled more rapidly than unbiased grooves although some of the narrow and deep biased grooves showed no net gain after deposition cycle No. 4.

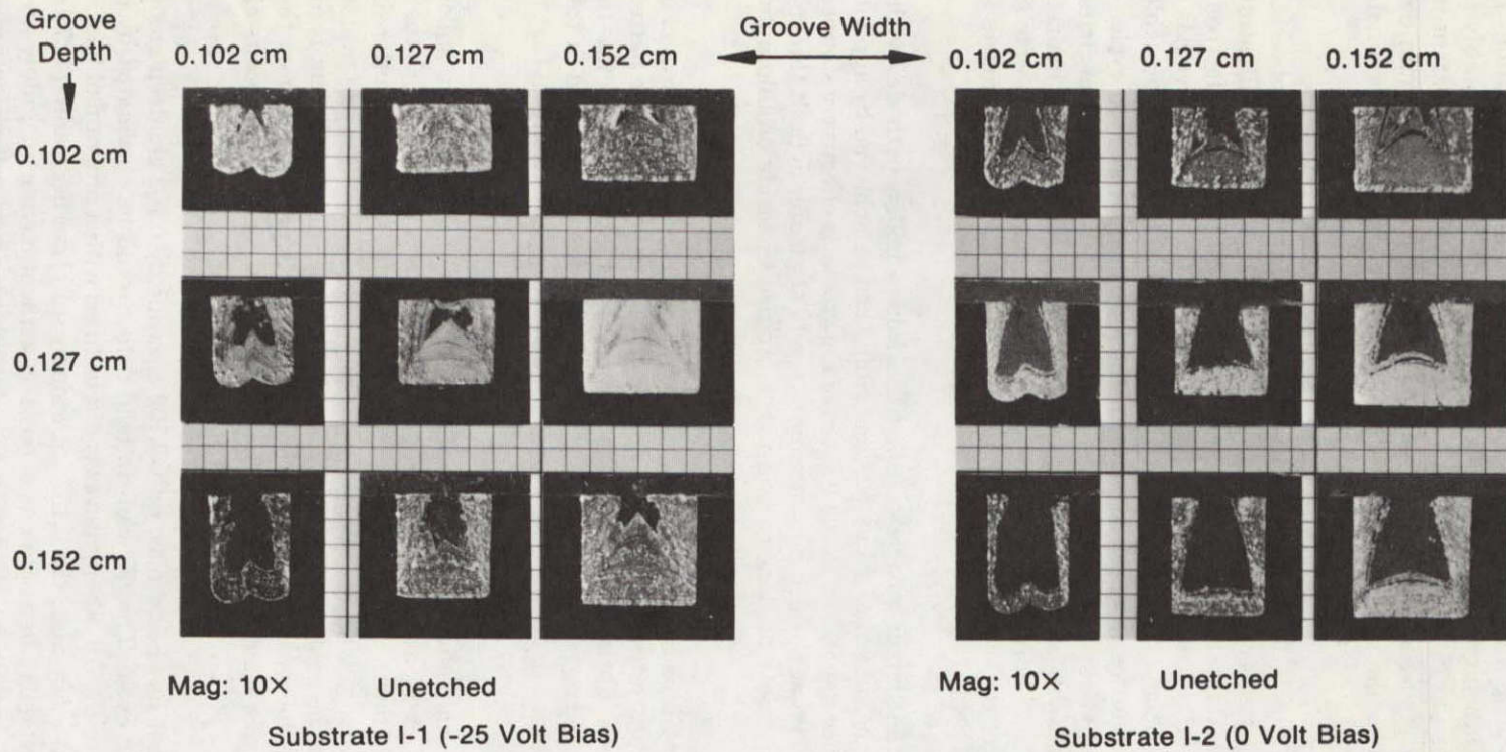
This work showed that larger grooves can be filled from a hollow cathode by the use of a negative bias voltage on the substrate. More efficient filling can be achieved by applying thinner layers, 0.051 cm or so, since deposition to the bottom of the groove is effectively stopped once the groove is shielded by wall growth which becomes more severe at greater deposit thicknesses. The machining between layers must be done carefully to minimize smearing of aluminum over the grooves.

The object of groove filling from post cathodes also was to determine the effect of bias on the degree of filling. Three substrates were grooved on the ID with the same groove pattern as used on the flat and OD grooved substrates. Substrate treatment after groove cutting was the same as for the hollow cathode filled substrates. Deposition parameters are summarized in table 6. The substrates were not machined to original thickness between every deposition run that made up a deposition cycle.

Figure 15 illustrates the salient qualities of filling from post cathodes. As for hollow cathode filling, more filling of all groove sizes for a given deposit thickness is achieved with the -50v bias on the substrate. Inward growth of the wall is also more rapid with subsequent intensification of the corner defects. Conversely, with 0v bias, the substrate grooves are filled less rapidly and the deposit on the bottom of the groove is less peaked and the corner defect problem is minimal. A new problem arises with the zero bias and that is a void defect is propagated from the rib wall-rib land interface. This was seen for all groove sizes. Also, at 0v bias, wall deposits exhibited a more open structure.

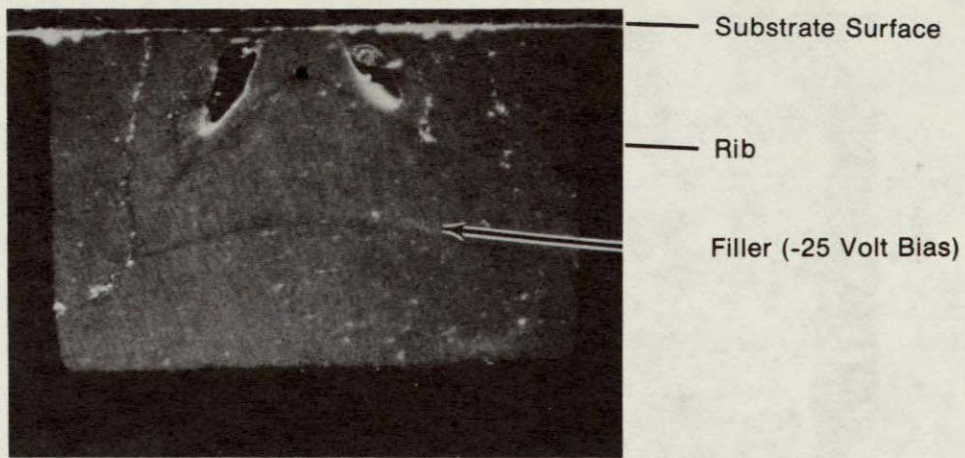
This work shows that for the 0v bias, only 0.152 cm wide by 0.102 cm deep grooves can be filled with one deposition cycle. The rib wall-rib land defect could be eliminated by machining past the original substrate ID. All other grooves could be filled with a program of backmachining and deposition cycles. At -50v bias, the 0.152 cm wide by 0.102 cm deep and 0.127 cm wide by 0.152 cm deep grooves could be filled with one deposition without having an unduly severe corner problem. All other grooves could be filled with a backmachining and deposition program.

A -25v bias may offer a good compromise between the 0v and -50v bias features. However, the deposition time at -25v (substrate I-1P) was too short to substantiate this conclusion.



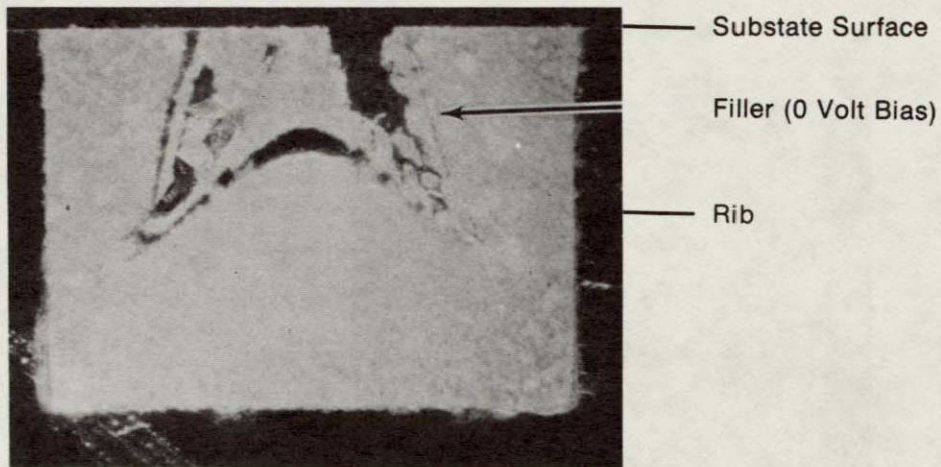
FD 104560

Figure 12. Filling Grooves by Sputtering from a Hollow Cathode - Effect of Bias



Mag: 47X

Unetched Filler In I-1

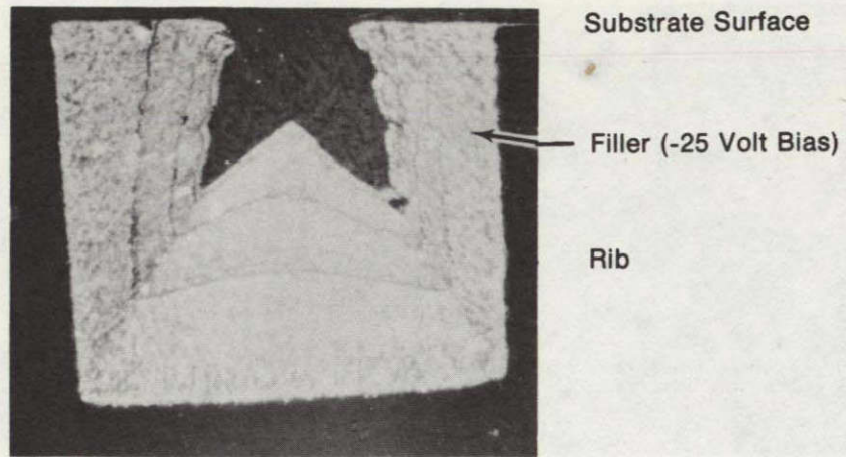


Mag: 47X

Unetched Filler In I-2

FD 104561

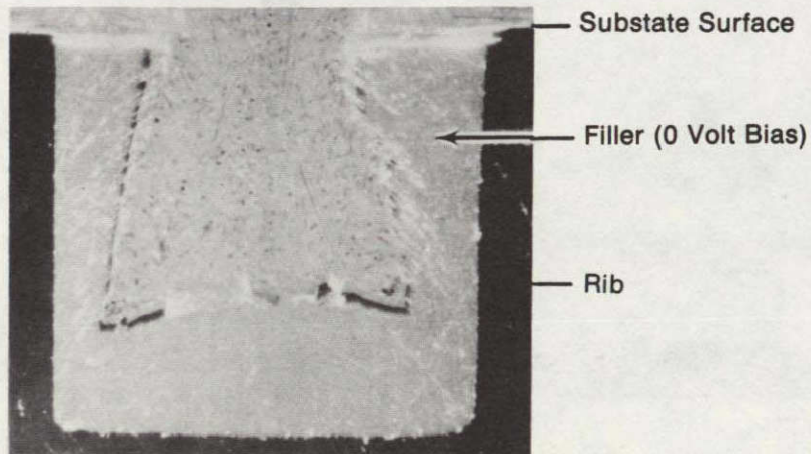
Figure 13. Typical Detail of Sputtered Aluminum Filling on 0.152 cm Wide by 0.102 cm Deep Grooves as a Function of Substrate Bias - Void Formation - Hollow Cathode



Mag: 47X

I-1

Unetched



Mag: 47X

I-2

Unetched

FD 104562

Figure 14. Typical Filling of 0.127 cm Wide by 0.127 cm Deep Grooves With Sputtered Aluminum as a Function of Substrate Bias - Hollow Cathode

TABLE 6. SPUTTER DEPOSITION PARAMETERS FOR ID GROOVED CYLINDRICAL SUBSTRATES (1100 Series Aluminum Post Cathode, System No. 2)

Substrate Number	Deposition Cycle No. ¹	Substrate		Target		Time		Pressure		Coating Thickness ¹		Groove Filling ²
		Current (ma/cm ²)	Voltage (volts)	Current (ma/cm ²)	Voltage (volts)	(hr)	(ks)	(N)	(N/m ²)	(mils)	(mm)	(mils)
I-1P	1	6.7*	-50	8.9	-400	5	18	5.1	0.66			
	2	5.2*	-25	6.0	-450	10	36	3.1	0.40			
	3	5.1*	-25	6.3	-500	15	54	2.5	0.33			
	4	6.7	-25	7.4	-450	5	18	3.6	0.47			
	5	6.5	-0	7.1	-500	13	46.8	3.7	0.48			
	6	6.3	-0	7.1	-500	7	25.2	3.7	0.48	23	0.58	19
I-2P	1	5.6	0	6.0	-500	15	54	3.4	0.44			
	2	5.3	0	5.2	-500	16	57.6	5.1	0.66			
	3	5.3	0	4.8	-500	36	129.6	3.6	0.47			
	4	7.2	0	9.4	-500	1	3.6	6.8	0.88			
	5	7.1	0	9.4	-500	5	18	6.0	0.78			
	6	7.5	0	9.4	-500	31	111.6	5.1	0.66			
	7	7.5	0	8.3	-500	72	259.2	5.1	0.66	50	1.27	31
I-3P	1	6.0*	-50	9.3	-500	1	3.6	6.5	0.85			
	2	5.1*	-50	7.8	-500	11	39.6	6.4	0.83			
	3	6.5*	-50	8.9	-500	123	442.8	6.1	0.79	35	0.89	30

*3 ϕ DC Power Supply

¹Thickness scaled from photomicrograph of groove cross section.

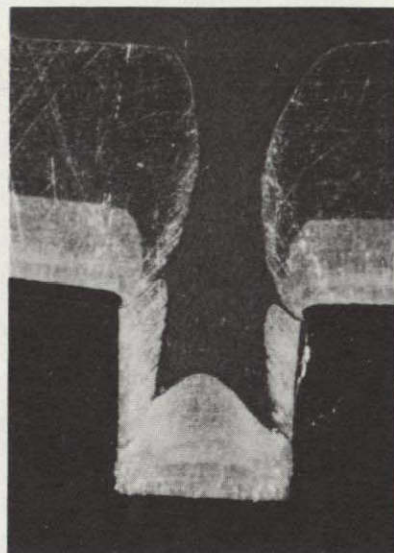
²Height of aluminum deposit (bottom of groove to peak of deposit) in nominal 0.152 cm wide by 0.102 cm deep groove measured from 47 magnification photomicrograph of groove cross section.

4. Aluminum Wire

Pressing aluminum wire into substrate grooves would have several advantages as a filling system. Filling would be relatively rapid, requiring only lathe machining of the filler back to the original substrate diameter after the wire laying operation. After closeout layer deposition, aluminum removal with NaOH solution would be facilitated by the channel which would run along each side of the wire at the bottom of the groove. (See figure 16.) A disadvantage of this technique from the vacuum point of view is that the same unfilled part of each groove is a virtual leak. This type of leak can lengthen pump down times and could possibly outgas excessively during sputter deposition.

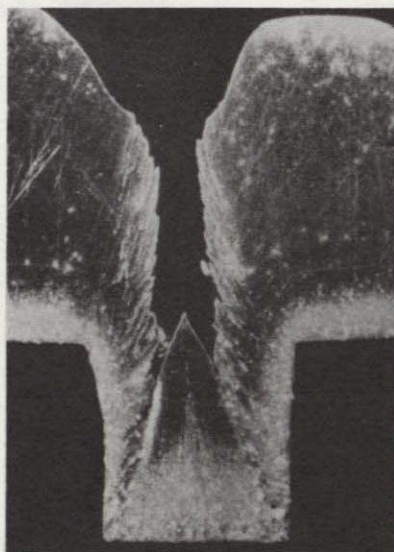
Straight pieces of type 1100 series aluminum wire, 0.159 cm in diameter were preformed into an approximate D shape in a die. The die consisted of a round bottom slot milled the length of a stainless steel block. The slot was 0.079 cm deep and had 0.079 cm radius. Aluminum wire laid in the slot was pressed to shape with approximately 2272 Kg (5000 lb) of force on a flat pusher block. The reasons for preforming the wire was to increase the wire diameter so the wire would be swaged into the substrate groove at the edges to preclude defect sites caused by bad filler to wall bond.

Prior to the filling operation, all substrates were vapor blasted, scrubbed with cleanser and rinsed in ethyl alcohol. The preforms were degreased in an ultrasonic Freon bath followed by ethyl alcohol rinse.



Mag: 20X

Unetched

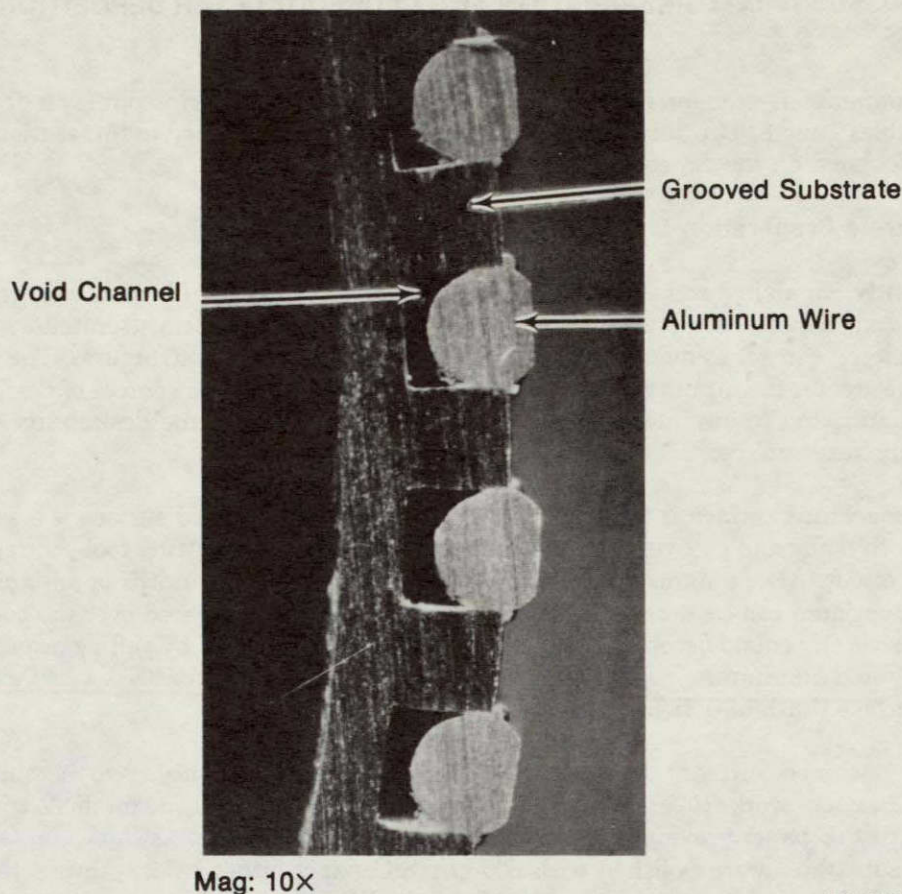


Mag: 20X

Unetched

FD 104563

Figure 15. Typical Filling of 0.127 cm Wide by 0.127 cm Deep Grooves With Sputtered Aluminum as a Function of Substrate Bias - Post Cathode



FD 104564

Figure 16. Aluminum Wire Before Machining

Substrate cylinders grooved on the OD were filled (on the ID) with CERROBEND to prevent cylinder deformation when the preforms were pressed into the grooves with 2272 Kg force on a flat pusher block. Substrates grooved on the ID were held in a retaining cylinder and the aluminum preforms were rolled individually into the grooves by passing the cylinder under a fixed arm with a roller at the end. An end view of substrate I-6 after the wire filling operation and removal of the CERROBEND is shown on figure 15. The aluminum is swaged into both sides of each groove and a large part of the groove is unfilled under each wire.

Substrate I-6 was the first wire filled substrate. Back machining to the substrate OD revealed a few places where wire to rib wall bonding was not complete. Substrate I-8 was filled with aluminum wire, back machined, and then the aluminum was vapor blasted away in each groove to a depth of 0.015 to 0.018 cm. Then aluminum was sputtered to refill each groove. The cap was sputtered on with -50v , 5.3 ma/cm^2 bias in System 1. (Cathode: -500v at 6.4 ma/cm^2 ; pressure 4.4 microns.) The sputtered aluminum was then machined back to the substrate OD. The reason for this capping operation was to provide a good filler to rib wall bond. Also, substrates I-6 and I-8 would show whether or not there was any significant difference in closeout layer growth over machined aluminum wire and machined sputtered aluminum. This will be discussed further in the Results Section of this report.

In view of the time needed to sputter fill grooves and of the problems associated with CERROTRU, aluminum wire was chosen as the filler for most of Task I work.

C. FINAL SUBSTRATE PREPARATION AND CLOSEOUT LAYER DEPOSITION PARAMETERS

The parameters used for Task I final substrate preparation and closeout layer deposition are given in tables 7 and 8. The data entries in these tables will be explained in this section along with a brief discussion on the expected significance of each parameter.

1. Substrate Preparation

Recently, Spalvins and Brainard (Reference 3) have shown effect of substrate surface roughness on deposit structure. Briefly, substrate surface defects (scratches, inclusions, impurities, etc.) can act as nucleation sites for the growth of modular structures. The rougher the surface, the greater the number of modular growths. The modes act as sources of cracks when the deposit is subjected to any mechanical loading. Their work shows the desirability of having a smooth substrate surface.

The machined surface is far from smooth. At best the machined surface is a succession of fairly smooth lands and grooves whose exact shape depend on the cutting tool configuration and the depth of cut. Also, a damage layer can extend to several thousandths of an inch below the surface. Aluminum can be dragged from the groove area and be smeared over the copper due to imperfect shearing cuts. Discontinuities in the surface can be caused by galling, especially in the softer sputtered aluminum or aluminum wire filler. The substrates for Task I had an estimated average surface finish of $0.81 \mu\text{m rms}$.

The machined surface, then, should receive additional smoothing to be suitable for a substrate. Previous work (Reference 1) in this program showed that of the methods tried, sanding with 600-grit SiC paper provided the best post machining treatment. As shown on table 7, most of Task I substrates were polished with 600-grit SiC paper either by lengthwise (by hand) or circumferential (on a lathe) sanding. The 1000-grit SiC paper was used on some substrates to provide a still smoother surface. The scouring powder scrubbing provided a final degreasing. Ethyl alcohol was used to remove water traces left from flushing the scouring powder.

2. Sputter Cleaning

As mentioned in connection with groove filling work, sputter cleaning is necessary to achieve a good deposit to substrate bond. The machined and sanded surface is still a rather rough and dirty surface. The aluminum has a thin oxide layer, copper oxides may fill defects on the rib land surface, and atmospheric gases are absorbed on the surface. Although an atomically clean surface cannot be obtained by sputter cleaning in these experiments, surface dirt can be reduced to a level that allows good adhesion.

Typically, after system pumpdown to $u\text{hV}$, the triode discharge is established, and a -25 volt bias is applied to the substrate for 5 minutes. At the beginning of this cycle, system pressure rises several microns, showing that the primary effect of the low energy ion bombardment is outgassing of the substrate surface*. Since the threshold energy for sputtering copper and aluminum by krypton ions is 15 and 16 volts respectively (Reference 4), small amounts of metal may also be sputtered. Also, on the initial application of voltage to the substrate, arcing may occur on the substrate due to local heating and subsequent electrical breakdown at aluminum oxide sites. Substrate heating by an arc can produce pressure bursts.

*Outgassing is caused by sputtering of the adsorbed gas species and by substrate heating.

TABLE 8. SUMMARY OF TASK I CLOSEOUT DEPOSITION PARAMETERS

ORIGINAL PAGE IS
OF POOR QUALITY

Substrate Number	Substrate		Cathode		Deposition Time ¹		Maximum Deposit Thickness		Maximum Deposition Rate		Pressure	
	Current ma/cm ²	Voltage volts	Current ma/cm ²	Voltage volts	hr	ks	mm	mils	nm/sec	mils/hr	N	N/m ²
Hollow Cathode												
I-3	8.6*	-25	7.4	-500	12.5	45					2.9	0.37
	9.1*	-50	7.4	-500	12	43.2	0.64	25	7.2	1.02	4.2	0.54
I-4	3.7	-50	3.3	-500	5	18					8.8	1.13
	3.9	-50	3.7	-500	21	75.6	0.30	12	3.2	0.46	5.3	0.68
I-5	6.9*	-50	5.8	-500	40	144					4.8	0.61
	8.6*	-50	6.4	-500	42	151.2	2.36	93	6.2	0.88	4.8	0.61
I-6	3.6 ¹	-50	3.4	-500	11	39.6					2.7	0.35
	4.1	-50	3.9	-500	42	151.2	0.81	32	4.2	0.60	4.4	0.56
I-7	8.2	-50	7.1	-500	56	201.6					4.3	0.55
	8.0*	-50	6.8	-500	40	144	1.60	63	4.6	0.66	4.8	0.61
I-8	9.1	-50	7.9	-500	16	57.6					3.6	0.46
	9.3	-50	7.8	-500	9	32.4					4.6	0.59
	8.6	-50	6.7	-500	22	79.2					3.7	0.47
System Vented												
	8.6	-50	6.8	-500	17	61.2					3.9	0.50
	8.9	-50	6.4	-500	64	224.4	2.41	95	10.3	1.46	4.1	0.53
I-9	8.3*	-50	6.0	-500	40	144					4.2	0.54
	8.0*	-50	6.0	-500	16	57.6	1.27	50	6.3	0.89	3.7	0.47
I-11	7.1	-25		-500	15	54					2.3	0.30
	6.9	-25		-500	10	36					3.4	0.44
System Vented												
	8.0	-25	6.2	-500	10	36					4.4	0.56
	7.4	-25	5.7	-500	16	57.6	1.40	55	7.6	1.08	4.0	0.51
I-12	3.3	-50	4.0	-500	88	316.8	1.02	40	3.2	0.45	7.6	0.97
I-13	4.1	-50	5.3	-500	47.5	171					4.1	0.55
	2.8	-50	3.6	-500	77	277.2	1.32	52	2.94	0.42	3.7	0.47
Anode voltage dropped from 40 to 30v												
I-14	4.6	-50	3.1	-500	10	36					5.4	0.69
	4.0	-50	2.6	-500	3	10.8					3.4	0.44
	4.1	-50	2.7	-500	7	25.2					3.7	0.47
	3.7	-50	2.6	-500	10	36					2.7	0.35
	4.0	-50	2.7	-500	18	64.4					3.7	0.47
	3.9	-50	2.6	-500	15	54					3.3	0.42
	3.9	-50	2.6	-500	20	72					3.2	0.41
	4.0	-50	2.6	-500	14	51.4					3.6	0.46
	4.0	-50	2.6	-500	18	64.4					3.6	0.46
	4.4	-50	2.8	-500	12	43.2	2.44	96	6.35	0.76	4.2	0.54
	Post Cathode											
I-4P	5.3*	-50	7.1	-500	15	54					5.4	0.69
	5.3*	-50	6.7	-500	10	36					5.9	0.76
	5.3*	-50	6.7	-500	11	39.6					6.4	0.82
	6.1*	-50	6.1	-500	48	172.8					7.5	0.96
System Vented												
	5.9*	-50	7.8	-500	16	57.6					6.8	0.87
	5.9*	-50	7.4	-500	24	86.4	2.97	117	6.60	0.94	6.5	0.83
I-5P	5.3*	-25	7.8	-500	14	51.4					5.4	0.69
	5.6*	-25	6.3	-500	84	302.4	2.34	92	6.60	0.94	6.2	0.80
I-6P	5.6*	-50	6.8	-500	2.25	8.1					4.8	0.61
	7.1*	-50	8.1	-500	10	36					7.4	0.75
	6.4*	-50	7.8	-500	15	54					11.2	1.44
	6.7*	-50	7.3	-500	52	187.2	2.28	90	8.00	1.14	5.4	0.69

* 3 ϕ DC power supply

¹ Substrate's sputter cleaned at least 0.9 kiloseconds at -50 volts between each deposition run.

² Argon pressure

At the end of 300 seconds the system is again evacuated to uhv. The reason for this is that the system atmosphere no longer is pure krypton but a complex mixture of krypton and outgassed species which can effectively stop cleaning and which may recontaminate the surface with chemical compounds due to the catalytic action of the discharge plasma.

After pumpdown to uhv, the discharge is restarted and the negative voltage again applied to the substrate. This second cleaning cycle is usually done with -50 volts on the substrate. Metal is being removed. Once the aluminum oxide layer is removed from the aluminum filler, aluminum is sputtered at about one-half the rate of copper. During this cycle additional substrate heating takes place which promotes further substrate outgassing. Cleaning was usually carried on until the system pressure stabilized. Sputter cleaning of AMZIRC for too long a time may increase surface roughness due to a low sputtering yield (atoms/ion) for the unevenly distributed zirconium bearing clusters. The zirconium could effectively shield the underlying copper from sputtering and the resultant effect would be a surface of sharp cones.

The substrate current density given in the tables (ma/cm^2) is computed by dividing the total current to the substrate by the area of the substrate and holder being bombarded. This was done to allow a rough comparison between post and hollow cathodes and between the different systems. This does not imply that the substrates receive a uniform ion density over the surface.

For the range of ion energy used for sputter cleaning, material removal varies nearly linearly with the number of ions (measured by substrate current) and with the ion energy (measured by substrate voltage).

It should be noted that in these experiments neither substrate current density nor sputtering time is a quantitative measure of sputter cleaning. To make sputter cleaning quantitative, the substrate surface would have to be reproducible on an atomic scale and the substrate current density would have to be reproducible. Neither of these requirements could be met for these experiments. Separate experiments would have been needed to characterize a surface as a function of low energy ion bombardment. Such experiments were outside the scope of this program. The conclusion is that if a deposit adheres, then sputter cleaning can be declared sufficient. The converse is not true; if a deposit to substrate bond fails, insufficient sputter cleaning may be only part of the problem and other failure mechanisms may dominate.

3. Substrate Bias

Previous work (Reference 1) in this program showed that deposits sputtered onto cooled substrates (in a magnetically supported diode discharge) had open grain boundaries with subsequent low mechanical strength. The substrate temperature had to be raised nearly to the melting point of copper to obtain a dense columnar structure. The origin of the columnar structure has been discussed by Thornton (Reference 5) for OFHC copper sputtered from a hollow cathode. The open columnar structure is attributed to low adatom and bulk mobility at low temperatures. Crystallites start growing from disconnected islands on the substrate. The growing crystallite can shade neighboring crystallites from the flux of coating material to the extent that boundaries between crystallites are actually voids equivalent to fine cracks. The shadowing effect would be found even on atomically flat substrates. Of course, large scale shadowing would be caused by any raised feature on a substrate surface.

Low energy ion (or neutral) bombardment is one way to obtain a dense structure at low substrate temperatures. In the experiments performed for this program, deposition is started by increasing the cathode voltage and adjusting the negative voltage (bias) on the substrate to the desired level. The ion bombardment caused by the bias voltage is able to greatly influence the deposit structure. But not enough work has been done to allow an accurate prediction of just what effect a certain bias will have on a deposit in a particular sputtering system. However, some general effects should be found in all systems.

First, a certain fraction of the depositing material is resputtered. The amount resputtered depends on the ion energy and density. Obviously some of the resputtered metal leaves the substrate, but in a model proposed by Bland, Kominiak and Mattox (Reference 6) some metal also is resputtered forward, i.e., metal is sputtered from the sides of the growing crystallites and deposited in the shaded zones between crystallites. The net effect is a smoothing of the deposit as sputtering progresses which effectively eliminates the open grain boundaries. Below a certain ion density, for example in some magnetically maintained discharges (Reference 1), the fraction of material resputtered will be too low to be effective.

Traditionally, biasing of a substrate has been done to keep the deposit clean during deposition. Gaseous impurities arriving at the substrate have a high yield for sputtering by inert gas ions. Patten, McClanahan and Johnston (Reference 7) have shown that, in an uhv system a negative bias reduced the oxygen level in OFHC copper sputtered deposits. Oxygen is always present in an unbaked vacuum system due to the disassociation of water vapor by the discharge. Oxygen is a usual impurity in OFHC and AMZIRC copper cathodes and can be released to the system during sputtering. The amount of oxygen present in the system will depend on system outgassing rate, on gas throughput, and on the effectiveness of the system geometry for gas pumping (covering of gas by sputtered material).

A third effect is that biasing can cause the inert sputtering gas to be buried in the deposit. The exact mechanism for gas trapping is not known but some possible mechanisms are discussed by Lee and Oblas (Reference 8). However, many experiments have shown that the gas content of the deposit is a minimum for a certain range of bias voltage. Increasing the bias voltage beyond this range will cause a sharp increase in gas content.

The above discussion shows that it should be possible to find a bias that will produce a relatively gas free, dense deposit -- dense for strength and gas free for weldability.

In table 8, the substrate current density was calculated as explained above for sputter cleaning. A bias current is registered at 0 volts (power supply reading) by the nature of the triode discharge. All electrodes in a triode system have a characteristic voltage to current relationship. Zero current is obtained at a small positive voltage in these systems.

4. System Geometry

The geometry of systems used in this program is shown on figure 1. The word geometry refers to the size, distance between, electrical potential, and the shape of system components. The effect of some of these geometric aspects on closeout layer thickness will be discussed.

The closeout layer thickness distribution along the length of a 12.7 cm long substrate in a hollow cathode is also shown on figure 1 for each system. Thicknesses have been normalized to the center thickness and each broad curve shows the range of measurements for several depositions. The deposits for systems 1 and 2 are thicker at the bottom (end near the filaments) than at the top. System 2 geometry differs from system 1 only in the orientation of the filaments and in the length of the ground potential casing around the filaments. The discharge cannot be maintained in system 2 at anode voltages much below 40 volts. Consequently, higher cathode and substrate current densities are maintained and cathode erosion at the bottom of the system 2 cathode is greater than for the system 1 cathode. Another consequence of the higher anode voltage is a greater sputtering rate for ground potential surfaces in system 2. The stainless steel filament holder is sputtered fairly rapidly in system 2, but not in system 1 which runs well at anode voltages of 30 volts or lower. In system 3 the cathode is sputtered more rapidly at each end than in the center. The discharge can be maintained at voltages as low as 20 volts. Operation of system 3 will be illustrated further in the discussion for substrates I-13 and II-1.

Gill and Kay (Reference 9) have shown by experiment and calculation how the deposit thickness varies along the length of a substrate in a magnetically supported diode discharge. The hollow cathode was nearly the same length as the substrate. The deposit was thickest at the center and decreased smoothly to about 20% of the center thickness at the ends of the substrate. This is the deposit shape when the cathode is evenly sputtered over its length. To get an evenly thick deposit over the whole substrate, the cathode has to be made longer (still having even sputtering) or the shorter cathode has to be sputtered at a greater rate at both ends. In previous work on this program (Reference 1) the deposit thickness distribution was improved in the magnetically supported diode discharge by positioning the magnetic field coils and by increasing cathode length.

The distance between system components can greatly affect the substrate deposit by affecting the degree of shielding. A ground potential piece placed close to a cathode (approximately $\frac{1}{8}$ -inch) effectively stops cathode sputtering (shields the cathode) at the surface behind the piece. In these systems the substrate also shields the cathode to some extent. Also, if the cathode and substrate are not perfectly coaxially aligned, one side of the cathode will be shielded more than the other. The resultant uneven sputtering of the cathode will cause a variation in deposit thickness around the substrate circumference.

If the cathode is shielded by the substrate, the substrate is also shielded by the cathode and bias current density will be reduced accordingly. A consequence of this mutual shielding is that the shadowing problem can be amplified by having a greater fraction of deposit material arriving from an obtuse angle just when the bias current density is too low to control the structure.

In systems 1 and 2, the shielding causes the cathode to be sputtered rapidly at the level of the top of the shield ring. This can contribute to the increased deposit thickness at the bottom of the substrate. The increased sputtering is apparently caused by the electric field between the top of the ring and the cathode as is observed in sputtering from a flat cathode in a diode discharge.

If the substrate bias voltage is raised sufficiently high, another geometric effect known as the hollow cathode discharge may be introduced. Two cathodes at the same voltage and at the proper separation will draw a much higher current for a given voltage than two single cathodes at the same conditions. The greater electron population in the hollow cathode discharge causes a much greater percentage of sputtered species to be ionized or excited (as in a spectroscopic light source). The extent of this effect in the triode discharge at the spacings used in these systems is not known. The apparent evidence for ion plating mentioned in the section on groove filling may indicate the start of a hollow cathode effect.

Systems 1 and 2 were used for post cathode work. The hollow cathode was replaced with a substrate holder and a post cathode installed. The rest of the geometry stayed the same. The remarks for the hollow cathode apply also to the post cathode. However, the shadowing effect is greatly reduced since a greater percentage of sputtered material arrives at the substrate at an angle more nearly equal to 90 deg. All deposits for post cathode work were thicker at the center of the substrate. Post cathodes were eroded more at the bottom end (free end) and at the center than at the top.

5. Cathode Voltage

In the triode discharge ion energy is very nearly equal to the cathode (or substrate) voltage. Increasing cathode voltage increases the energy of the bombarding ions. Since the sputtering yield (atoms/ion) increases with ion energy, the sputtering rate is increased with cathode voltage. The yield has a nonlinear dependence on ion energy, rising rapidly from the threshold to several hundred eV and then increasing more slowly with the higher energies. Note that in the triode discharge cathode current remains constant with increasing voltage from about -25 volts.

Another effect of cathode voltage is difficult to assess. Experiments have shown that ions approaching a cathode surface can be neutralized by Auger electrons and reflected at high energy. Lee and Oblas (Reference 8) have shown experimentally that the argon entrapped in their triode sputtered tungsten films (ground potential) increased from 0.5 wt% at -1000v to 2.5 wt% at 2000v. They postulated that much of this gas load was trapped high energy neutrals.

6. System Pressure (Gas Density)

The model in Thornton's paper (Reference 5) also shows (schematically) the effect of argon gas pressure on deposit structure. This model shows that, at low substrate temperatures, the columnar growth habit grows increasingly porous up to 30×10^{-3} torr for a hollow cathode. This pressure effect is reduced for the post cathode. The mechanism proposed to explain the increase in porosity is the decrease in adatom mobility due to the increased adsorption of the inert gas at higher pressures. Again Lee and Oblas have an interesting curve in their paper which shows that the argon content of their films reaches a peak at about 5 microns (-1500v cathode voltage).

The effect of pressure is difficult enough to correlate from one system to the next when a pressure gage somewhat remote from the discharge (by necessity) is the only indicator. What is really needed is a measure of gas density in the discharge. The correlation of gage reading to actual gas density in the discharge requires a separate set of experiments. A constant gage pressure reading is no guarantee of a constant gas density in the region between a cathode and substrate.

7. Deposition Rate

The deposition rates listed in table 8 are calculated by dividing the maximum deposit thickness in each experiment by the time needed to make the deposit. This rate is of course a net rate, i.e., the difference between the rate of arrival of sputtered material and the rate at which it is resputtered from the substrate by low energy ions and high energy neutrals. A correlation of rate to closeout layer structure would require a knowledge of these two rates which cannot be determined per se in these experiments.

The net rate can be increased by increasing the cathode current density or cathode voltage. The cathode current density can be increased by raising the anode voltage and/or filament temperature. Net rate can also be increased by cutting the substrate bias voltage. Raising the net rate by increasing system power will increase the temperature of the deposit and other system components. Structure may be affected by this temperature increase as well as by the increased outgassing which would occur in an unbaked vacuum system.

A complete study of the effects of discharge parameters on closeout layer structure would require Langmuir type probe work to determine ion and electron energies and densities and mass spectrographic work to determine the relative abundance of species (metal and gas) arriving at the substrate surface. This type of work is outside the scope of this program. Also, the interrelation of sputtering parameters precludes doing the ideal experiment in which one variable at a time is changed.

D. RESULTS

Task I results will be presented and discussed in this section. First, general remarks pertaining to the burst, tensile, etc., test results will be made. Then filler system performance will be evaluated. And, finally, the effects of deposition parameters on closeout layer bond strength and structures will be given.

1. Test Results

Most of the closeout layer thicknesses were within $\pm 15\%$ of the average coating thickness over the substrate circumference. A few variations were greater than $\pm 15\%$ and will be discussed in the text. This variation was caused by deviations of the substrate and target from perfect coaxial alignment. Variations in thickness along the substrate length are due mainly to system geometry and are shown for each system on figure 1. The maximum closeout layer thickness for each substrate has been tabulated in table 8.

Burst test specimens were cut where the closeout layer thickness permitted and obvious debonding or cracking did not occur. Results of hydrostatic burst tests are given in table 9. The test rig was sensitive to slight out of tolerance machining of the cylindrical specimens. The force on the closeout layer bond is equal to the pressure given since the rib lands and grooves were the same width. Specimens from post cathode depositions were not tested because of an out of tolerance machining of the test rig and some specimens.

TABLE 9. BURST TEST RESULTS FOR
TASK I HOLLOW CATHODE
SPUTTERED SPECIMENS

Substrate Number	Hydrostatic Burst Strength		
	(psi)	(MN/m ²)	
I-4	1,800	12.4	Failed
I-7	5,500*	37.8*	DNF
I-7	10,000	68.8	DNF
I-9	9,900	67.3	DNF
I-11	10,000	68.8	DNF
I-13	9,000	61.9	Failed
**Wrought AMZIRC	6,500*	44.7*	DNF

DNF=Did Not Fail
 * O-Rings failed at the indicated pressures
 ** Holes drilled into conventional wrought AMZIRC and pressurized.

Tensile specimens were cut from areas remote from the substrate grooves whenever the closeout layer was thick enough. All sputtered AMZIRC had a much higher tensile (table 10) strength than the wrought AMZIRC (wrought data in table 15 in Task II).

VICKERS microhardness for substrates and sputtered closeout layers are given in table 11. No correlation was found between hardness and deposition rate or distance from the substrate for hollow cathode closeout layers. The lower hardness near the substrate for most post cathode deposits was attributed to difference in structure and not to substrate heating. This structure difference for post cathode deposits will be discussed in detail.

The zirconium content of several substrates and closeout layers was measured. Representative values will be given in the text. Substrate and cathode zirconium content varied widely from the averages given, clearly showing that the zirconium in wrought AMZIRC is in clusters of various sizes. The zirconium in sputtered deposits was evenly dispersed. An electron microprobe was used to determine bulk zirconium content and interface trace elements which will also be given in the text.

The adequateness of substrate sputter cleaning will be judged by whether or not the closeout layer is debonded. If a bond fails, though, other mechanisms may have entered which could not be studied in this program.

TABLE 10. TENSILE PROPERTIES OF AMZIRC CLOSEOUT LAYERS (ROOM TEMPERATURE)

Substrate Number	0.2% Offset Yield Strength		Tensile Strength		Elongation (%)
	(ksi)	(NM/m ²)	(ksi)	(NM/m ²)	
Hollow Cathode					
I-5	93.4	642.6	118.8	817.3	15.0
I-5	86.2	593.1	120.1	826.3	12.6
I-7	87.5	602.0	127.9	880.0	10.2
I-8	85.4	587.6	127.5	877.2	3.6
I-8	90.3	621.3	128.5	884.1	8.8
I-9	91.9	632.3	125.7	864.8	14.8
I-9	93.1	640.5	124.4	855.9	12.6
Post Cathode					
I-4P	95.3	655.7	95.3	655.7	13.0
I-4P	117.5	808.4	118.2	813.2	4.0
I-5P	115.2	792.6	115.2	792.6	4.0
I-5P	117.6	809.1	117.2	806.3	4.0

TABLE 11. VICKERS HARDNESS FOR AS DEPOSITED AMZIRC CLOSEOUT LAYERS FOR TASK I

Substrate Number	Substrate Material	Substrate Hardness VPN	Closeout Layer Hardness ¹ VPN
Deposited from flat cathodes			
I-1A	AMZIRC	118-133	174-210
I-2A	AMZIRC	110-127	153-220
Deposit from hollow cathodes			
I-3	OFHC Copper	105	² 237-270
I-4	OFHC Copper	105-110	223-236
I-5	OFHC Copper	93-100	210-220
I-6	OFHC Copper	110	220-237
I-7	OFHC Copper	110-114	220-225
I-8	OFHC Copper	110-116	237-243
I-9	AMZIRC	118-127	210
I-11	AMZIRC	112-123	215-236
I-12	AMZIRC	118	231-243
I-13	AMZIRC	118-121	231-256
I-14	AMZIRC	116-118	³ 285-294
Deposit from post cathode			
I-4P	AMZIRC	121	⁴ 256
I-5P	AMZIRC	118	231-243
I-6P	AMZIRC	-	⁵ 237-248

¹ Range of hardness found over entire closeout layer.

² Hardness near substrate 132-137.

³ Hardness near substrate 243-249.

⁴ Hardness near substrate 183.

⁵ Hardness near substrate 196-205.

All sputtered structures were dense and, except for substrate I-14, closed. The growth habit was columnar for all hollow cathode deposits. Post cathode deposits all started columnar (very narrow crystallites) but at some point in the deposition turned into what will be called a fine structure in which the columnar habit could not be detected. All microstructures are viewed parallel to the substrate length (longitudinal view).

2. Filler System Performance

The effectiveness of each of the filler systems will be judged by the ease and completeness of filler removal and by the effect of the system on the closeout layer structure and bond strength. The bond strength will show how well the filler system holds up under machining and sputter cleaning. All sputtering work reported in this section was done in a hollow cathode.

Substrates I-3, -4, and -5 were filled by the CERROTRU sputtered aluminum cap system. Misindexing during backmachining of the CERROTRU left a layer of CERROTRU on the side of almost every groove on each substrate. This resulted in a thin line of CERROTRU being present on the substrate surface running the length of each groove. Sputter cleaning before closeout layer deposition provided enough heat to melt the CERROTRU which was then able to wet the complete substrate surface. Bi and Sn were present at the rib lands of substrates I-3 and -5 in sufficient quantity to give a dense X-ray image in the electron microprobe. Lesser amounts of both elements were detected 180 degrees from the grooves. The indexing on substrate I-4 was somewhat better and only trace amounts of Bi and Sn were found at the interface.

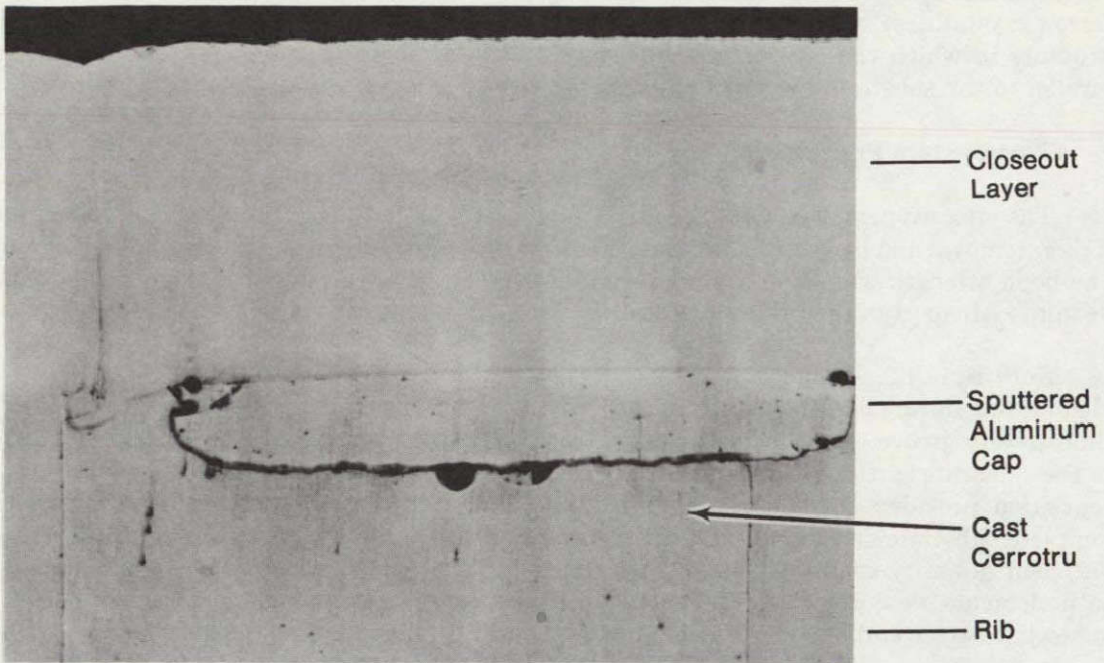
Typically, closeout layer cracking was observed over areas of exposed CERROTRU. Such a crack can be seen in figure 17 which shows a correctly and incorrectly indexed groove. A typical microstructure is shown (for I-5) in figure 18. The growth of small cracks and "leaders" is stopped by the action of the substrate bias, and the closeout layer structure is the same over grooves as over the rib lands. The origin of the cracks and leaders will be discussed later in the analysis of substrate I-7.

A burst test specimen machined from I-4 failed at 1800 psi. The closeout layer cracked in an area remote from the grooves indicating that the closeout layer was poorly bonded due to either insufficient sputter cleaning or to the CERROTRU contamination.

Removal of the CERROTRU from substrate I-3, -4, and -5 required repeated heating of the substrates to 400°F (481°K). The sputtered aluminum cap was leached in 6.5 molar NaOH solution at 355°K. This removal technique left a CERROTRU residue over most of the groove. Previous work (Reference 1) showed that etching in a concentrated HCl solution would have been necessary to completely remove all of the CERROTRU.

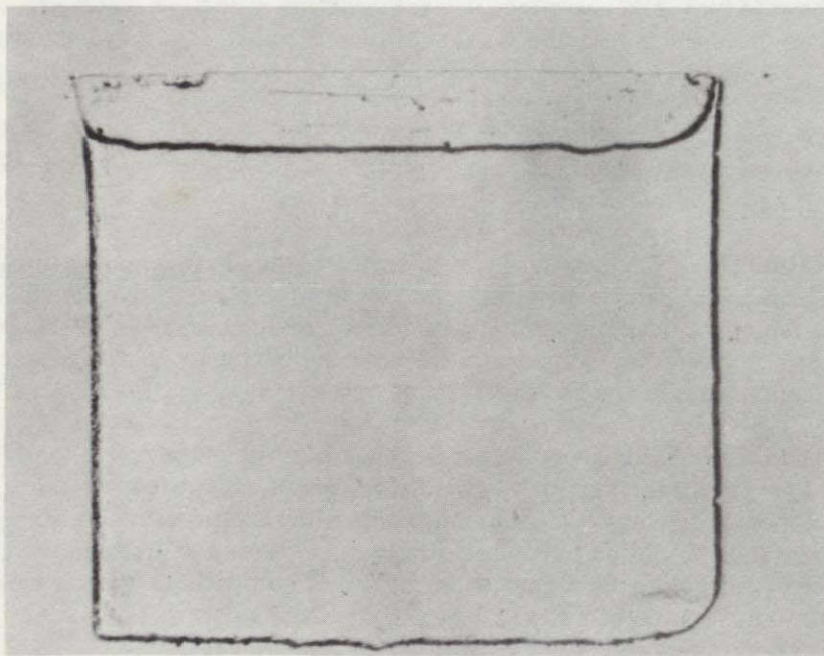
This work on capped CERROTRU showed that the back machining operation would have to be perfectly indexed to avoid winding up with CERROTRU at the substrate interface. This is beyond the capability of most machinery. One possible solution to this problem (if a step in the groove walls could be tolerated) would be to cut back the slot for the cap wider than the groove width (either straight or beveled sides) and sputter in the aluminum without sputter cleaning. The sputtered aluminum cap would then have to be effectively bonded to the rib wall by a bidirectional machining operation on a lathe.

CERROTRU encased in sputtered aluminum (substrate I-7) proved to be a better filler system than the capped CERROTRU. Some misindexing still exposed the CERROTRU to the closeout layer. However, cracking was much less severe than for I-3, -4 and -5. The interface contained 0.12 wt% Bi and 0.03 wt% Sn. The detection of 0.10 wt% of Fe and 0.08 wt% of Cr indicated that stainless steel sputtered from the filament holder was reaching the substrate as shown previously in figure 2b. No aluminum was detected in the interface.



Mag: 50X

Incorrectly Indexed

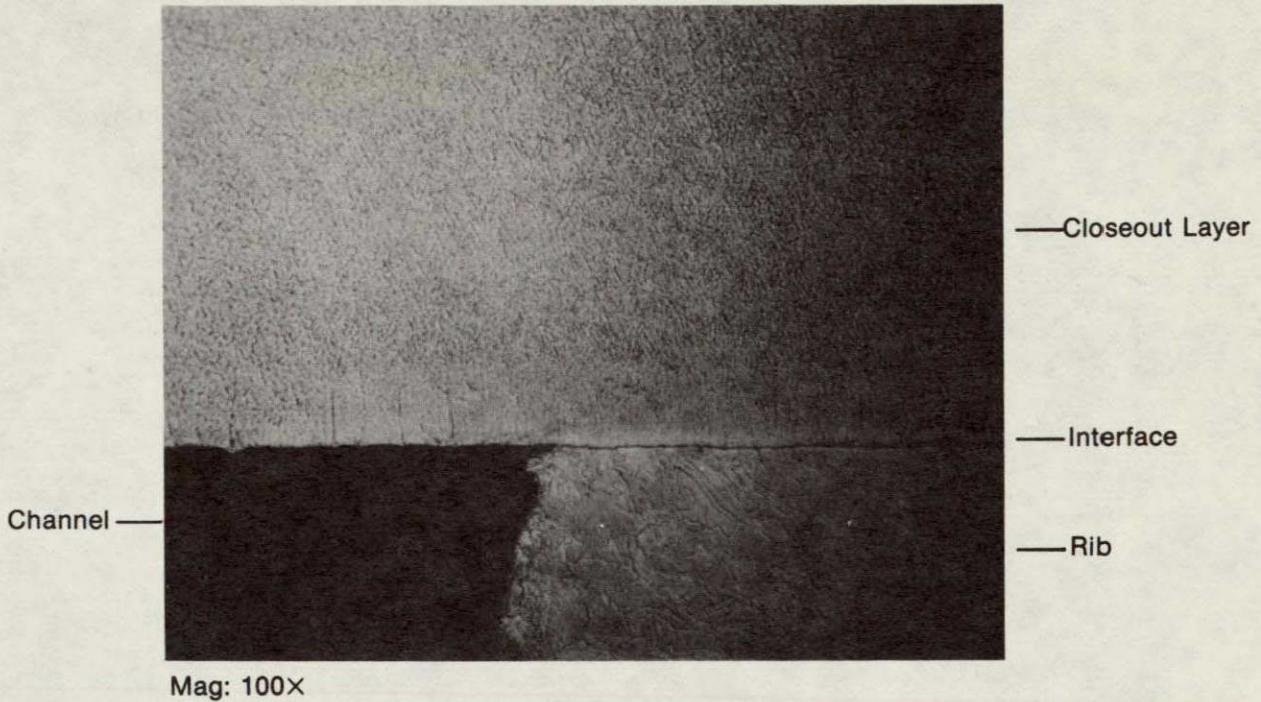


Mag: 50X

Correctly Indexed

FD 104565

Figure 17. Closeout Layer Over Correctly and Incorrectly Indexed Cast CERROTRU® - Substrate 1-4



Mag: 100X

Etched - Filler Removed

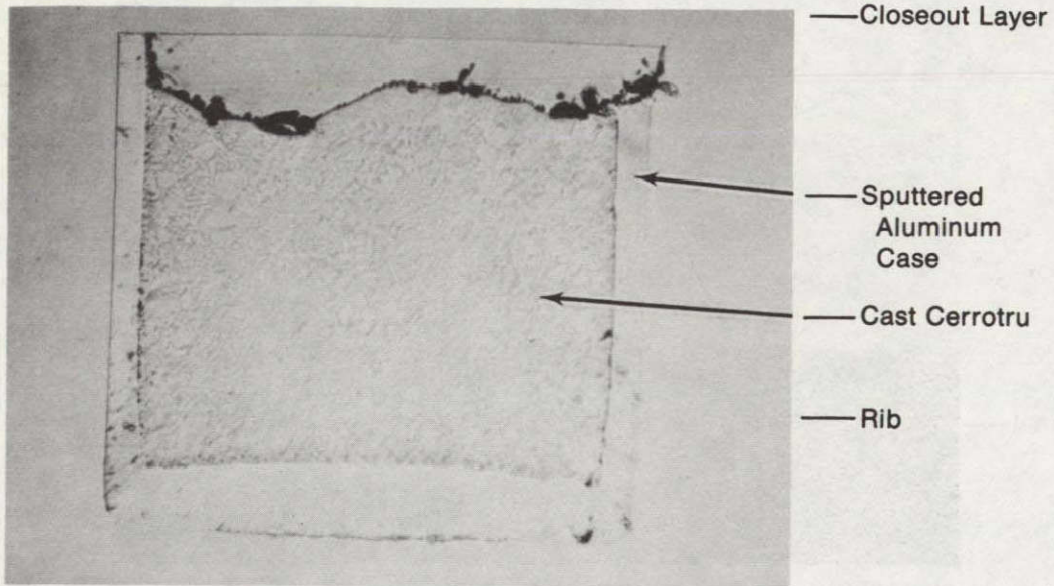
FD 104566

Figure 18. Typical Closeout Layer Microstructure Over Capped Cast CERROTRU® Filler - Substrate I-5

Figure 19 shows a properly and improperly indexed groove. No large cracks were noted over the exposed CERROTRU. A typical microstructure for I-7 is shown on figure 20. Closeout layer structure is the same over the grooves and rib lands. Small cracks and leaders are closed off in the first 0.0051 cm of deposit. A single phase dc bias power supply was used during the deposition of the first half of the closeout layer and a 3 ϕ dc supply for the second half (not shown on figure 20). No difference in structure was noted.

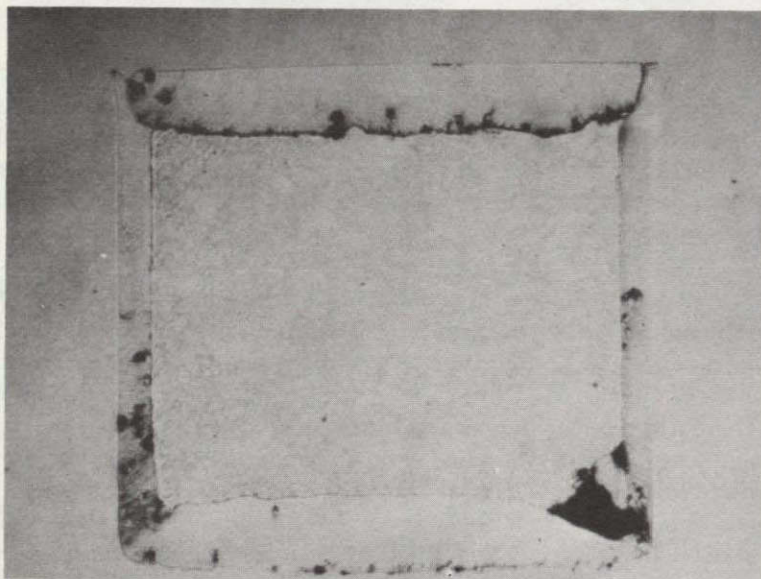
An example of the effect of a large defect on a substrate surface on closeout layer structure is shown in figure 21. Here the defect did not start at the surface, but was started after 0.0051 cm of the closeout layer had been deposited. Growth of the deposit is nearly perpendicular from the walls of the depression. As was seen in groove filling work with sputtered aluminum, this outward growth eventually shields the bottom of the depression from the sputtered material and a void is formed. This is a large scale example of the shadowing discussed previously for the hollow cathode geometry. The growth habit of the closeout layer over this defect is influenced through the entire deposit thickness. This particular defect may have originated from a pock in the CERROTRU that was too deep to be completely filled by the sputtered aluminum cap. The leader structure referenced on figure 20 is believed to be simply the growth habit over much smaller defects. This type of void defect would probably have a detrimental effect on low-cycle fatigue strength of the closeout layer.

Two burst test rings were cut from I-7. One specimen did not burst at 10,000 psi (68.8 MN/m²). The other specimen also did not burst but at 5500 psi (37.8 MN/m²) a test cell O-ring failed due to slight out of tolerance dimensions of the specimen.



Mag: 40X

Incorrectly Indexed

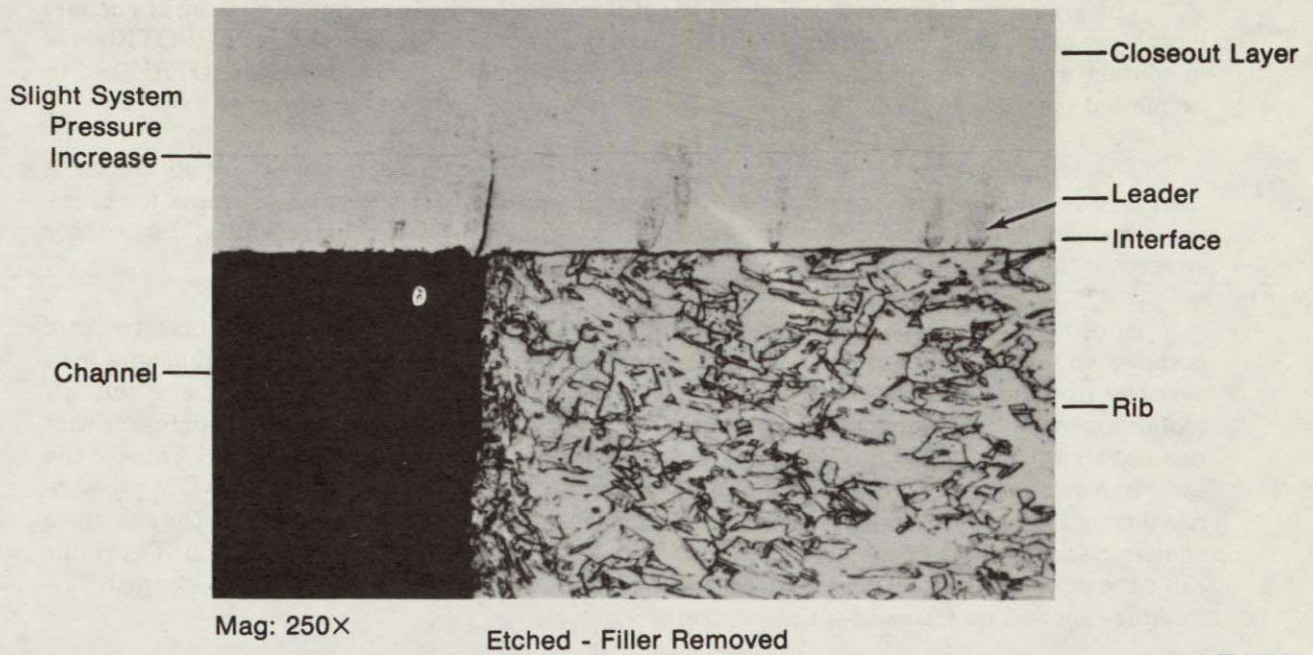


Mag: 40X

Correctly Indexed

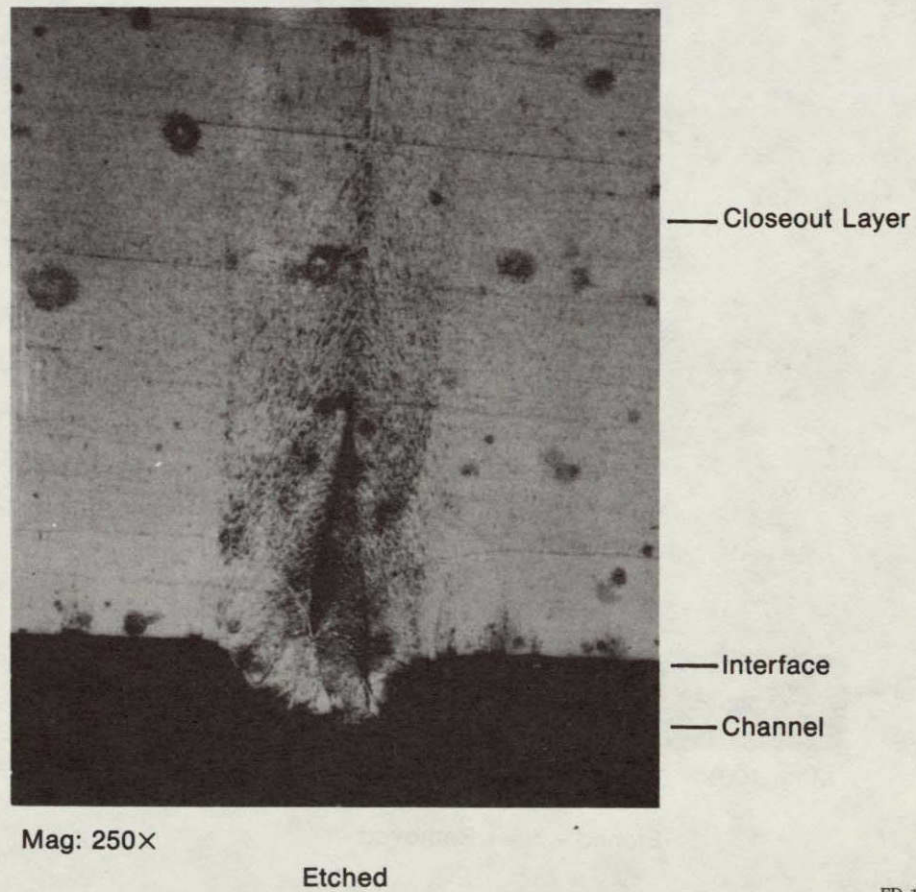
FD 104567

Figure 19. Closeout Layer Over Correctly and Incorrectly Indexed Encased CER-ROTRU® - Substrate 1-7



FD 104568

Figure 20. Typical Closeout Layer Microstructure Over Encased CERROTRU® -Substrate 1-7



FD 104569

Figure 21. Growth of Closeout Layer Over Large Defect On Surface of Filler - Void Formation Substrate 1-7

The aluminum liner (with CERROTRU still in) was leached at a rate of 6.03 cm of channel length per hour. The CERROTRU then fell out of the grooves except where the CERROTRU was in contact with the closeout layer due to misindexing. At these points, the CERROTRU had to be melted out.

The reliability of the encased CERROTRU system could be improved by sputtering a thicker aluminum liner which would eliminate problems due to misindexing. Elimination of the sputter cleaning cycle before cap deposition could also be considered if the cap could be tightly swaged to the aluminum walls during the final machining operation.

Substrate I-6 was the first of the aluminum wire filled substrates. A typical microstructure is shown on figure 22. The closeout layer structure has more leaders over the aluminum wire than over the rib land. This is caused by the greater roughness of the machined surface in the soft aluminum wire. The large crack apparently originated from an area where the aluminum wire was not tightly swaged to the groove wall. Some of the microstructure detail may be due to the excessive outgassing (and low throughput of system 1) observed by steady slight system pressure rise during the first 5 hr of deposition. The system was pumped to 10^{-5} microns and the substrate sputter cleaned for 1.8 kiloseconds at -50 volts before proceeding with the deposition. The result can be seen on figure 22. The growth of the large crack and leaders was effectively stopped. The interface showed no traces of stainless steel.

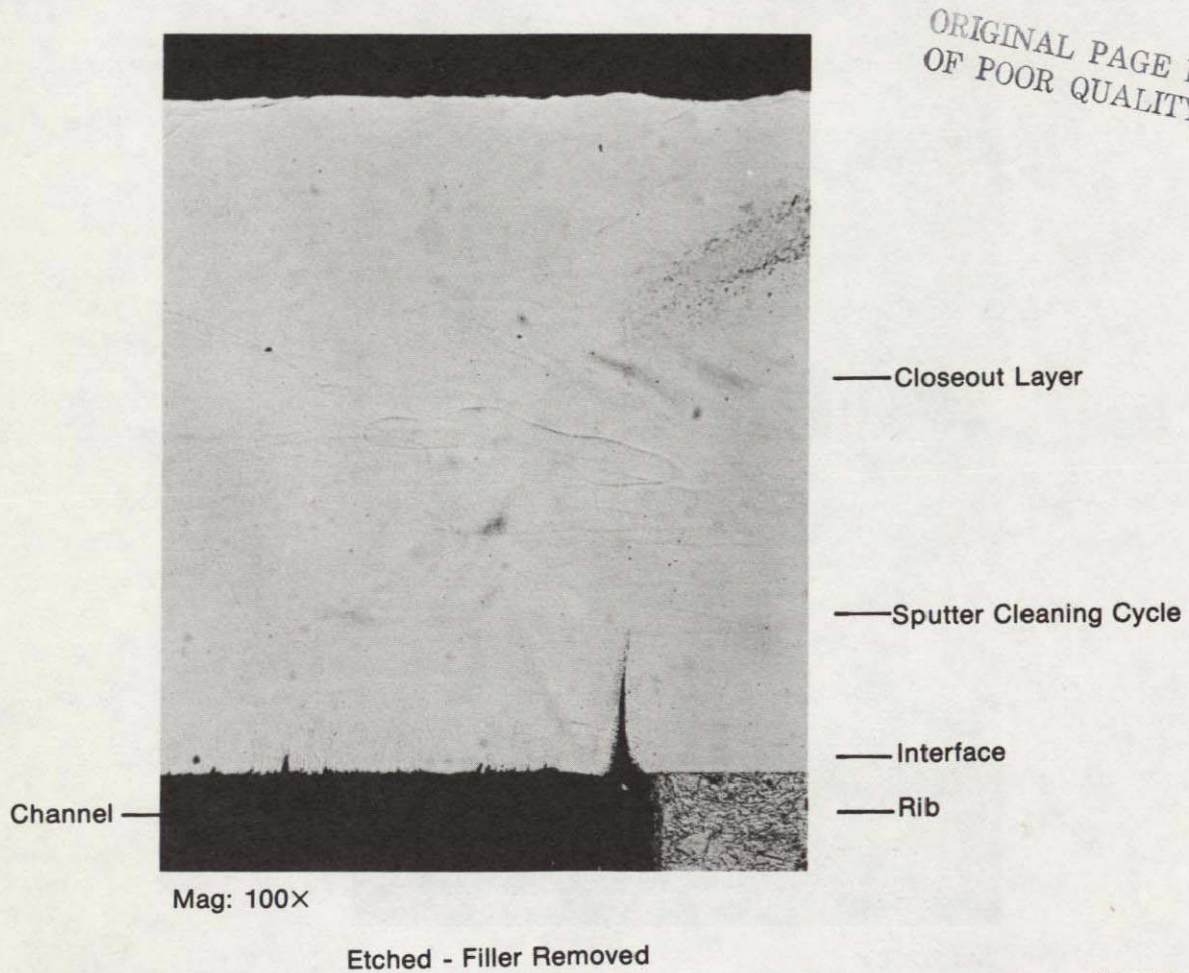


Figure 22. Typical Microstructure of Closeout Layer Over Aluminum Wire Filler - Substrate I-6

The aluminum wire was leached by the 6.5 molar NaOH solution (355°K) at a rate of 5.22 cm of channel length per hour. No traces of aluminum could be found in the channels.

A sputtered aluminum cap over the aluminum wire in substrate I-8 was used to test structure difference between a closeout layer over sputtered aluminum and a layer over aluminum wire. The sputtered aluminum had a smoother machined surface. Closeout layer microstructure is shown in figure 23. Only a slight difference in structure was seen over the grooves and no cracks were found. The difference in structure compared with I-6 is undoubtedly not due to the sputtered aluminum alone, since substrate preparation was quite different. Substrate I-8 was sanded with a finer grit SiC paper and the sputter cleaning cycle was four times as long. The interface had a trace amount of stainless steel.

The capped aluminum wire appears to be the best of the filler systems actually closed out. The sputtered aluminum cap machines to a smoother surface and makes a good bond with the walls of the grooves. This minimizes the number of defect-caused growths and ensures a homogeneous closeout layer structure. The wire and cap combination is rapidly leached from the grooves leaving no residue, and very little of the filler material is present in the interface. The only disadvantage may be the outgassing from the unfilled part of each channel.

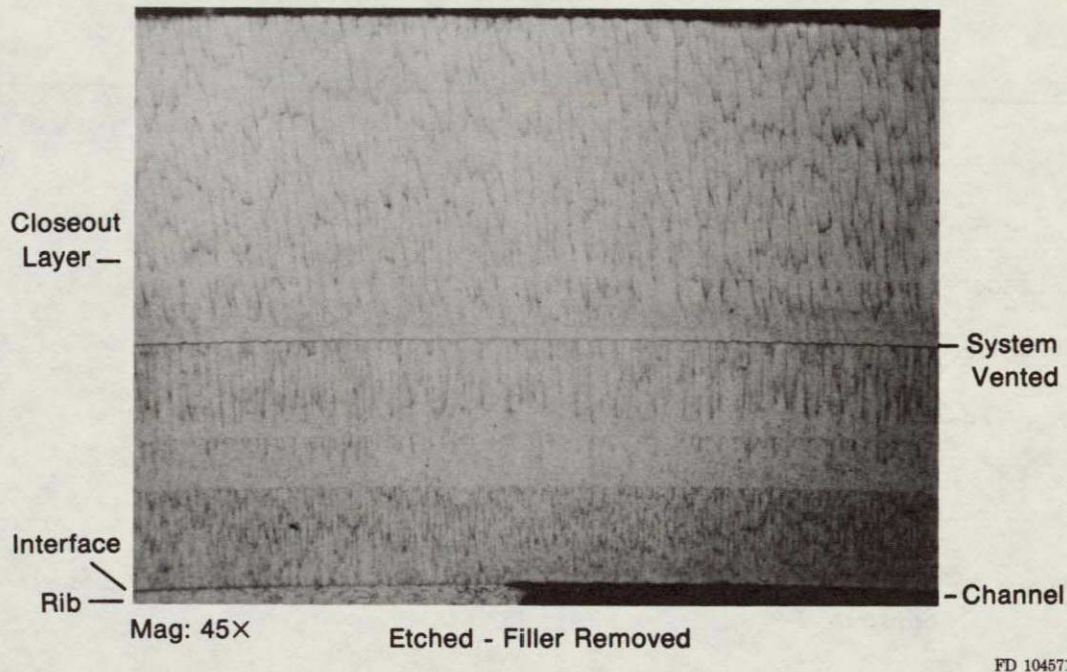


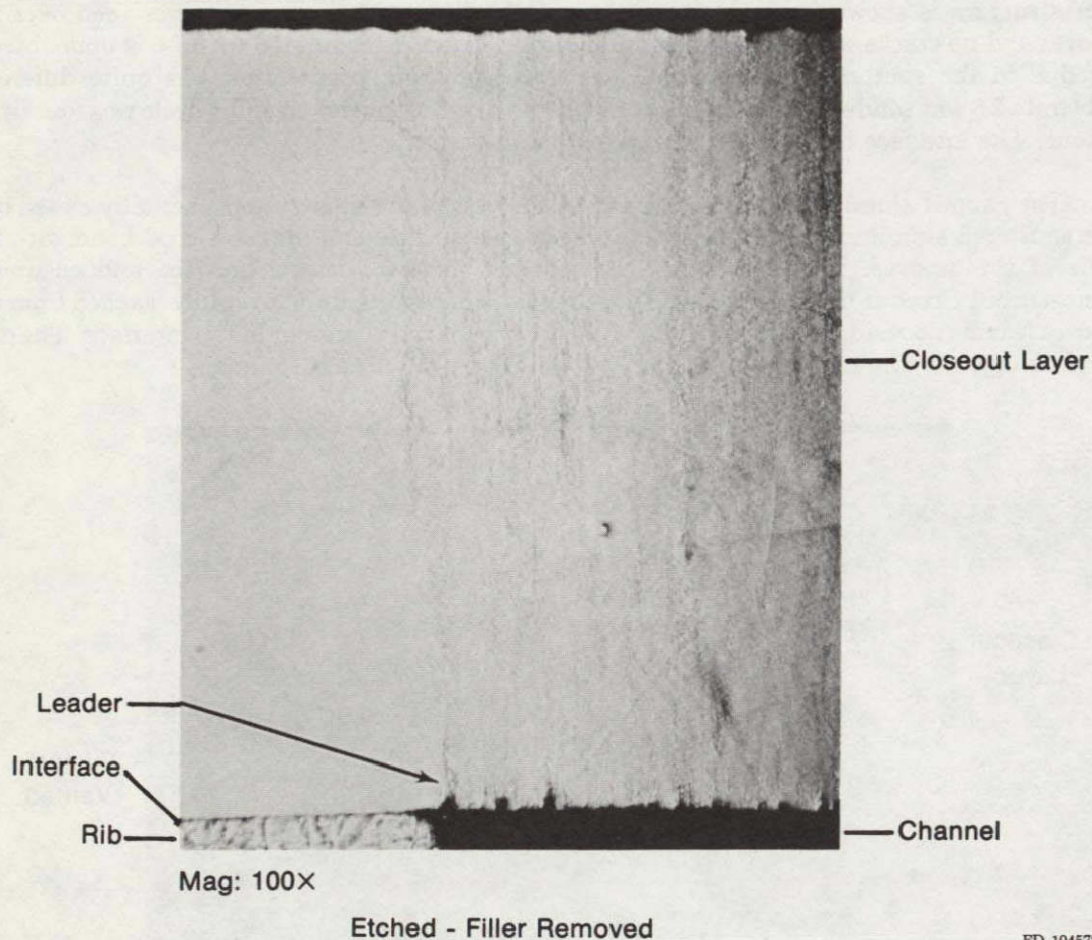
Figure 23. Typical Closeout Layer Microstructure Over Capped Aluminum Wire - Substrate I-8

3. Deposition Parameter Effects

The effects of sputtering parameters on closeout layer bond and structure were studied with wire filled substrates overcoated from both hollow and post cathodes. The effect of substrate surface preparation, sputter cleaning and bias current density will be demonstrated. All substrates were AMZIRC.

The first of the hollow cathode depositions was made onto substrate I-9. No cracks were observed over the grooves. However, the leader structure was present over the grooves and at

isolated points over the rib lands as shown on figure 24. The leaders definitely start at pits or other imperfections and the greater density over the filler shows again that the machined aluminum wire surface is rougher than the copper land surface. The leader structure apparently had no effect on closeout layer strength, since tensile properties were excellent and the burst test specimen did not fail. Traces of stainless steel and 0.4 wt% aluminum were found in the interface.



FD 104572

Figure 24. Typical Microstructure Over Aluminum Wire Filler - Origin Of Leaders - Substrate I-9

Substrate I-11 was sputter cleaned for only 5 minutes at -25 volts to determine if the sputter cleaning cycle was responsible for the aluminum content of the interface. I-11 and 0.2 wt% aluminum in the interface which indicates that the aluminum is not due to the sputter cleaning cycle, but most likely due to smearing from the machining. It is interesting to note that shortly after the start of deposition a system leak developed limiting system ultimate to $1 \text{ by } 10^{-3}$ microns. Deposition was deliberately continued to determine the effect of poor vacuum on closeout layer structure. The microstructure of the closeout layer, figure 25, shows that a smooth substrate finish reduces the number of leaders over the grooves and rib lands. The burst test specimen held to 10,000 psi (68.8 NM/m^2) but a tensile specimen could not be machined due to separation of the outer layer of the deposit. The substrate bias was apparently effective in keeping the deposit clean, but the interface was not cleaned after the system had been vented between deposition runs with the -50 volt, 30-minute cleaning cycle.

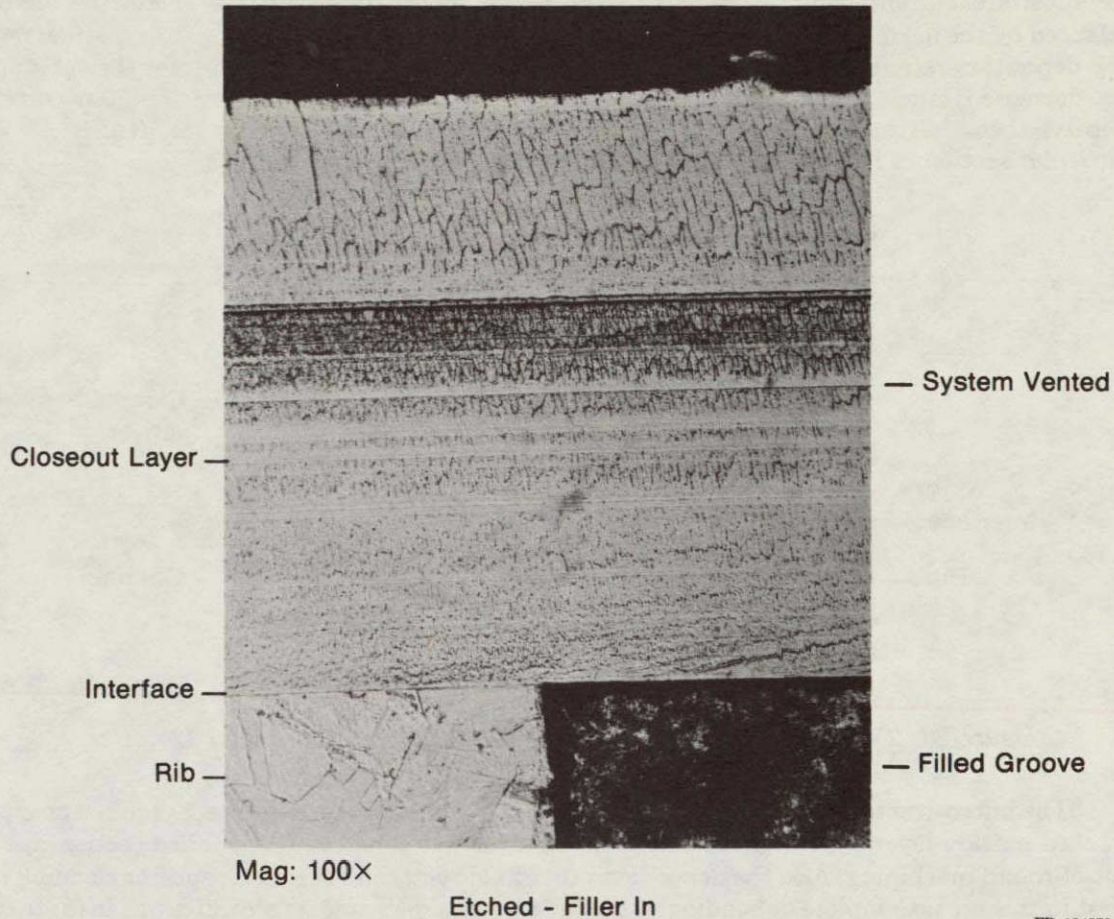


Figure 25. Microstructure Over Surface Sanded With 1000 Grit SiC Paper - No Leaders - Substrate I-11

Substrate I-12 was the first of the fully grooved wire filled cylinders to be closed out. A typical microstructure is shown in figure 26. No cracking was observed and closeout layer growth habit was slightly different over the grooves due to the rougher aluminum surface finish. No burst test sample was cut due to debonding of the closeout layer from the rib land. Insufficient sputter cleaning (low substrate current density) was the probable cause of bond failure.

The effect of substrate bias current density on closeout layer structure and subsequent strength was demonstrated with substrate I-13. Sputter cleaning of I-13 was carried out for a longer time and with a higher current density than I-12. The higher current density was achieved by raising the anode voltage from 30 to 40 volts. The higher current density was held through the first one-third of the closeout layer deposition and then the current density was lowered by dropping the anode voltage back to 30 volts.

The difference in microstructure caused by the different current densities is shown in figure 27. The structure starts out with a growth of fine columnar crystallites with the higher current density and then goes into the wider crystallite structure which indicates the shadowing effect is no longer controlled by ion bombardment of the substrate. The deposition rate of the outer layer is 17% greater than the rate for the inner layer even though both cathode and substrate current densities have decreased by 32%. If the rate of arrival of material at the substrate is directly proportional to the cathode current density and if the resputtering rate is directly proportional to

the substrate current density, then the decrease in material arrival rate should be almost balanced by the decrease in resputtering rate leaving a slight reduction in the net deposition rate. The deposition rate increase shows that the fraction of material resputtered from the substrate has decreased much faster than the decrease in substrate current density. The ion current density, then, has been reduced to below the average substrate ion current density at the particular section of I-13 studied.

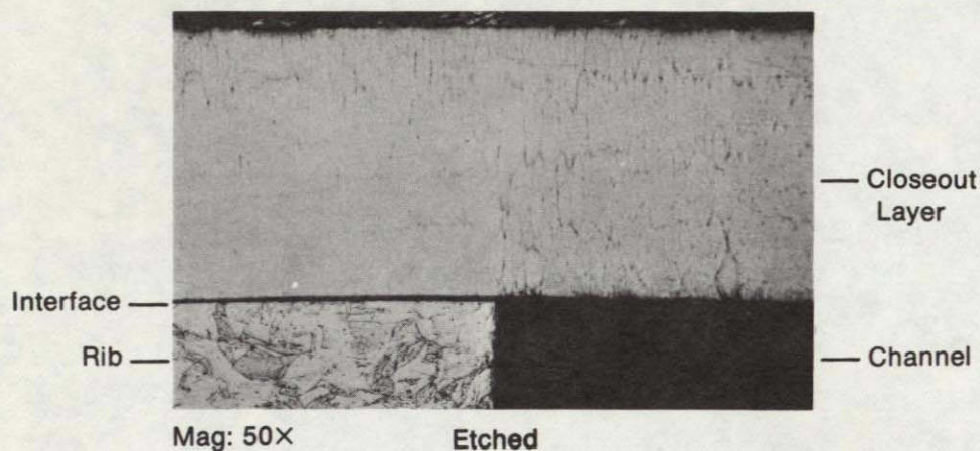


Figure 26. Typical Microstructure of Closeout Layer on Substrate I-12

The microstructures on figure 27 are taken from a section of the burst test specimen near the cracked outside layer which failed. The closeout layer was thinnest at the failed section due to out-of-round machining. Also the deposition rate was slowest, and therefore, sputter cleaning the least in this area. Complete debonding in the failed area shows sputter cleaning was inadequate.

The usual modification of structure over the rougher machined aluminum wire can be seen. The difference between structure over the grooves and lands was less at 180 degrees from the failed zone where the deposition rate was 30% greater. The average substrate zirconium content was 0.41 wt% and closeout layer zirconium content was a constant 0.20 wt% for both layers.

A comparison of microstructure for substrate I-12 and I-13 shows that the range of pressure used in these experiments had no noticeable effect on structure. The 7.6 micron pressure for substrate I-12 and the 3.7 micron pressure for the outer layer of substrate I-13 (same cathode and substrate voltages) had no visible effect on structure.

Substrate I-14 had the same surface preparation and was sputter cleaned three times as long, but at only half of the current density as substrate I-11. The closeout layer microstructure is pictured in figure 28 for the thinnest (0.071 cm) and thickest (0.243 cm) parts of the deposit. The large difference in thickness illustrates earlier remarks about shielding in these systems. Substrate I-14 was closed out in the hollow cathode which had been used to make the thick deposit for substrate II-4. At the end of the substrate II-4 deposition, this cathode had a 120-degree wide pocket sputtered into the center 4 inches of the cathode. Substrate I-14 was installed in the identical position of substrate II-4. The thick deposit on substrate I-14 was formed on the side of the substrate facing the cathode pocket. The greatest substrate to cathode distance was at this pocket area. The microstructure clearly shows:

1. No difference in structure over grooves and rib lands in the thick deposit, but a considerable difference for the thin deposit. This again shows that surface roughness can be overcome with a high substrate bias current density.

2. Vastly different structure for the two deposit thicknesses. This was manifested by the deposit surface finish. The thin section had a matte finish and the thick section was shiny.
3. The thin closeout layer had open crystallite boundaries and very little mechanical strength.
4. The directional growth of the thin deposit shows that very little sputtering, and correspondingly, very little ion bombardment of the substrate occurred on the cathode opposite this thin deposit. In fact, the cathode had a 0.030 cm thick film deposited in this area.

The closeout layer was poorly bonded (failed during specimen cut-up) over the whole substrate surface. This indicates that sputter cleaning was inadequate because of a low current density, or to a dirtier surface (when compared to substrate I-11), or to extreme outgassing of the substrate. The rib land under the thin closeout layer was probed and the following elements by wt% were found to be 1.01 Al; 0.05 Si; 0.19 Fe; 0.02 Cr; 0.22 W; and 0.75 Zr. A piece of the wrought cathode cut from an area opposite the thin deposit had 0.4 Zr wt% and less than 0.02 Fe wt% (no other elements found). The high Zr content is not due to any sputtering enrichment since very little ion bombardment took place. Likewise the aluminum which remained must have been smeared on the rib lands during final machining. The Si may have been present due to the presence of imbedded SiC chips from final machining. Tungsten and stainless steel were from the filaments and holder, respectively.

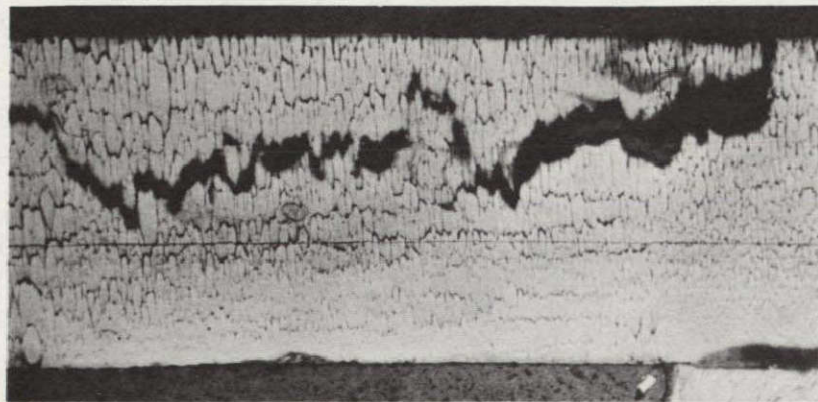
The average current density was the same as in other runs in System No. 1 due to the total current to the substrate being the same. However, the ion current density to the bottom substrate holder cap was much greater for substrate I-14 (and substrate II-4). The bottom cap was highly eroded instead of being heavily coated as usual.

Post cathode depositions onto aluminum wire filled AMZIRC substrates were done in System No. 2. Surface preparation of substrates I-4P, -5P and -6P was limited to scrubbing after the final machining. The substrates were not directly cooled. Possible effects due to substrate heating will be discussed. All three substrates had a bright surface after closeout was completed. No difference in closeout layer structure over lands and grooves was noted indicating the lack of shadowing which was prominent in the hollow cathode depositions.

Microstructures for two sections of I-4P are shown in figure 29. Sputter cleaning was inadequate as evidenced by the debonding of both sections. The deposit thickness distribution was especially poor after the first distribution cycle so the substrate was turned 180 degrees and a new post cathode installed. This time sputter cleaning was increased and a good bond was achieved over the original low deposition rate area, but not over the original high rate area.

The deposit hardness varied from 183 VPN for the coarser structure (original high rate area) to 256 VPN for the finer structure (over the original low rate area). The effect on tensile properties was evident as the lower strength specimen was machined mostly from the coarse layer and the higher strength specimen entirely from the fine layer.

The line marked DEMARCATION on the original low rate deposit microstructure was apparently caused by a slight increase in gas pressure from 6.8 to 7.3 microns. The deposition rate increased almost 20%. The effect was not detected in the original higher rate deposition area.



Mag: 50X

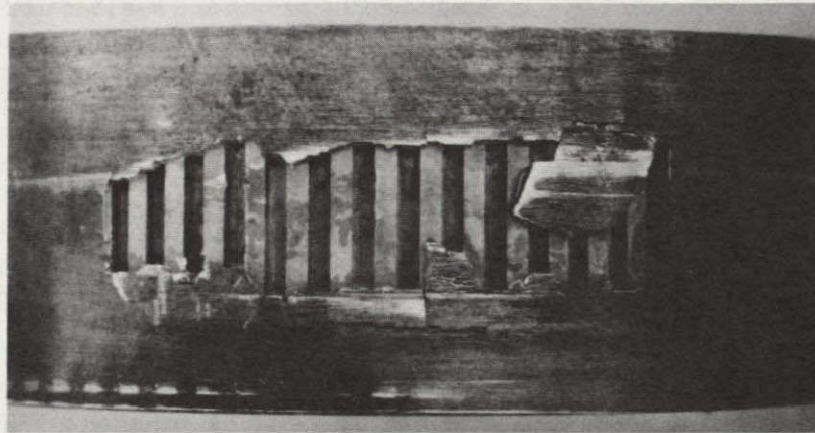
Etched - Filler Removed

Bias Current
Density

— 2.8 ma/cm²

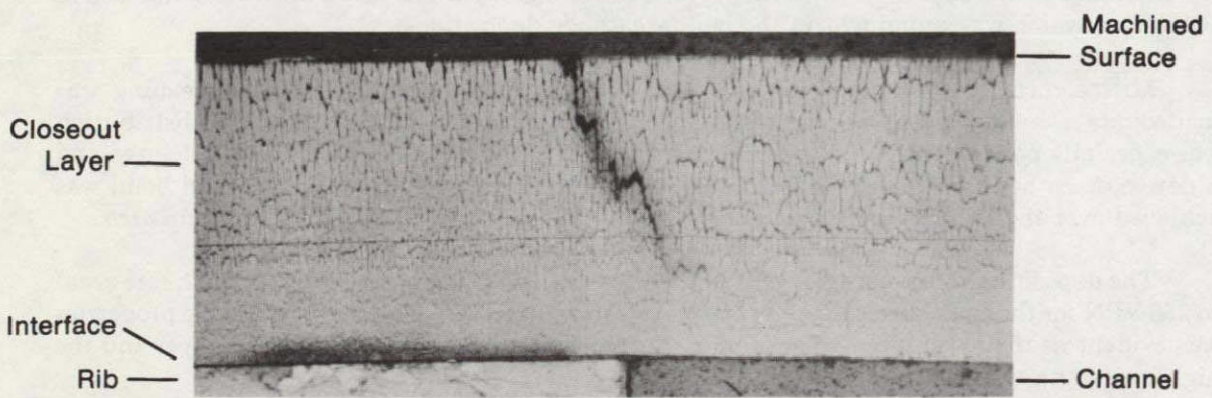
Current
Change

— 4.1 ma/cm²



Mag: 2X

Burst Specimen



Mag: 50X

Etched - Filler Removed

Machined
Surface

Closeout
Layer

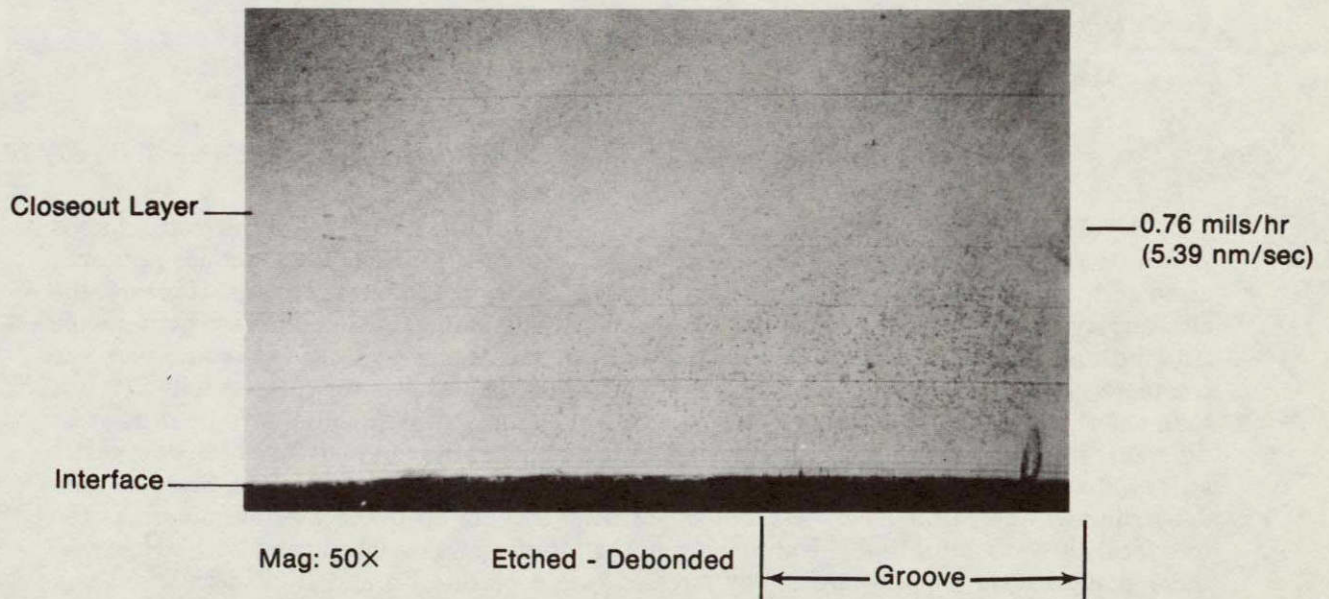
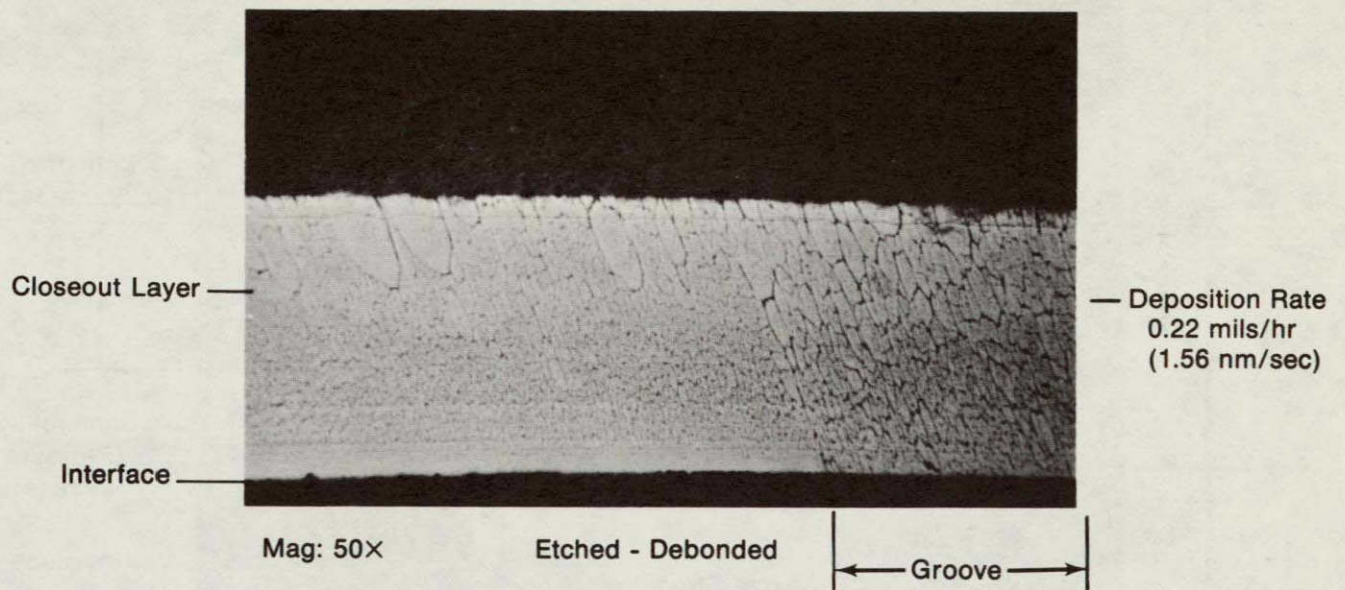
Interface

Rib

Channel

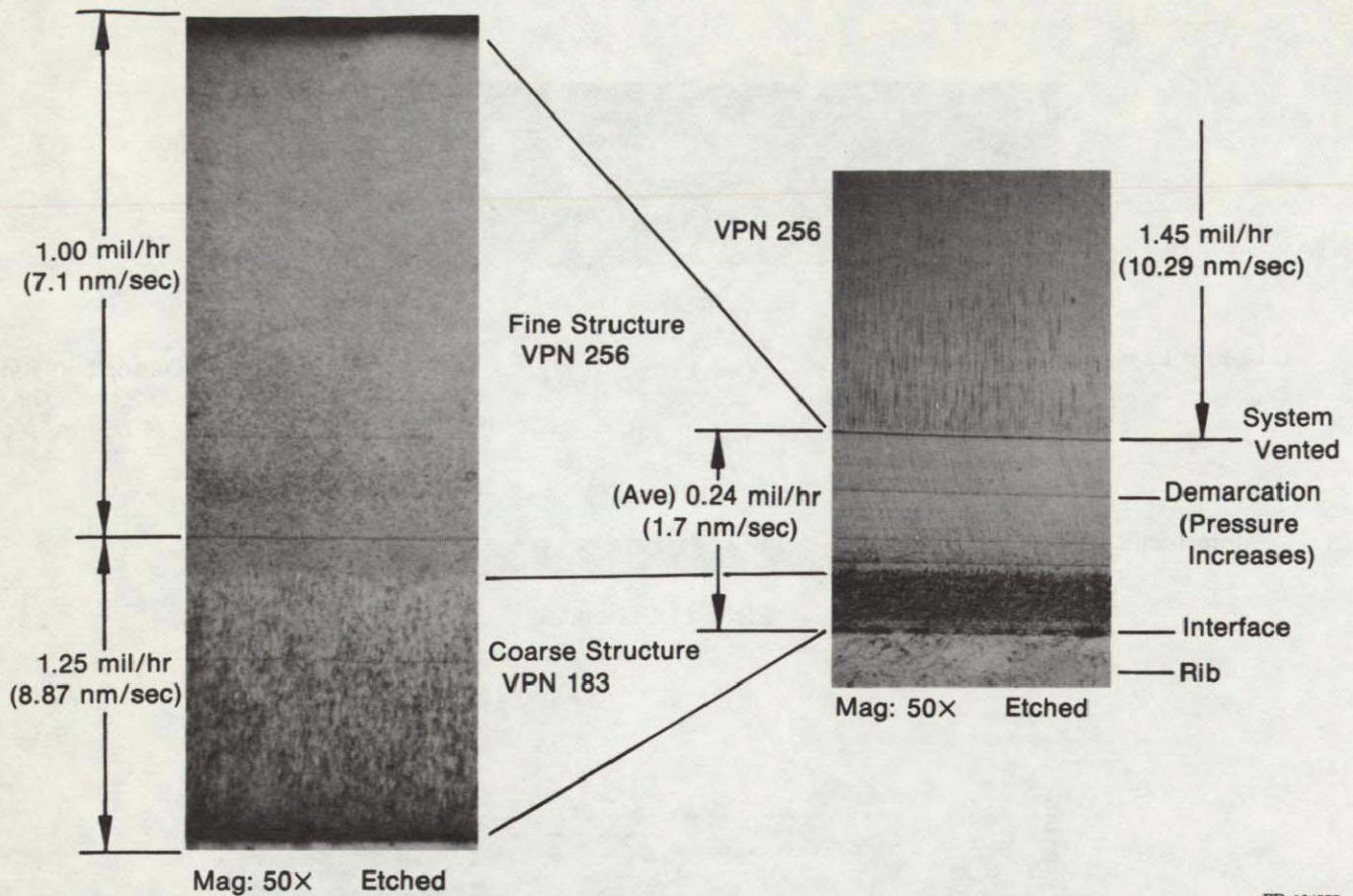
FD 104575

Figure 27. Microstructure Near Burst Specimen Failure Showing Crack Propagation - Substrate I-13



FD 104576

Figure 28. Microstructure of Closeout Layer Deposited at Two Different Rates Showing Effect of Bias Current Density, Substrate I-14



FD 104577

Figure 29. Coarse and Fine Microstructure for Two Closeout Layer Growth Rates; Substrate I-4P, 50V Bias

Substrate I-5P was sputter cleaned twice as long as substrate I-4P. The microstructure is shown on figure 30. Sputter cleaning effectiveness was hard to judge. The interface appeared clean and the closeout layer well bonded for the area 180 degrees from the grooves. However, the closeout layer debonded during tensile specimen machining. A fine line could be seen between the rib land and the closeout layer. After the aluminum was leached out, the closeout layer was completely debonded from the substrate. Since deposit thickness over the ribs was only 27% less than the thickness at 180 degrees (the apparent bonded area) there should have been no gross difference in substrate cleaning current density. Debonding at the ribs may have been due, partly at least, to the leaching of the 1.2 wt% aluminum that was found in the interface. Since no such debonding was noted for hollow cathode depositions (having up to 0.4 wt% aluminum at the interface), it is doubtful that the aluminum in the interface was leached completely. However, these post cathode deposits are highly stressed (see substrate I-6 and II-2P discussion) and leaching aluminum from the side of each rib may act as a stress riser between the closeout layer and the rib land which could have initiated a crack along the interface. Machining may have started a similar cracking mechanism during tensile specimen machining.

The change in microstructure from coarse to fine apparently was initiated by a small 0.1 micron increase in pressure. Tensile specimens were machined from the outer fine structure. The variation in hardness with structure appearance was not as great as substrate I-4P. Hardness for the coarse grain structure was 241 VPN and 253 VPN for the fine structure. The smaller hardness change for the grain structure change of substrate I-5P was due to the -25 volt bias. Substrates I-4P and I-6P were closed out with a -50 volt bias.

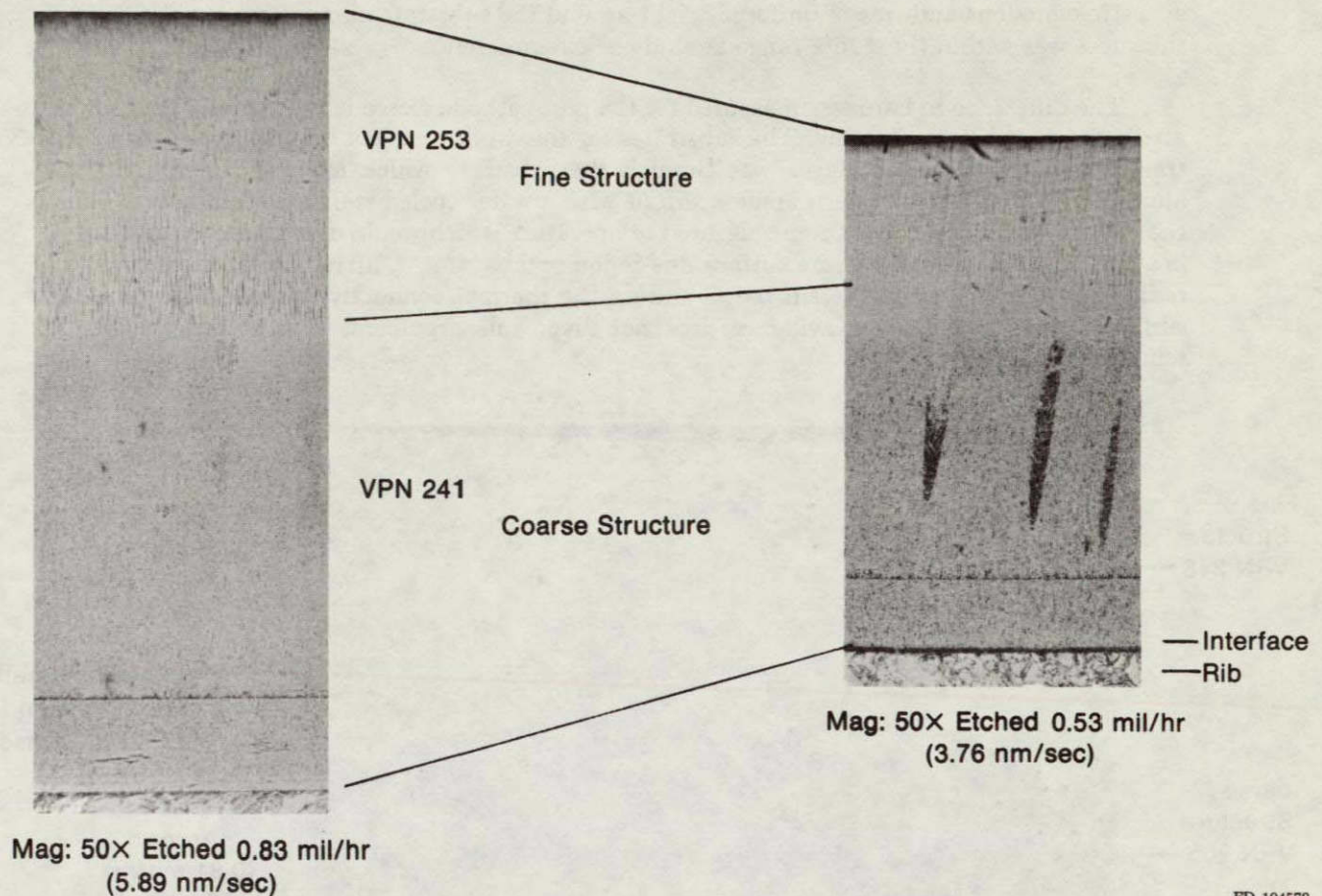


Figure 30. Coarse and Fine Microstructure for Two Closeout Layer Rates; Substrate I-5P, -25V Bias

The effect of sputtering gas species on closeout layer structure was studied with substrate I-6P. The substrate was sputter cleaned exactly as I-5P with krypton and the deposition started. After about 0.0051 cm of closeout layer was deposited, argon was substituted for the krypton. The system was effectively vented when the gas line was evacuated after changing bottles. The next 0.051 cm of closeout layer was made with argon (in two runs). Krypton was then used to finish the closeout layer.

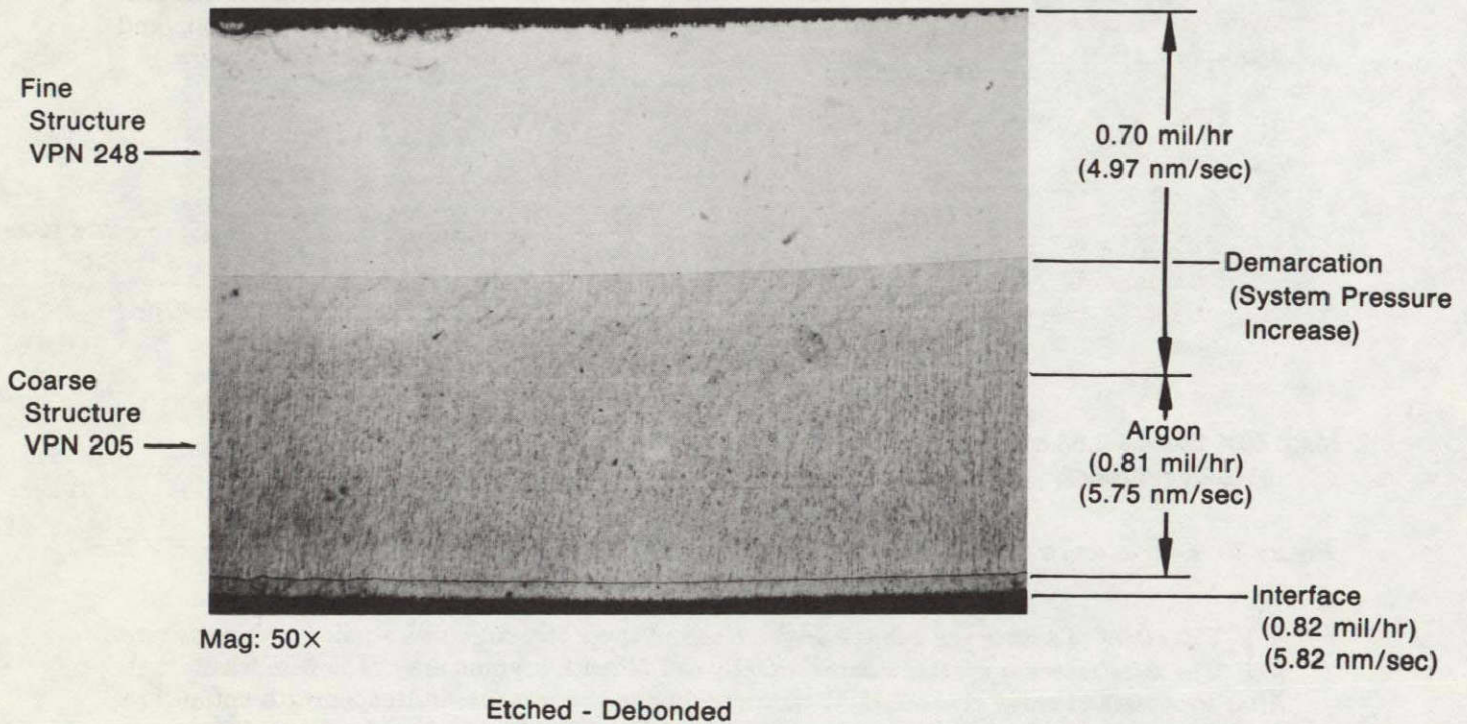
The microstructure for the I-6P closeout layer is shown on figure 31. No change in structure can be attributed to the argon. The system pressure had to be raised for the argon to maintain the discharge. Again, the abrupt change in structure can only be attributed to a slight increase in krypton pressure. Harness changed from 196-205 VPN for the coarse grain structure to 237-248 VPN for the fine grain structure which correlates well with substrate I-4P.

Deposition rates have been included on figure 31. The decrease in rate for the second krypton deposition cycle from the rate obtained for argon may be due to a combination of reasons, i.e., to pressure differences, to difference in resputtering rate, and to decrease in post cathode dimension with sputtering time.

When the end of substrate I-6P was cut off for a burst specimen ring, bond failure was evident. Shortly after cutoff, the closeout layer on the remainder of the cylinder stretched about 0.0025 cm higher than the substrate surface. The stretch was accompanied by several audible

acoustic emissions and was of uniform height around the substrate circumference. The deposit thickness was within the $\pm 15\%$ range around the circumference.

The difference in hardness measured for the post cathode closeout layers could possibly be attributed to substrate heating. The substrates for this work were not directly cooled and heat transfer from the closeout layer was through the substrate which made a slip fit with its aluminum holder which in turn made a slip fit with a water cooled stainless steel jacket. Thus, the closeout layer could be at some elevated temperature which would depend on the amount of heat introduced at the substrate surface due to ion bombardment, arriving sputtered material, radiant heat from heated system parts, and on the thermal conductivity through the mating surfaces. But the following evidence does not favor this argument of structure change by temperature change.



FD 104579

Figure 31. Microstructure Showing Coarse and Fine Regions for Substrate I-6P

In previous work for this contract (Reference 1), a relatively coarse grain structure deposited at a -50 volt (7.2 ma/cm^2) bias had a VPN hardness of 230 and a fine grain structured layer (sputtered immediately after the coarse layer) at -25 volts (6.7 ma/cm^2) bias had a VPN 270 hardness. Upper limits on temperature were 855°F (730.2°K) for the -50 volt bias and 730°F for the -25 volt bias. Deposition rate was 0.44 and 0.82 mil/hr (3.1 and 5.8 mm/sec) respectively for the -50 volt and -25 volt bias. Since in the previous experiments the substrates were deliberately thermally lagged by use of a thick walled low thermal conductivity holder and the substrate bias current densities were approximately the same, substrate temperatures should have been considerably lower in the present experiments. Further evidence for low substrate temperature is obtained from the hardness of the OFHC substrate I-1P which was deposited with aluminum at the same current densities as for substrates I-4P, -5P and -6P. Substrate hardness for substrate I-1P was 110 VPN which indicates that the substrate was not heated over 400°F (477°K).

2. Substrate Surface Preparation

1. The surface should be as smooth as is practical to obtain on a given substrate material. As mentioned for the aluminum wire, surface roughness resulted in a more open columnar structure in the closeout layer on hollow cathode sputtered substrates. Gross defects may be closed over (with substrate bias) leaving a void which would undoubtedly affect closeout layer life. Lathe machining followed by sanding lengthwise with 600 or 1000 grit SiC paper provided a good surface finish on the hollow cathode substrates.
2. No structural effects due to surface roughness were noted on the post cathode closeout layers. However, a smooth surface may be beneficial since sputter cleaning would then be more effective.

3. Sputter Cleaning

1. Judging from the burst test and structure results and debonding during specimen preparation, hollow cathode substrate sputter cleaning was adequate in system number 2, but not in systems 1 and 3. The poor substrate cleaning in the latter two systems is primarily due to lower substrate ion current density. Some of the cause, however, may have been due to the increased complexity of the fully grooved substrates which were cleaned in these systems.
2. Sputter cleaning of all post cathode substrates (in system number 2) has been described as inadequate by definition, since all closeout layers separated from the substrates. Substrate current density was lower than the current density on the successfully cleaned hollow cathode substrates. The sputter cleaning process was definitely complicated by the presence of grooves and the aluminum traces on the rib lands (see discussion of II-1P, -2P, and -3P which were successfully bonded to substrates cleaned with less current density than I-4P, -5P and -6P).

4. Substrate Bias

1. Substrate bias was very effective in controlling the structure of closeout layers deposited in the hollow cathode. At high enough current densities (and voltage) the effect of surface roughness on structure can be minimized. Evidence for the forward sputtering of closeout material was seen in the resultant shiny and smooth closeout layer surfaces at the end of deposition. Low bias current density, and therefore low resputtering rate, at any voltage was not effective in controlling structure.
2. The onset of the coarse to fine grain structure transition observed for the post cathode deposits is affected by bias voltage (current density constant). This will be seen more clearly in the Task II discussion.

5. System Geometry

1. The necessity of having an even closeout layer thickness was demonstrated for the hollow cathode. An even deposit thickness implied even substrate ion bombardment which (at high enough density) is crucial to obtaining a good structure on a substrate surface. Coaxial alignment of cathode and substrate

is essential to obtaining an even deposit due to the mutual shielding (of substrate and cathode) at the low pressures and spacings used in these experiments.

2. The closeout layer formed by the post cathode also needs to be uniform in thickness due to the high stress levels which may be able to crack the deposit at a thin section. Again, an evenly distributed deposit is obtained by coaxial alignment of cathode and substrate. The uneven current density to the substrate resulting from nonalignment may not have as great an effect on closeout layer structure as it has in the hollow cathode case.

6. System Pressure

The small differences in pressure recorded during a deposition, or from one experiment to the next, caused no noticeable change in closeout layer structure except possibly for the post cathode deposits. The structure change from coarse to fine grains could possibly have been due to the small pressure changes.

SECTION IV
TASK II
PROPERTIES OF TRIODE SPUTTERED COPPER - 0.15 WT%
ZIRCONIUM (AMZIRC®) MATERIAL

The objective of Task II was to evaluate the effect of triode mode sputtering parameter variations on the tensile properties and hardness of AMZIRC sputtered from both a post and hollow cathode.

A. EQUIPMENT AND PROCEDURES

The equipment and general procedures for Task II were the same as those used for Task I. Depositions were made to ungrooved substrates from hollow and post cathodes. The majority of deposits were made without interrupting the discharge to eliminate any layering effects on deposit structure. The discussion of expected effects of parameters on closeout layers applies to this work also.

Substrate preparation and deposition parameters are given in tables 12 and 13, respectively. Tensile strength and elongation are given in table 14 for sputtered and wrought AMZIRC. Both flat and round tensile specimens were cut from wrought AMZIRC. The small difference in tensile strengths between the two types of specimens is probably due to the statistically insignificant inhomogeneity of the wrought material. Results show the sputtered AMZIRC to have at least twice the tensile strength of the wrought material. Vickers microhardness for all substrates and Task II deposits is given in table 15.

The gas content of the thick sputtered AMZIRC is given in table 16. Oxygen and hydrogen analysis was done in standard LECO gas analyzers. Krypton analysis was done by mass spectrometry by the Gollob Analytical Service Corp., Berkeley Heights, N.J.

TABLE 12. SUMMARY OF TASK II SUBSTRATE PREPARATION

<i>Substrate Number</i>	<i>Substrate Material</i>	<i>Surface Preparation</i>	<i>Current ma/cm²</i>	<i>Voltage volts</i>	<i>Time min</i>	<i>ks</i>	<i>Pressure N</i>	<i>N/m²</i>	<i>System Number</i>
Hollow Cathode									
II-1	OFHC	600 grit SiC paper, scrubbing powder scrub, ethyl alcohol rinse	8.0	-25	5	0.3	3.4	0.44	3
			7.4	-25	15	0.9	3.7	0.48	
			7.9	-50	15	0.9	6.4	0.83	
II-2	AMZIRC	600 grit SiC paper (on lathe) scrubbing powder scrub, ethyl alcohol rinse	2.0	-25	5	0.3	3.4	0.44	3
			4.1	-50	5	0.3	3.4	0.44	
			3.3	-50	50	3.0	3.6	0.47	
II-3	AMZIRC	1000 grit SiC paper	No Ion Bombardment Cleaning						3
II-4	AMZIRC	600 grit SiC paper (on lathe) scrubbing powder scrub, ethyl alcohol rinse	3.1	-25	5	0.3	3.6	0.47	1
			3.8	-50	70	4.2	2.4	0.31	
Post Cathode									
II-1P	AMZIRC	As machined, scrubbing powder scrub, ethyl alcohol rinse	3.3	-25	5	0.3	2.0	0.26	1
			3.3	-50	30	1.8	2.8	0.36	
II-2P	AMZIRC	Same as II-1P	2.7	-25	5	0.3	3.4	0.44	1
			4.3	-50	30	1.8	4.2	0.55	
II-3P	AMZIRC	Same as II-1P	3.2	-25	5	0.3	5	0.65	1
			4.0	-50	30	1.8	30	0.39	

TABLE 13. SUMMARY OF TASK II DEPOSITION PARAMETERS

Substrate Number	Substrate		Cathode		Deposition Time ¹		Maximum Deposit Thickness		Maximum Deposition Rate		Pressure	
	Current ma/cm ²	Voltage volts	Current ma/cm ²	Voltage volts	hr	ks	mm	mils	nm/s	mils/hr	N	N/m ²
II-1	7.4	-50	8.8	-500	16	57.6					6.4	0.82
	2.1	-50	2.8	-1000	24	86.4	1.19	47	7.9	1.13	5.6	0.72
II-2	3.6	-50	3.8	-1000	166	597.6	2.79	110	4.3	0.61	3.4	0.44
II-3	0	ground	4.2	-500	204	734.4	2.69	106	3.7	0.52	5.3	0.68
II-4	4.0	-50	3.0	-500	319	1148.4	7.70	303	6.7	0.95	3.7	0.47
Post Cathode												
II-1P	3.9	-50	6.1	-500	181	651.6	3.33	131	5.1	0.72	2.7	0.35
II-2P	4.0	-25	5.9	-500	20	72					4.4	0.56
	4.1	-25	6.1	-500	20	72					3.7	0.47
	4.4	-25	6.1	-500	55	198					5.2	0.67
	4.7	-25	5.4	-500	45	162	2.57	101	5.1	0.72	5.6	0.72
II-3P	2.9	0	6.2	-500	108	388.8	3.66	144	9.3	1.33	3.7	0.47

TABLE 14. TENSILE PROPERTIES OF DEPOSITED AND WROUGHT AMZIRC (ROOM TEMPERATURE)

Substrate Number	0.2% Offset Yield Strength		Tensile Strength		Elongation %
	(ksi)	(NM/m ²)	(ksi)	(NM/m ²)	
Hollow Cathode Deposit					
II-2	112.0	770.6	129.5	891.0	4.6
II-4	125.2	861.4	127.5	877.2	4.0
II-4	125.3	862.1	129.6	891.6	6.0
Post Cathode Deposit					
II-1P	123.7	851.1	133.5	918.5	7.0
II-1P	123.3	848.3	129.2		5.4
II-2P	114.6	788.4	114.6	788.4	3.0
II-2P	112.5	774.0	116.2	799.5	5.0
II-3P	97.2	668.7	97.2	668.7	3.0
II-3P	95.9	659.8	95.9	659.8	3.0
Wrought AMZIRC ¹					
² Flat - 1	40.8	280.7	48.3	332.3	17.0
Flat - 2	41.3	284.1	47.7	328.2	19.0
³ Round - 1	40.1	275.9	50.7	348.8	20.0
Round - 2	38.6	265.6	50.6	348.1	21.0

¹ Tensiles cut from substrate blank.

² Tensile specimen as shown in figure 5.

³ Round tensile, 0.241 cm diameter at gage.

ORIGINAL PAGE IS
OF POOR QUALITY

**TABLE 15. VICKERS HARDNESS
FOR AS-DEPOSITED
AMZIRC FOR TASK II**

<i>Substrate Number</i>	<i>Substrate Material</i>	<i>Substrate Hardness VPN</i>	<i>Deposit Hardness VPN</i>
Hollow Cathode Deposit			
II-1	OFHC Copper	106-116	215-220
II-2	AMZIRC	112-132	220-243
II-3	AMZIRC	-	220-226
II-4	AMZIRC	116-134	225-249
Post Cathode Deposit			
II-1P	AMZIRC	137	231-262
II-2P	AMZIRC	132	220-236
II-3P	AMZIRC	123	220-243

**TABLE 16. GAS CONTENT OF
TASK II DEPOSITS**

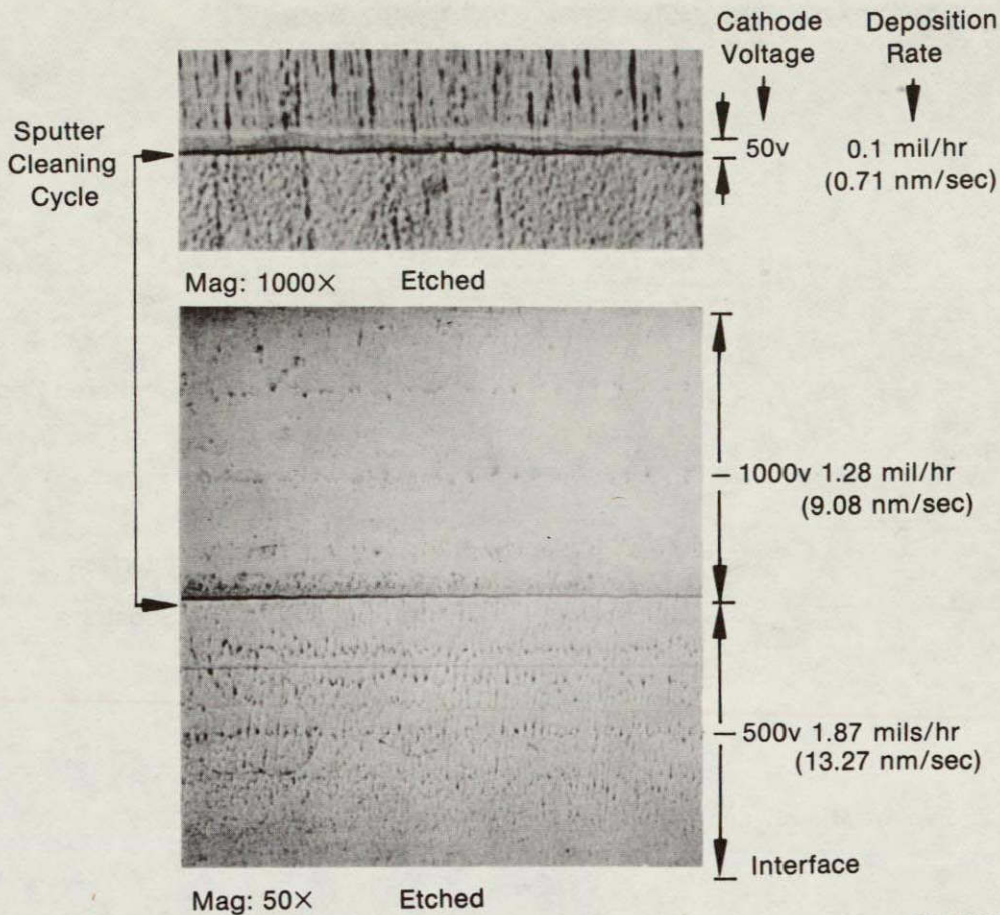
<i>Substrate Number</i>	<i>Oxygen ppm</i>	<i>Hydrogen ppm</i>	<i>Krypton ppm</i>
Hollow Cathode			
II-1	230	5.5	72
II-2	50	6.0	13
II-3	150	3.0	ND
II-4	32	1.0	ND
Post Cathode			
II-1P	40	2.5	15
II-2P	40	2.0	ND
II-3P	60	7.5	ND
Wrought AMZIRC			
Cathode	17.5	3.0	

ND= None Detected - Less than 0.5 ppm.

B. HOLLOW CATHODE RESULTS AND DISCUSSION

The first deposition of Task II was done to determine the effect of higher rate and voltage on deposit structure. Substrate II-1 was coated in two runs in system 3. The microstructure is shown in figure 32. The higher rate was achieved by using only the top anode and increasing the anode voltage to 54 volts (39 amps). At the higher voltage, both anodes were used as usual (30v at 39 amps). Substrate bias was -50 volts for both runs.

The average substrate current density of 7.4 ma/cm² measured during deposition of the high rate region was in the same range as current densities obtained in Task I in system 2. However, the structure is that of a deposit made at low current density. The deposit debonded from the substrate showing that sputter cleaning (at the same current density) was ineffective. Further evidence of actual low substrate current density can be seen in the insert to figure 32. The substrate actually had a net gain of sputtered material from the hollow cathode which also was at -50 volts. This accumulation was not seen in system 2 for substrates cleaned under identical time (30 minutes) and voltage (-50 volts), e.g., substrate I-9.



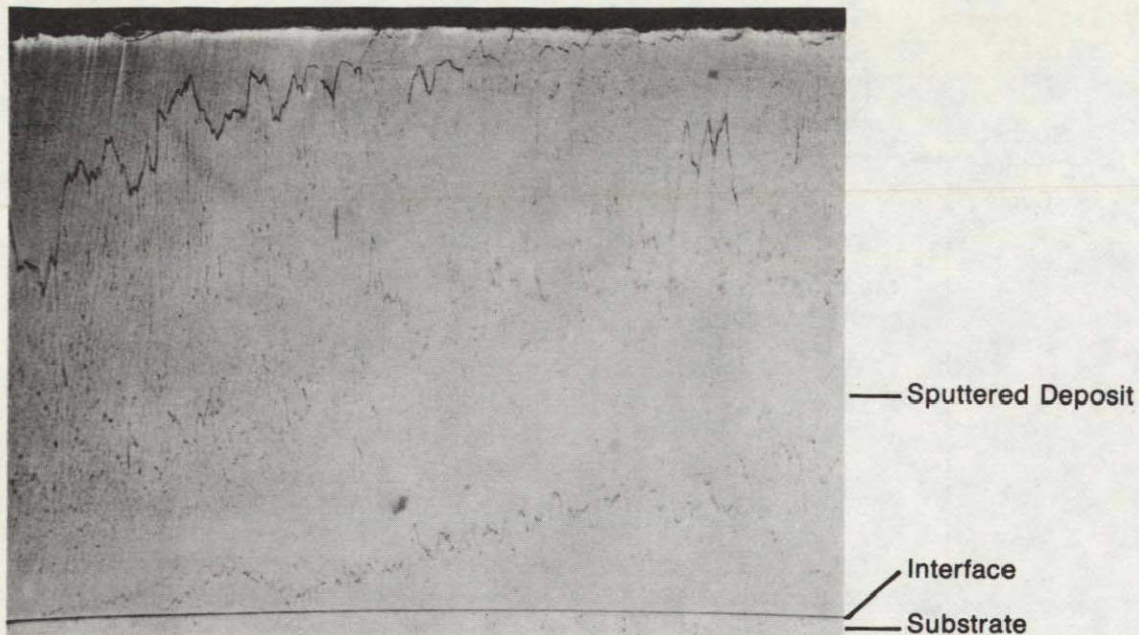
FD 104580

Figure 32. Microstructure of Sputtered AMZIRC at Higher Voltage and Higher Rate, Substrate II-1

The high voltage region shows a possibly better microstructure. The layered structure in this region (and in the high rate region) is due to the growth habit and not to any change of system parameters.

Substrate II-2 was coated without stop with -1000 volts on the cathode. Filament current was increased from that used in deposition II-1 to increase current density to the cathode and substrate. The current density increase was 36% and 71% for the cathode and substrate respectively. The average deposition rate decreased 44% showing that the resputtering was much greater than for substrate II-1 at the same cathode and substrate voltages. The substrate was more effectively sputter cleaned also as no debonding of the deposit was noted. The oxygen content of the deposit was considerably lower than for substrate II-1 which shows that the bias current density was enough to be effective.

The microstructure for II-2 is shown in figure 33. The structure is similar to that of substrate II-2P (figure 37) and may be indicative of high stress.



Mag: 45X

Etched

FD 104581

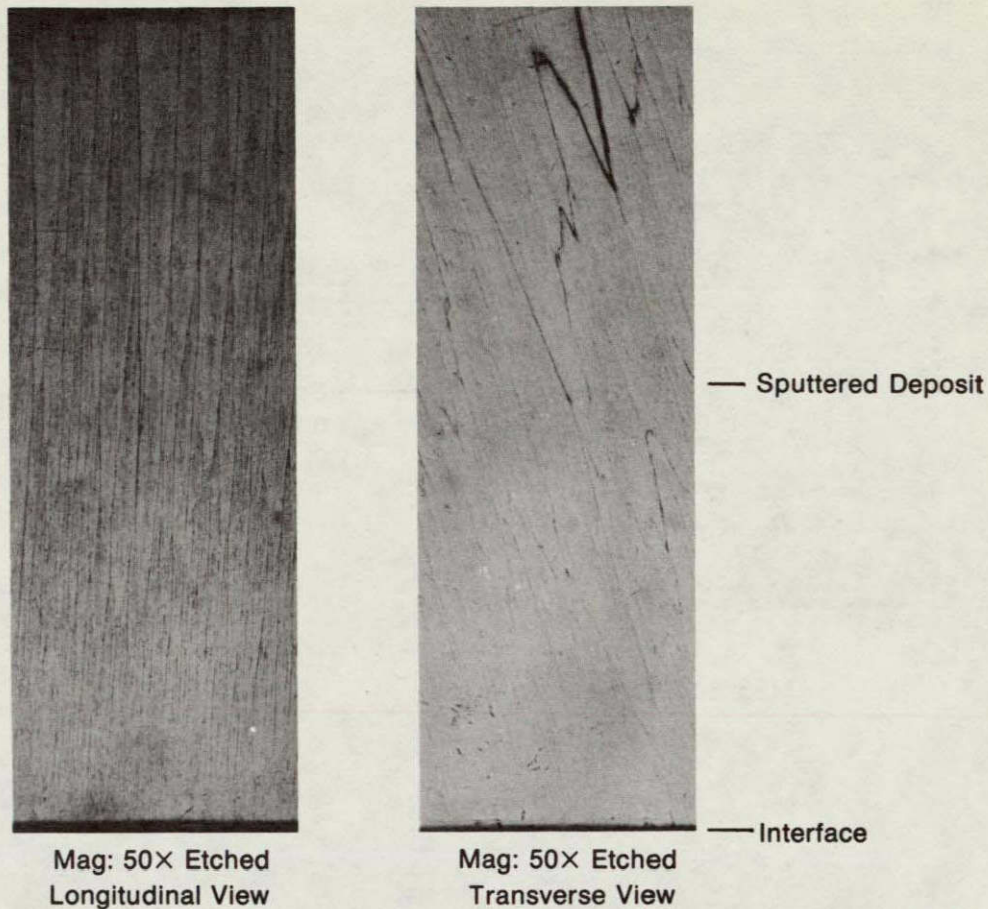
Figure 33. Typical Microstructure for Substrate II-2; Cathode Voltage $-1000V$

The substrate for deposition II-3 was not sputter cleaned to determine the effect of insufficient sputter cleaning on a bulk deposit. The microstructure is shown in figure 34. The growth habit is typical of deposits with insufficient bias current density. The growth is oriented in the direction of arrival of sputtered material when viewed tangentially to the substrate circumference (transverse view). This illustrates that sputtered material arrives primarily from the ends of the cathode in system 3. No tensile specimens were cut since the deposit was severely cracked and pulled away from the substrate by the high internal stress and zero adhesion. The oxygen level was high from lack of bias current.

As discussed for substrate I-14, mutual shielding has caused the uneven deposit on substrate II-4. The microstructure of a thick and thin section is shown in figure 35. The thick deposit is very fine grained while the thin section shows the usual structure attributed to low bias current density. The hardness is lower than that of I-14 which may be due to the absence of layers. The surface of the 0.76 cm thick section was shiny and smooth.

C. POST CATHODE RESULTS AND DISCUSSIONS

Task II post cathode work was done on three AMZIRC substrates, II-1P, -2P and -3P which were processed identically and sputter cleaned for the same length of time. All deposits were made in system number 1. Substrates II-1P and II-3P were coated without stop. The deposit for II-2P was made in four layers. The object of the post work was to study the effect of substrate bias on thick deposits. Because of slight misalignment between the post cathodes and substrates, deposition rate was also studied. All structures were dense and no debonding of the deposit from the substrate was observed before or after sample cut-up.



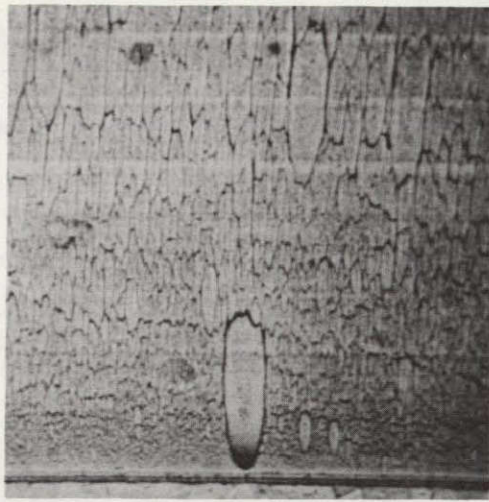
FD 104582

Figure 34. Typical Longitudinal and Traverse Microstructure for Substrate II-3

Typical microstructures for these deposits are shown in figure 36. The coarse structure is representative of the entire II-3P deposit and of the higher rate part of the II-2P deposit.

The coarse to fine structure phenomena are shown clearly for substrate II-1P at both low and high rates (-50 volt bias). The effect is only barely observable for II-2P (-25 volt bias) at the low rate and no change in structure was observed for II-3P (0 volt bias). As for Task I post work, the fine structure is harder than the coarse structure for the low rate deposits. However, the hardness for II-1P apparently passes through a maximum in the fine structure. The change from coarse to fine structure for II-1P was not triggered by any noticeable change in deposition parameters. The difference between the coarse and fine structures could be seen on the substrate surfaces. Substrate II-3P was matte and II-2P and -1P were shiny.

If the thickness for the onset of the coarse to fine structure change is plotted vs deposition rate, a rough pattern can be seen. The onset thickness increases for increasing deposition rate and also for decreasing substrate bias voltage. This would indicate that this structure change is associated with a geometric packing effect which is the opposite of the shadowing effect seen in the hollow cathode. The structure does not seem to be dependent on substrate bias current density.



— Sputtered Deposit
0.22 mil/hr (1.56 nm/sec)

Mag: 50× Etched



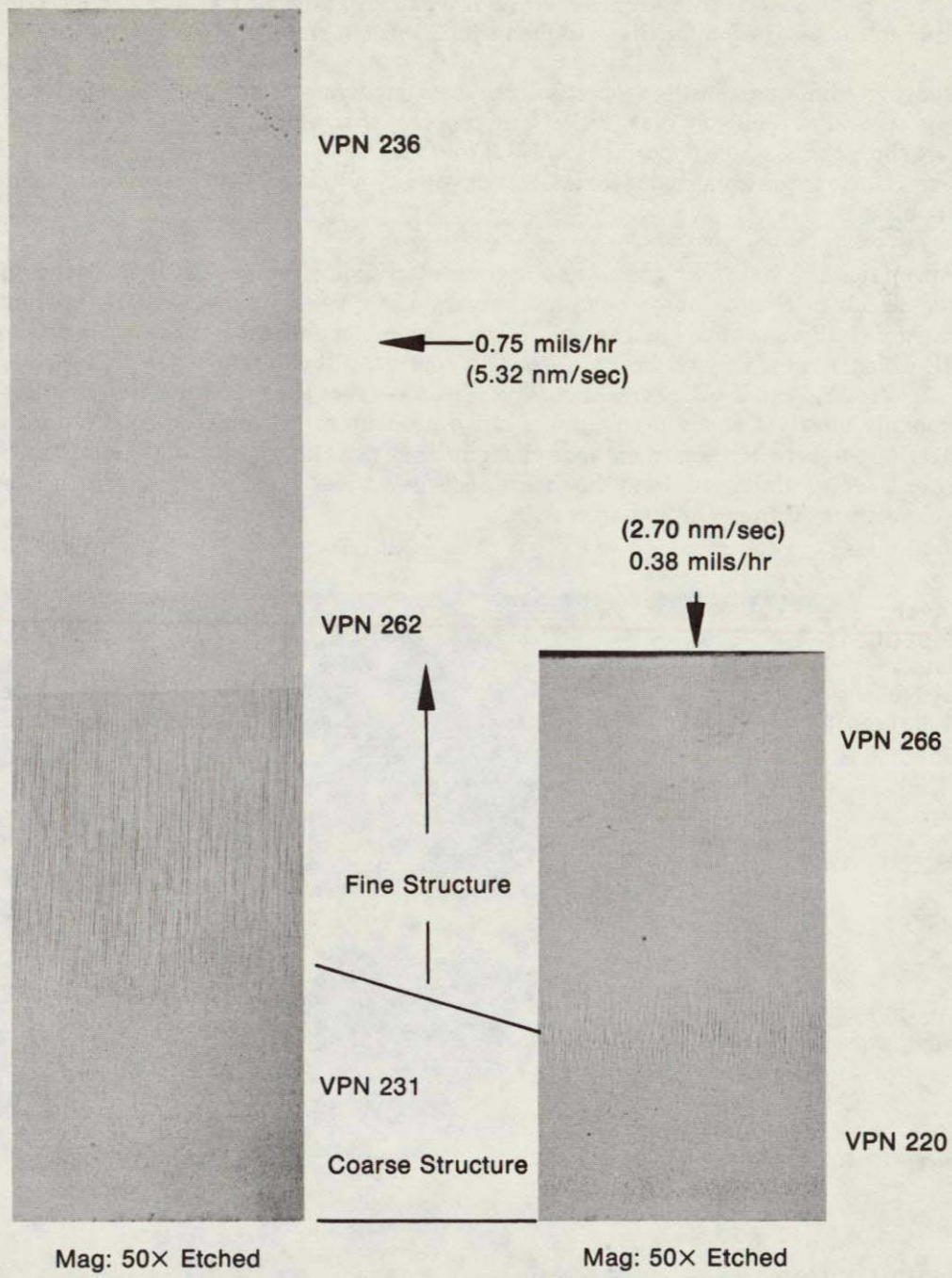
— Sputtered Deposit
0.91 mil/hr (6.46 nm/sec)

— Interface
— Substrate

Mag: 50× Etched

FD 104583

Figure 35. Microstructure of Deposit Formed at Two Rates Showing Effect of Bias Current Density - Substrate II-4



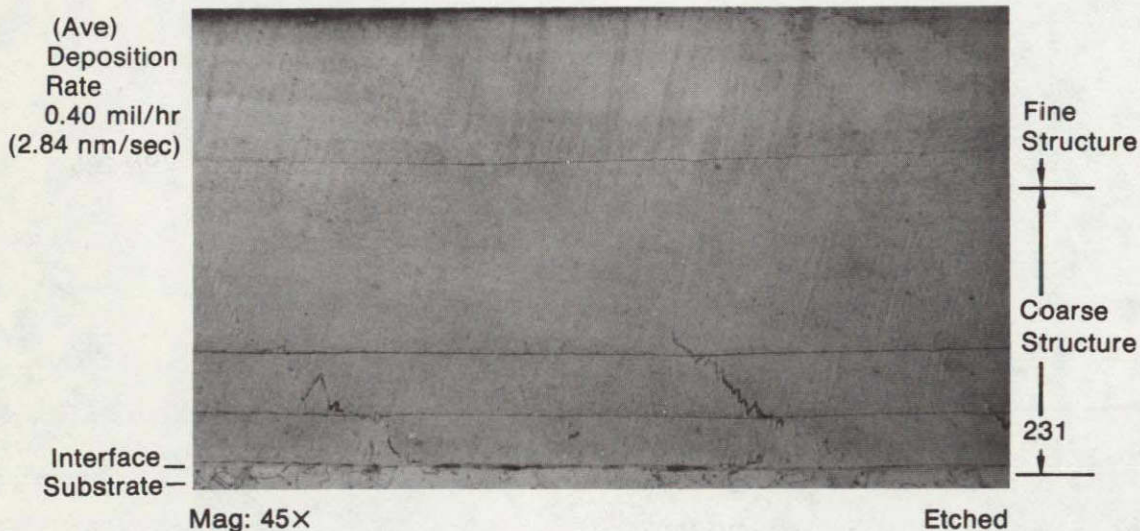
FD 104584

Figure 36. Microstructure of Deposit From Post Cathode Showing Onset of Fine Structure at Two Deposit Rates; -50 Volt Bias, Substrate II-10

Tensile properties for these post cathode deposits are dependent on substrate bias voltage (table 14). The all coarse structure of substrate II-3 had lower tensile strength and low elongation compared to the elongation for the specimen which was cut from the coarse structure of I-4P.

Judging from the tensile properties, the best structure would be the relatively coarse structure formed at -50 volt bias (I-4P). The problem then becomes one of keeping the coarse structure through the whole deposit thickness. From the discussion of the dependence of the onset of the structure change from coarse to fine, one possibility would be to increase the deposition rate at -50 v bias.

An interesting feature of the low sputtering rate microstructure for II-2P is the apparent cracking which originates at or near the substrate surface. (See figure 37) Apparently the substrate for II-2P was not cleaned as well by the sputter cleaning as were the substrates for II-1P and -3P which show a very clean interface. The poor bond then allowed the thin section of the deposit to stress relieve itself by cracking. This illustrates that the debonding in I-4P, -5P and -6P was probably mostly a stress problem and not a problem of leaching out aluminum from the interface. Apparently in the post cathode closeout layer work any action on the substrate such as cutting or leaching aluminum from the grooves acts as a stress raiser which can result in spalling of the closeout layer from the substrate.



FD 104585

Figure 37. Microstructure of Deposit II-28 at Low Rate -25 V Bias

D. CONCLUSIONS

Tensile strengths of thick deposits made in one deposition run were practically the same as the strengths of the layer deposits made in Task I. The conclusions reached in Task I, as concern the dependence of deposit structure on deposition parameters, should therefore be applicable to Task II work. The structure of continuous deposits appeared the same as for a layered deposit, e.g., II-1 compared with I-14, formed with the same parameters. The coarse to fine structure observed in the post cathode deposits was not a function of starting and stopping the deposition. If deposit fatigue life is not degraded, a layered deposit could be more desirable. Sputter cleaning at sufficient bias current density between layers can effectively stop defect growth which would ordinarily be carried completely through a continuous deposit.

SECTION V PROGRAM SUMMARY

In this program techniques were developed for coating and fabricating advanced high performance regeneratively cooled thrust chambers by sputtering Cu-0.15 Zr from hollow and post cathodes. Thrust chambers were simulated by grooved and plain cylinders (substrates) approximately 12.5 cm long by 6.3 cm in diameter.

As a part of Task I, several filler material systems were evaluated. CERROTRU® encased in aluminum, aluminum wire, and sputtered aluminum were found to be suitable filler materials as judged by the ease of filler material removal and closeout layer bond strength and structure. The balance of Task I work was done with substrates filled with aluminum wire.

The effect of deposition parameters on closeout layer bond and structure were studied in three coater geometries. Work with hollow cathodes showed that high bond strengths and dense structures could be obtained with sufficiently high bias ion current density and voltage. Also, the use of substrate bias was effective in curing the leader structure associated with defects on substrate surfaces. Closeout layer thickness, structure and bond strength was dependent on system geometry. Closeout layers sputtered from post cathodes showed a duplex structure that was dependent on bias voltage. The tensile strengths of closeout layers was in turn dependent on this duplex structure. Post cathode closeout layers were highly stressed and not as well bonded as hollow cathode closeout layers.

In Task II thick deposits were continuously sputtered on smooth substrates. Tensile strengths and structures were practically the same as those obtained in Task I. Substrate bias was effective in reducing the oxygen content of the deposits.

SECTION VI

REFERENCES

1. Mullaly, J. R., T. E. Schmid, C. T. Torrey and R. J. Hecht, *Development of Sputtered Techniques for Thrust Chambers*, NASA CR134824, March 1975.
2. McClanahan, E. D., R. Busch, and R. W. Moss, *Property Investigation and Sputter Deposition of Dispersion-Hardened Copper for Fatigue Specimen Fabrication*, Contract NAS3-134480, November 1973.
3. Spalvins, T. and W. A. Brainard, "Nodular Growth in Thick Sputtered Metallic Coatings," *J. of Vac. Sci. Technol.* 11 (6), pp 1186 - 94, 1974.
4. Wehner, G. K., "Physical Sputtering," *Proceedings of Fifth International Conference on Ionization Phenomena in Gases*, Munich 1961, North-Holland Publishing Co., Amsterdam, pp 1141 - 56.
5. Thornton, J. A., "Influence of Apparatus Geometry and Deposition Conditions on the Structure and Topography of Thick Sputtered Coatings," *J. Vac. Sci. Technol.* 11, No. 4, pp 666-70, July/Aug 1974.
6. Bland, R. D., G. J. Kominiak and D. M. Mattox, "Effect of Ion Bombardment During Deposition on Thick Metal and Ceramic Deposits," *J. Sci. Vac. Technol.* 11, No. 4, pp. 671-4, July/Aug 1974.
7. Patten, J. W., E. D. McClanahan, and J. W. Johnston, "Room-Temperature Recrystallization in Thick Bias- Sputtered Copper Deposits," *J. Appl. Phys.* 42, No. 11, pp 4371-4377, October 1971.
8. Lee, W. W., and D. Oblas, "Argon Concentration in Tungsten Films Deposited by dc Sputtering," *J. Vac. Sci. Technol.* 7, No. 1, pp 129-33, Jan/Feb 1970.
9. Gill, W. D. and E. Kay, "Efficient Low-Pressure Sputtering in a Large Inverted Magnetron Suitable for Film Synthesis," *Rev. Sci. Instrum.*, 36, No. 3, pp 277-282, March 1965.

DISTRIBUTION LIST FOR FINAL REPORT NASA CR 135153

National Aeronautics and Space Administration
Lewis Research Center
21000 Brookpark Road
Cleveland, Ohio 44135

Attn: W. Fleming, MS 500-313
E. A. Bourke, MS 500-205 (5 copies)
Technical Utilization Office, MS 3-19
Technical Report Control Office, MS 5-5
AFSC Liaison Office, MS 501-3 (2 copies)
Library, MS 60-3 (2 copies)
Office of Reliability and Quality Assurance, MS 500-211
J. M. Kazaroff, Project Manager, MS 500-204 (25 copies)

National Aeronautics and Space Administration
Headquarters
Washington, DC 20546

Attn: RP/Director, Space Propulsion and Power (2 copies)
RS/Director, Manned Space Technology
SV/Director, Launch Vehicles and Propulsion
RW/Director, Materials and Structures
MT/Director, Advanced Missions
SG/Director, Physics and Astronomy Programs
SL/Director, Planetary Programs
R/Office of Aeronautics and Space Technology
KT/Director, Technology Utilization Division

National Aeronautics and Space Administration
Ames Research Center
Moffett Field, California 94035

Attn: Library

National Aeronautics and Space Administration
Goddard Space Flight Center
Greenbelt, Maryland 20771

Attn: Library
620/Merland L. Moseson

National Aeronautics and Space Administration
Flight Research Center
P.O. Box 273
Edwards, California 93523

Attn: Library

National Aeronautics and Space Administration
John F. Kennedy Space Center
Cocoa Beach, Florida 32931

Attn: Library
CD/Kurt H. Debus

DISTRIBUTION LIST (Continued)

National Aeronautics and Space Administration
Langley Research Center
Langley Station
Hampton, Virginia 23365
Attn: Library
Office of Director

National Aeronautics and Space Administration
Johnson Space Center
Houston, Texas 77001
Attn:
Library
EP/J. G. Thiobodaux, Jr.

National Aeronautics and Space Administration
George C. Marshall Space Flight Center
Huntsville, Alabama 35812
Attn: Library
S&E-ASTN-P/Hans G. Paul
S&E-ASTN-MM/James Hess

Office of the Director of Defense
Research and Engineering
Washington, D.C. 20301
Attn: Office of Asst. Dir. (Chem. Technology)

NASA Scientific and Technical Information Facility
P.O. Box 33
College Park, Maryland 20740
Attn: NASA Representative (10 copies)

Jet Propulsion Laboratory
4800 Oak Grove Drive
Pasadena, California 91103
Attn: Library
Henry Burlage, Jr.
Duane Dipprey

Defense Documentation Center
Cameron Station - Bldg. 5
5010 Duke Street
Alexandria, Virginia 22314
Attn: TISIA

RTD (RTNP)
Bolling Air Force Base
Washington, D.C. 20332

Advanced Research Projects Agency
Washington, D.C. 20525
Attn: Library

DISTRIBUTION LIST (Continued)

Air Force Rocket Propulsion Laboratory (RPR)
Edwards, California 93523
Attn: Library
Donald Penn

Air Force FTC (FTAT-2)
Edwards Air Force Base, California 93523
Attn: Library

Air Force Office of Scientific Research
Washington, D.C. 20333
Attn: Library
SREP/Dr. J. F. Masi

Space and Missile Systems Organization
Air Force Unit Post Office
Los Angeles, California 90045
Attn: Technical Data Center

U.S. Air Force
Washington, D.C.
Attn: Library
AFRST/Col. C. K. Stambaugh

U.S. Army Research Office (Durham)
Box CM, Duke Station
Durham, North Carolina 27706
Attn: Library
Commanding Officer

U.S. Army Missile Command
Redstone Scientific Information Center
Redstone Arsenal, Alabama 35808
Attn: Document Section
Dr. W. Wharton

Bureau of Naval Weapons
Department of the Navy
Washington, D.C.
Attn: Library
RTM-41/J. Kay

U.S. Naval Weapons Center
China Lake, California 93555
Attn: Library
Commander
H. E. Bennett

U. S. Naval Missile Center
Point Mugu, California 93041
Attn: Commander
Library

DISTRIBUTION LIST (Continued)

Naval Research Branch Office
1030 E. Green Street
Pasadena, California 91101
Attn: Library
Commanding Officer

U.S. Naval Research Laboratory
Washington, D. C. 20390
Attn: 6180/Director
Library

Picatinny Arsenal
Dover, New Jersey 07801
Attn: Library

Air Force Aero Propulsion Laboratory
Research and Technology Division
Air Force Systems Command
United States Air Force
Wright-Patterson AFB, Ohio 45433
Attn: APRP (Library)

Aerojet Liquid Rocket Company
P.O. Box 15847
Sacramento, California 95813
Attn: Technical Library 2484-2015A
V. Frick
Larry Bassham

American Society for Metals
Metals Park, Ohio 44073
Attn: Ralph G. Dermott

Sandia Laboratories
Box 969
Livermore, California 94550
Attn: H. R. Johnson
J. W. Dini

Chemical Propulsion Information Agency
Applied Physics Laboratory
8621 Georgia Avenue
Silver Spring, Maryland 20910
Attn: Tom Reedy

Watervliet Arsenal
Watervliet, New York
Attn: Peter Greco
F. K. Sautter

DISTRIBUTION LIST (Continued)

Metrophysics, Inc.
Arizona Division
P.O. Box 3126
117 S. Hayden Road
Tempe, Arizona 85281

Battelle Memorial Institute
Pacific Northwest Laboratories
P.O. Box 999
Richland, Washington 99352
Attn: Howard R. Gardner (2 copies)
Edwin D. McClanahan
Dr. Raymond A. Busch

Rocketdyne
Division of Rockwell International Corporation
6633 Canoga Avenue
Canoga Park, CA 91304
Attn: Mr. H. Diem